Schweizerische Eidgenossenschaft
Confédération suisse
Confederazione Svizzera
Confederaziun svizra

Eidgenössisches Departement für
Umwelt, Verkehr, Energie und Kommunikation UVEK

Bundesamt für Energie BFE

Schlussbericht 31.08.2015

WindRail – a modular system to produce building based electricity from wind, pressure difference, and solar radiation

WindRail wind turbine energy assessment

Subventionsgeberin:

Schweizerische Eidgenossenschaft, handelnd durch das
Bundesamt für Energie BFE
Sektion Cleantech
Pilot- und Demonstrationsprogramm
CH-3003 Bern
www.bfe.admin.ch

Kofinanzierung:

Anerdgy AG

Subventionsempfänger:

Anerdgy AG
Technoparksstrasse 1
CH-8005 Zürich
www.anerdgy.ch

Zürcher Hochschule für Angewandte Wissenschaften
Institut für Energiesysteme und Fluid-Engineering IEFE
Technikumstrasse 9
Postfach 805
CH - 8401 Winterthur
www.iefe.zhaw.ch

Autoren:	Peter Shaw, Anerdgy AG, peter.shaw@anerdgy.ch Sven Koehler, Anerdgy AG, sven.koehler@anerdgy.ch Adrian Täschler MSc. FHO, ZHAW Manuel Räber MSc. ETH, ZHAW Prof. Dr.-Ing. Andreas Heinzelmann, ZHAW
BFE-Programmleitung:	Yasmine Calisesi, Leiterin P+D-Programm yasmine.calisesi@bfe.admin.ch
BFE-Projektbegleitung:	Lionel Perret, Leiter Forschungsprogramm Windenergie lionel.perret@planair.ch
BFE-Vertragsnummer:	SI/501132-01

Zusammenfassung

Im Rahmen des Energiekonzepts 2050 soll der Anteil an erneuerbaren, dezentralen Energieerzeugern erhöht werden. Ziel dieser Studie ist es, das energetische Potential des WindRails zu evaluieren. Das WindRail ist ein modulares System, das aus Wind- und Sonnenenergie am Gebäude elektrische Energie erzeugt und ins Netz einspeist. Die Untersuchung zeigt, dass das geprüfte Modul einen Mehrertrag an elektrischer Energie von 45 % pro Quadratmeter aktiver Rotorfläche im Vergleich zur Aventa AV-7 Anlage produziert; im relevanten Windbereich von ±30 ° Anströmung werden 38 % des kinetischen Windenergiepotentials in Strom umgewandelt. Trotz der positiven Ergebnisse kann keine abschliessende Beurteilung des energetischen Potentials und der Wirtschaftlichkeit des Systems erfolgen. Dies aufgrund des Aufbaus als Einzelmodul, einer fehlenden Netzeinspeisung und der zu kurzen Untersuchungsdauer. Daher wird empfohlen ein Referenzprojekt in voller Anlagengrösse zu realisieren und dies entsprechend zu begleiten.

Résumé

La proportion en générateurs d'énergies renouvelables décentralisés doit être augmentée, dans le cadre du concept d'énergie 2050. Le but de cette étude est d'évaluer le potentiel énergétique du WindRail. Il s'agit d'un système modulaire qui transforme l'énergie solaire et éolienne au bâtiment en énergie électrique, transférable au réseau. En comparaison avec l'installation Aventa AV-7 le module WindRail examiné montre un rendement supérieur de 45 % par mètre carré de surface active du rotor; au secteur du vent pertinent, dans un angle de ±30 % par rapport au Windrail, 38 % du potentiel énergétique cinétique du vent sont transformé en courant. Malgré ce résultat positif, il n'est pas possible de juger le potentiel et l'économie du système de façon concluante. L'emploi d'un seul module, la période d'essai limitée et l'absence du transfert au réseau en sont les causes. Par conséquent, il est recommandable de réaliser un projet de référence en pleine taille et de l'accompagner de façon convenable.

Abstract

Within the energy concept 2050, the renewable, decentralized energy supply will be increased significantly. The goal of this study is to evaluate the WindRail technology; which is a modular system that transforms buildings exposed to wind and solar radiation into electricity to be fed into the building electricity grid. This report shows that the tested WindRail single module has an increased wind turbine power output of 45 % per square meter active rotor surface in comparison to the Aventa AV-7 wind turbine; at the relevant wind direction of ±30° the kinetic wind energy is converted into electricity with 38 % efficiency. Nevertheless, a final evaluation of the energy potential and its economics are not yet possible because only a single module was evaluated, no wind turbine grid input was realized and the test period was too short. Therefore, it is highly recommended to realize and scientifically evaluate a WindRail full-installation reference project.

Contents

1 Initial position

WindRail is a product developed by Anerdgy for year-round local energy production, utilizing energy from a combination of natural sources: wind, pressure and solar radiation. The system uses a newly developed wind turbine, encapsulated in a modular unit [11] [12], which enables its installation and maintenance on any type of flat roof. WindRail is suitable for both new buildings and buildings undergoing renovation. WindRail is integrated within the buildings and acts as a platform for other technologies and functions (e.g. rainwater harvesting, greenhouse). Thus, it enables the transforming of the building rooftop into a sustainability centre, in an ecological and cost-effective way. Figure 1 shows a typical installation integrated in a building.

Figure 1: WindRail functional principle

1.1 Innovation value

1. *Wind and solar energy generation coupling*

Combining two types of technology enables WindRail to optimize energy production levels, throughout the year, both day and night, and to increase the energy yield per square meter of footprint. Solar panels placed on the upper surface of the module are cooled by the wind flow, which helps to keep them efficient.

2. *Wind flow around the building*

WindRail makes effective use of the wind flow around the building along the façade and roof edge. To use the wind flow, the inlet area and guide vanes are designed and positioned on the edge of the roof on the building's façade.

3. *Using pressure differences*

The wind turbine converts wind speed into torque on the turbine axis. The yield is the ratio of the rotational energy on the shaft of the turbine over kinetic energy contained in the wind flow. The pressure difference between the inlet and outlet of the internal turbine is converted into mechanical energy on the rotor shaft. Simulation results indicate that this translates into an increased yield of the wind turbine by a factor up to 2 (i.e. an inlet wind speed of 6 m/s translates to 12 m/s at the rotor).

4. Integration with the building structure

A simple modular system integrates WindRail with the building structure and prevents landscape pollution. Each module is connected to the building using an ingenious interface system (base frame), which ensures safety and allows installation and maintenance. WindRail modules are designed to also enable the integration of other building based-technical solutions, e.g. building air conditioning and ventilation equipment.

1.2 Windrail applications

WindRail is suited for any form of building (Figure 2). The buildings may be used for industrial, residential, commercial and other purposes as long as they have flat roofs.

Figure 2: WindRail applied on industrial and residential buildings

1.3 Renewable energy generation on buildings

Renewable energy generation on buildings is dominated by crystalline PV-cell technology. Wind power generation on buildings is limited by the availability of accepted technologies and the higher cost compared to existing solutions. WindRail is a product, which combines three sources into one modular system. Figure 3 gives an overview of the market penetration versus the functionality of the system.

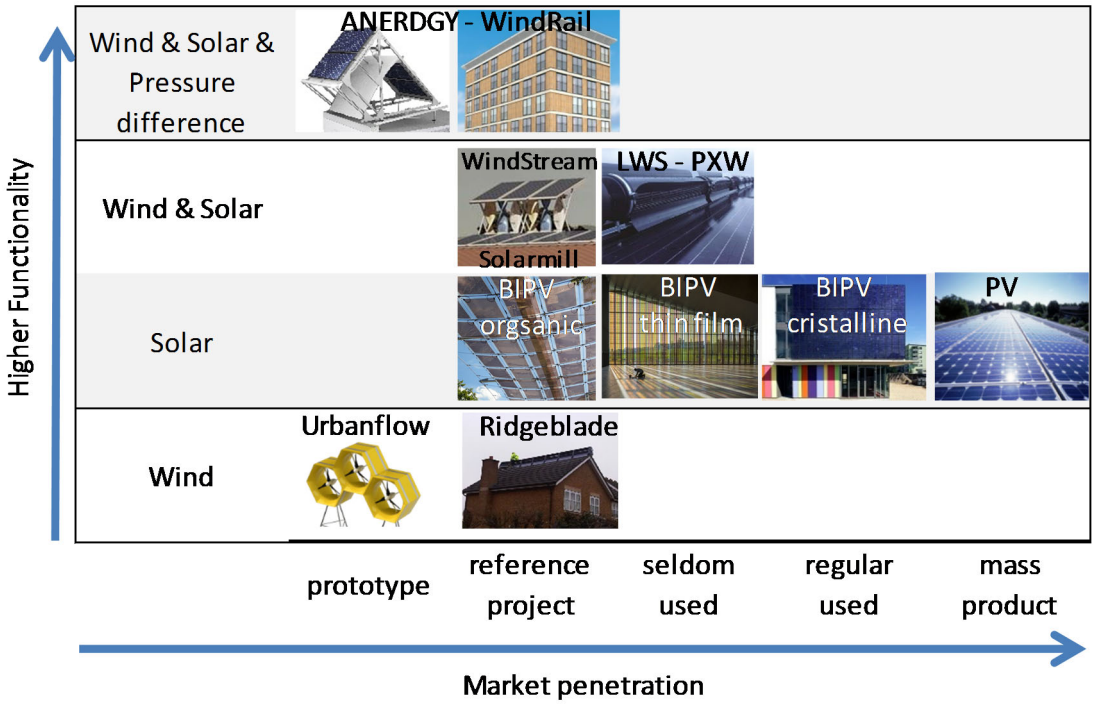

Figure 3: Building based energy generation solutions at 2015

1.4 The WindRail Prototype

The WindRail status according to the BFE nomenclature for R&D projects [1] is presented in Table 1. The Technology Readiness Level (TRS) corresponds to the current development stage of the project. The first four columns show the qualification for different BFE support projects as approved for energy research (F), pilot (P), demonstration (D), or lighthouse projects. The WindRail prototype is currently in the TRS 7 status.

Table 1: WindRail R&D steps

F	P	D	L			WindRail development	Goals	period
				TRS 9	To demonstrate the actual equipment / process in a full operational environment (hot commissioning).	regular Installation (full system)		
				TRS 8	To demonstrate the actual equipment / process in a limited operational environment (hot commissioning).	reference project (module row)		
				TRS 7	To demonstrate the actual equipment / process in the relevant operational environment (cold commissioning).	C model (1 module)	validation functional & efficiency	Oct. 14 - July 15
				TRS 6	To demonstrate an engineering-scale equipment / process testing in a relevant environment	B model (1 module)		July 14
				TRS 5	To demonstrate a bench-scale equipment / process in a relevant environment.	A model (1 module)		Nov. 14
				TRS 4	To complete laboratory-scale testing of similar equipment systems testing in a relevant environment.	not applicable, due to lack of laboratory-scale environment		
				TRS 3	To simulate the equipment and proof of concept in a simulated environment.	CFD Analyse		Sep. 13
				TRS 2	To formulate the equipment and process concept	A model design & construction		Aug. 13
				TRS 1	To observe and report the basic principals	Analytics model		Jul. 13

1.5 CFD simulation building with WindRail

A single WindRail module with turning rotors was fully installed and setup in Marthalen as part of this TRS 7 project. Around 30,000 CPU core hours of CFD simulations were performed to analyze wind flow and pressure around the buildings and the influences on WindRail. This process enabled continuous optimization of the product throughout the measurement period.

2 Project aim and objectives

The primary aim of this project was to prove the principal concept. Therefore the following objectives were initially defined:

1. Building based electricity generation using wind and solar within a single module concept
2. Wind turbine efficiency and control through output power comparison with a HAWT
3. PV combination functionality
4. Installation and maintenance concept
5. Functionality of a roof mounting and sliding system
6. Electrical building grid connection
7. Validation of low noise-level and vibrations

In addition, measurement goals were defined as follows:

- Continuous measurement of the generated energy
- Determining efficiency per module
- Validating the power generator and MPPT routines
- Validating easy installation
- Complying to environmental, health and safety standards

3 Location and basic conditions

3.1 Landi Marthalen location – grain silo

Landi Marthalen and its CEO, Christian Lutz, kindly allowed us continuous access to this location for the purposes of this project. The project location is the site of Landi Weinland in Marthalen, ZH (47.635560 N, 8.655449 E). An advantage of this location is that the ZHAW is able to measure and compare the WindRail module output versus the classical HAWT which is installed at the same place. However the average wind speed in this area is lower than the designed ideal efficiency of WindRail of 7.5 m/s. Table 2 shows the site parameters. Figures 4 and 5 show the yearly solar irradiation and wind speed.

Table 2: Project site input data

Parameter	**Input estimate**
Building height	40 m
Building orientation	NE/SW
Yearly solar irradiation	1200 kWh/m²
Building geometry	Smooth outer shape
Sea level	457 m
Initially estimated wind conditions:	
Wind distribution per orientation	NE:42 % ES:4 % SW:49 % WN:5 %
Average wind speed	2.4 m/s
Wind probability distribution [10]	A-Factor: 3.5 k-Factor: 1.4

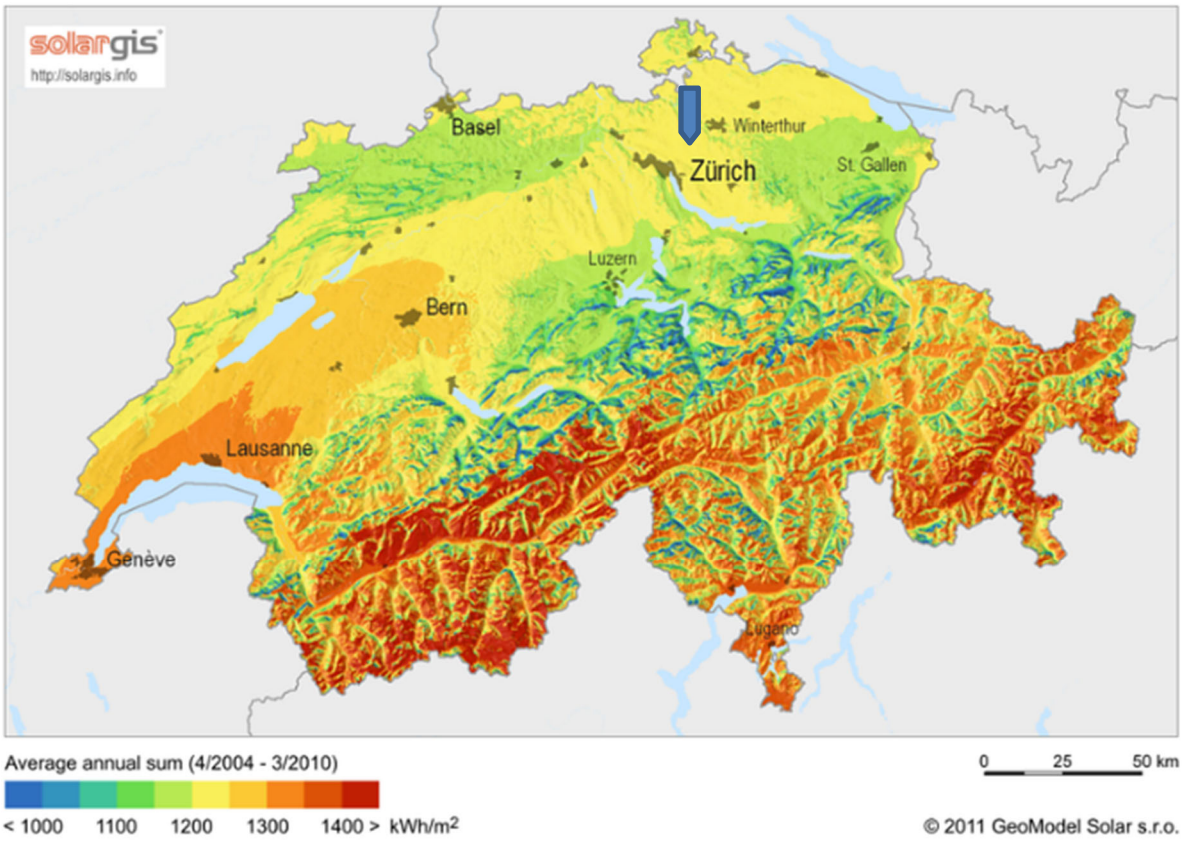

Figure 4: National solar radiation intensity

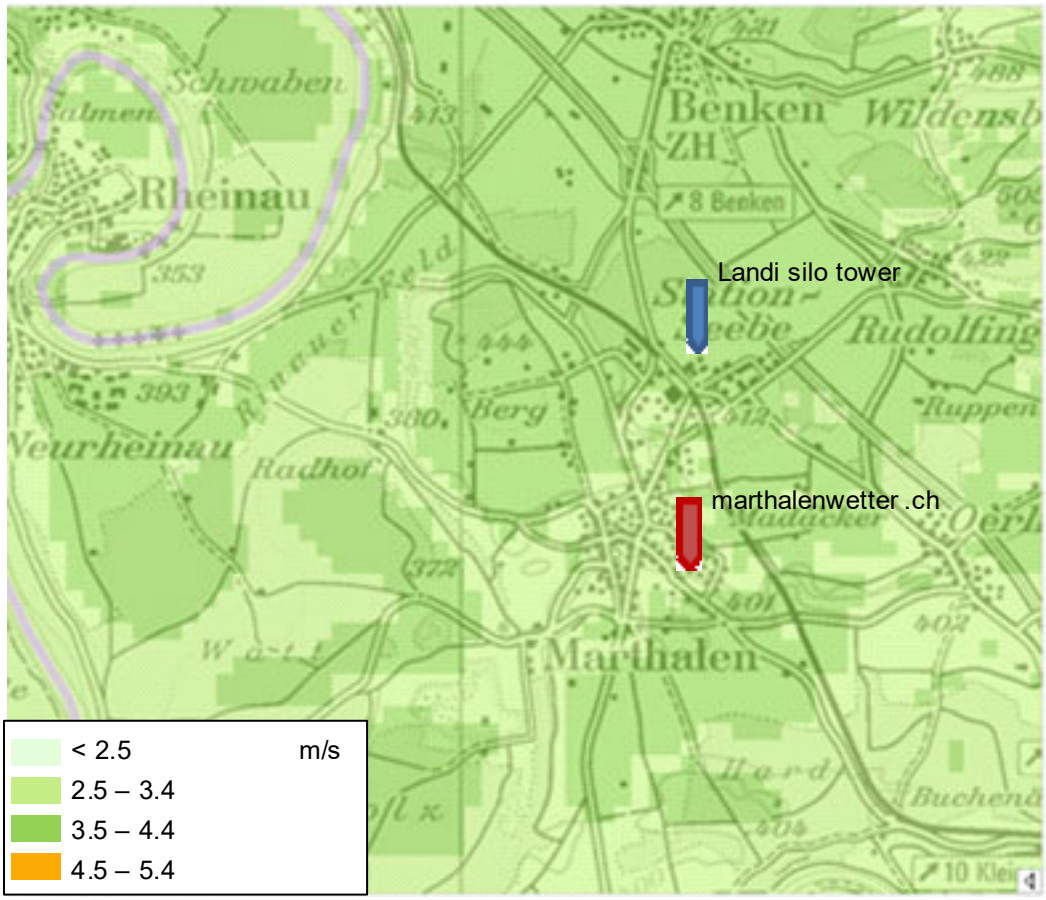

Figure 5: Project site wind speed chart

Based on the available wind direction data as well as the position of other constructions on the roof, Anerdgy decided to install the WindRail module for the project on the south-west side of the building. Figure 6 shows the roof and its constructions, whereas Figure 7 presents the project site from the ground.

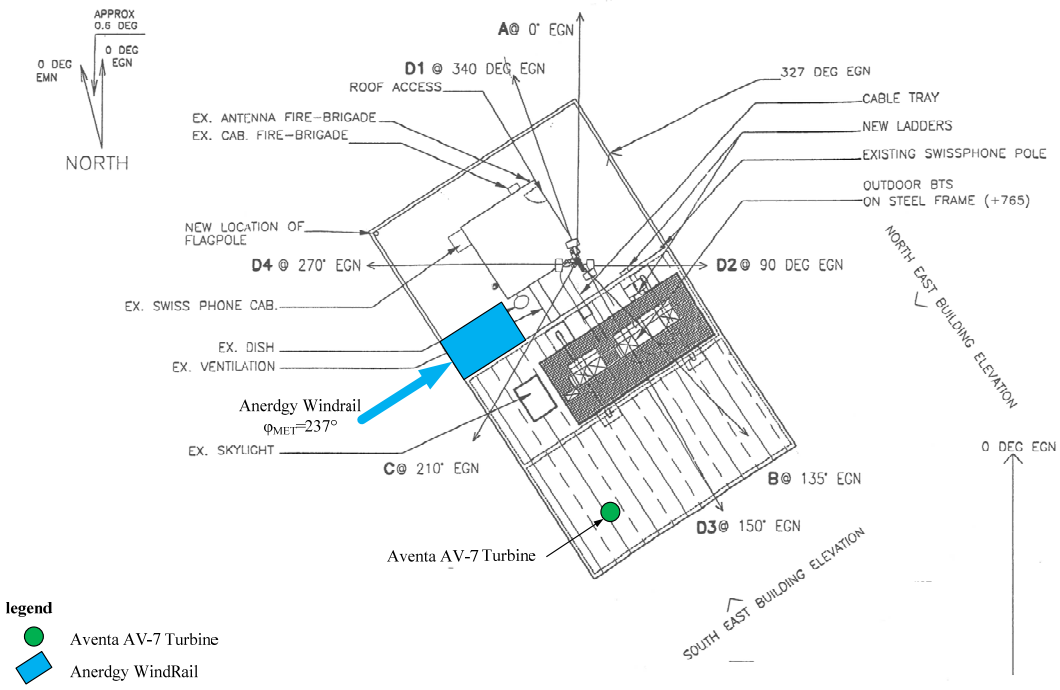

Figure 6: Project site plan

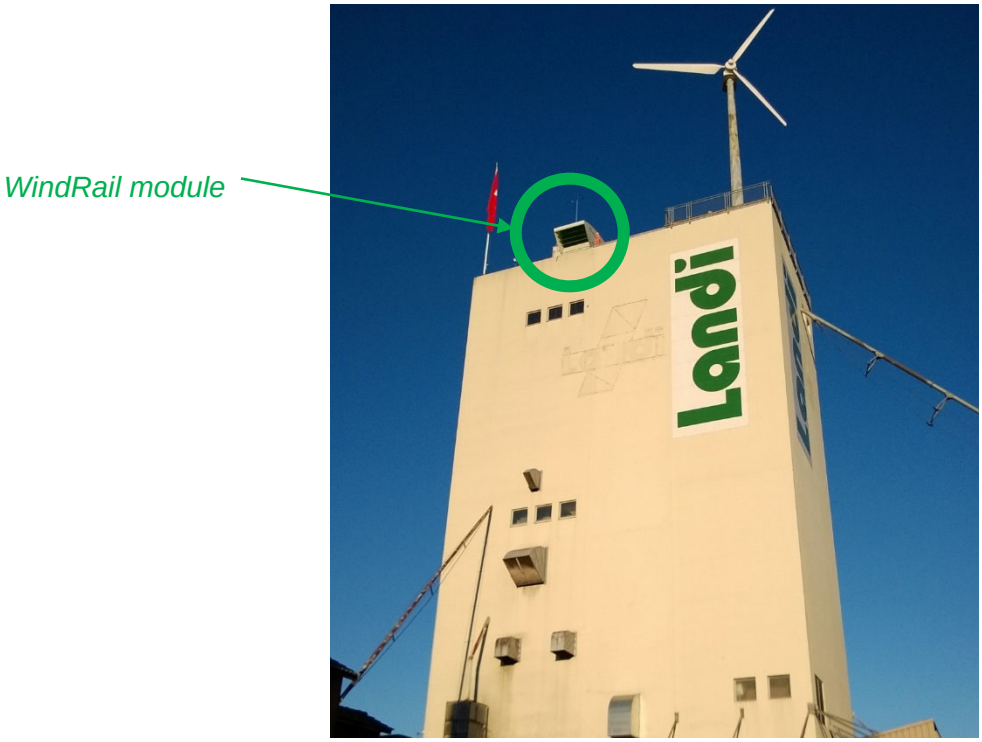

Figure 7: Street level view on the building site

3.2 Global wind data Marthalen

A local inhabitant of the area installed a meteorological station, which can be used for validation. Figures 8 and 9 show the wind speed and direction.

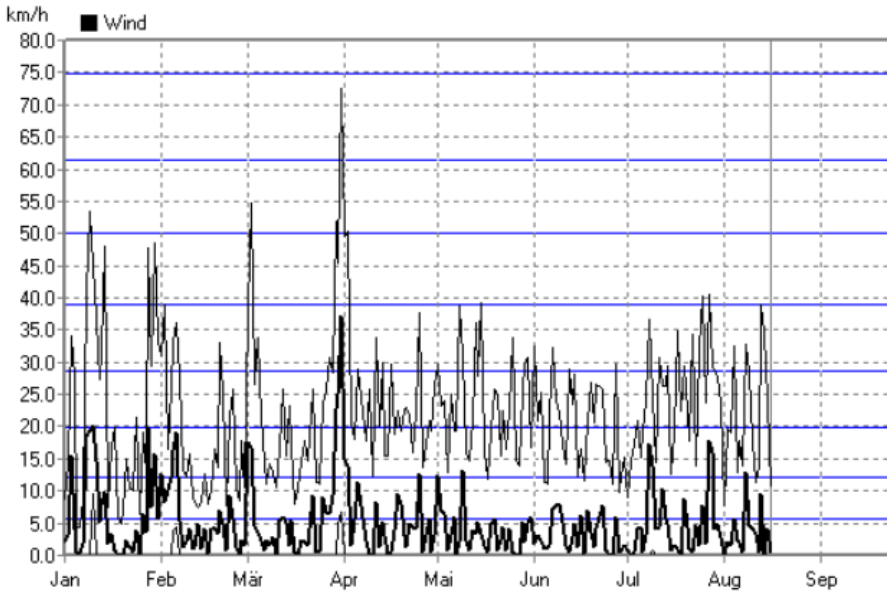

Figure 8: Wind data: www.marthalenwetter.ch

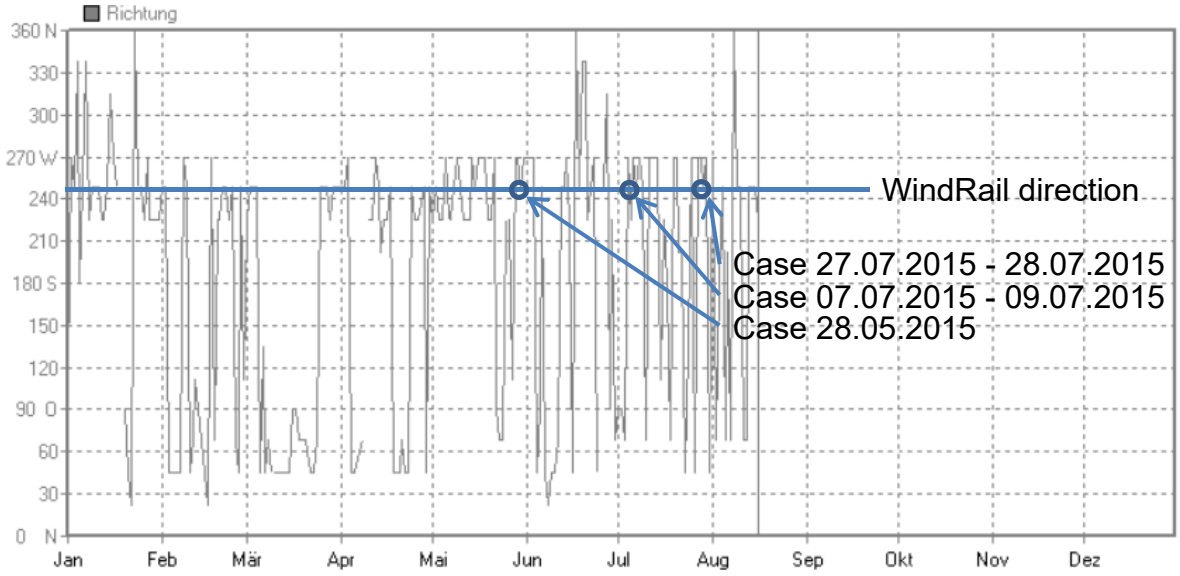

Figure 9: Wind direction data: www.marthalenwetter.ch

3.3 Prototype

The WindRail prototype uses standardized components for industrial drives, and these were never intended for energy production. In addition these drives are oversized for the attached nominal 0.75 kW generators. The Anerdgy software initializes the drives on power-up and continuously monitors the speed and the temperature. Once the generators start turning, the speed is compared with a power curve and the relevant Torque is applied in 20 ms-intervals to ensure maximum yield at all speeds. In high-wind conditions, the system shifts to the constant power mode. System improvements for higher power generation under storm conditions are being developed and will initially be evaluated on a test-bench as these wind conditions rarely occur at Marthalen. Because of the chosen test design by Anerdgy, no wind energy is fed back to the grid. Instead, the produced wind energy is absorbed by an attached brak-

ing resistor. This method was chosen as it ensured that the various control strategies could be tested and optimized independently of any power limitations in the grid inverter. The timing of this load is controlled by the DC bus voltage. This leads to current pulses, which differ in their width and which have a high harmonic content. The originally intended AC measurement with rated energy meters by ABB was revised. It was also not possible to measure this current with a high-resolving DC meter because the interferences between the meter and the drive would lead to a measurement error greater than 100 %.

3.4 Roof environment

EMC radiation and overheating created significant problems and blackouts during the measurement period as well as to the evaluation electronics. The massive radiation on the roof is produced by the GSM antenna, the large motors in use within the grain silo (building), and the wind turbine's frequency converters. Heating to temperatures greater than 85 °C was caused by the fact that the electrical cabinets are packed with test equipment, direct solar radiation heating, and hermetically closed. These cabinets are only used for test equipment and are not required for normal operation. In practice, the construction of any electrical cabinets will take these environmental conditions into consideration.

3.5 Energy efficiency definition

Currently there is no norm or standard available as to how to define efficiency for such systems. It comes mainly from two factors:

a) Parallel usage of wind & solar in one system
b) Usage of pressure difference on the wind turbine side (a function of the building geometry) is not reflected in classical wind turbine efficiency calculations as this is not applicable for a standalone wind turbine (as defined in IEC 61400-12-1, IEC/TS 61400-13 [2])
c) WindRail uses qualified PV panels according to IEC 61215

Consequently, Anerdgy proposes the following definition for WindRail efficiency:

1. Solar energy output = not part of this report
2. Wind energy output = Anerdgy wind measurement reference point

CFD analyses show that the 4 m point exhibits almost the same influence on the wind stream as the 6 m point. Therefore the 4 m reference point is chosen, because the installation is easier and it shows less pole swing. This means that the new Anerdgy definition is the horizontal wind speed 4 m above the building and 1 m inside from the façade corner. The given wind and energy figures, if not indicated otherwise, - always refer to the 4 m point. The Aventa AV7 turbine is installed 18 m above the building roof level (Figure 10).

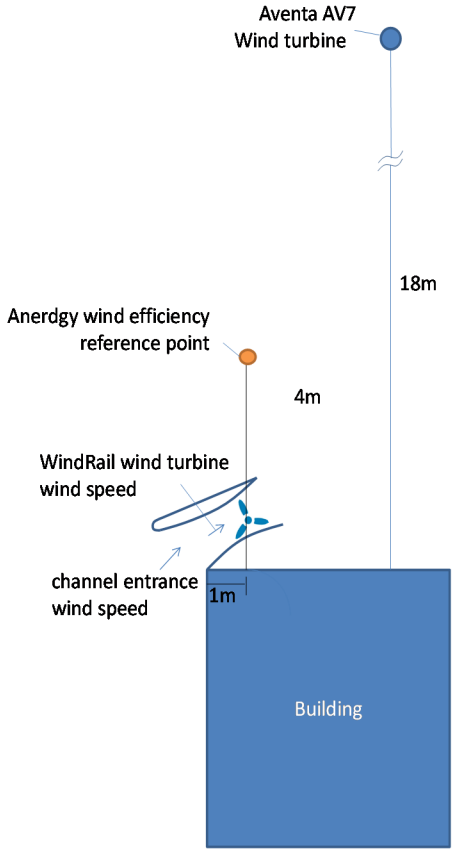

Figure 10: Efficiency reference point definition

3.6 Summary

The test location of Landi Marthalen and its wind conditions are not perfectly suited to the goals of this report but are reasonably sufficient. The prototype C30 C-Muster functions fully under wind, pressure, and solar radiation. Therefore it can produce the required dataset accordingly.

The proposed wind reference point is not yet fully validated nor defined by a standard. However, it performs adequately in the WindRail system, and it is comparable to the Aventa AV7 wind turbine.

A viable energy measurement was achieved by calculating a variable error coefficient. This enabled the computation of the produced energy output of the measured pulsed current (Appendix A).

4 System description

4.1 WindRail concept

The WindRail consists mainly of the base frame, the wind channel, the generators, the PV cells and the control cabinets (Figure 11). The rotor position is located towards the end of the wind channel. Two industrial crystalline PV panels are installed at the back and two above the wind channel.

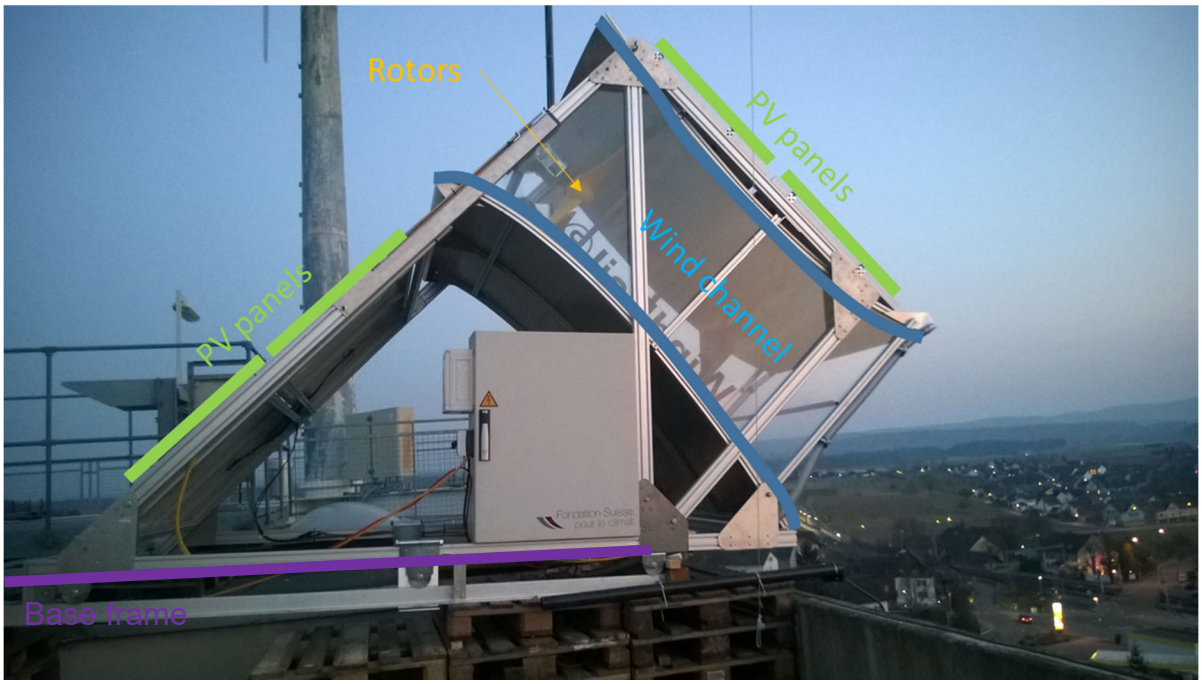

Figure 11: Main part of the WindRail system

4.2 Rotor & Generator

The WindRail rotors and generators were developed by Anerdgy AG. The rotor is double-bladed with 0.95 m diameter and a 120 mm fixed hub. No pitching is foreseen and the rotor has a direct connection to the generator. The 4Q FOC controlled three-phase AC generator provides 0-600 V output range. The generator efficiency is in the range of 0.87-0.95 [3].

4.3 Wind channel

The function of the wind channel is based on the Venturi effect and was designed by Anerdgy with CFD simulations and optimizations. The CFD calibration was performed through real life tests with the Anerdgy A & B prototypes.

4.4 Electronic Drive

On the realized prototype a modified standard drive from Baumüller Nürnberg GmbH is used to control the generators while the relevant software control algorithms are realized on a NI cRio system. Both systems are connected through EtherCAT. Figure 12 shows the drives and the NI cRio in the cabinets.

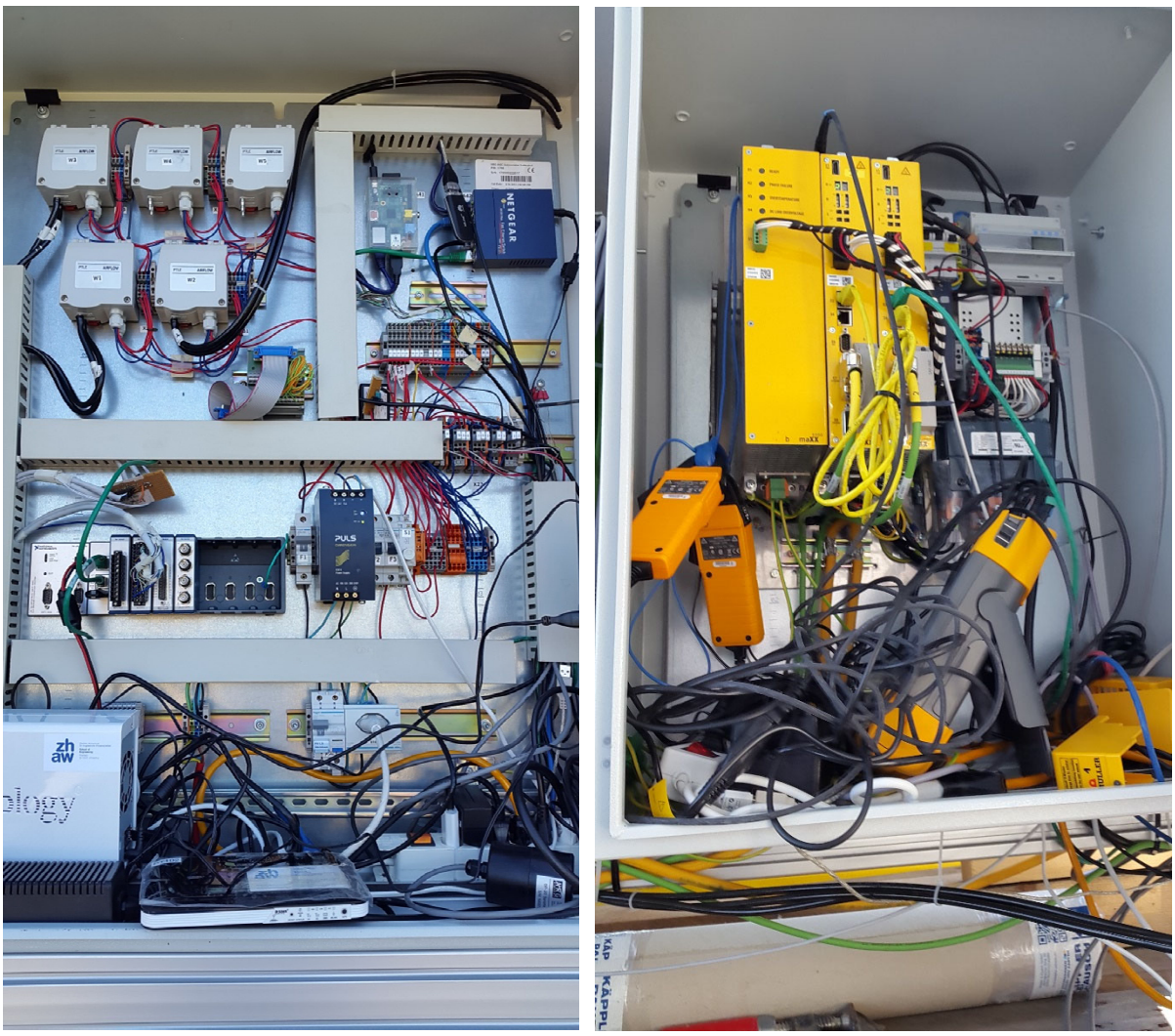

Figure 12: Control and electrical power cabinets

4.5 Software

The generator control algorithms as well as all the security relevant procedures are written in LabVIEW by Anerdgy. The simplified block diagram in Figure 13 shows the principle generator mode and its switching criteria.

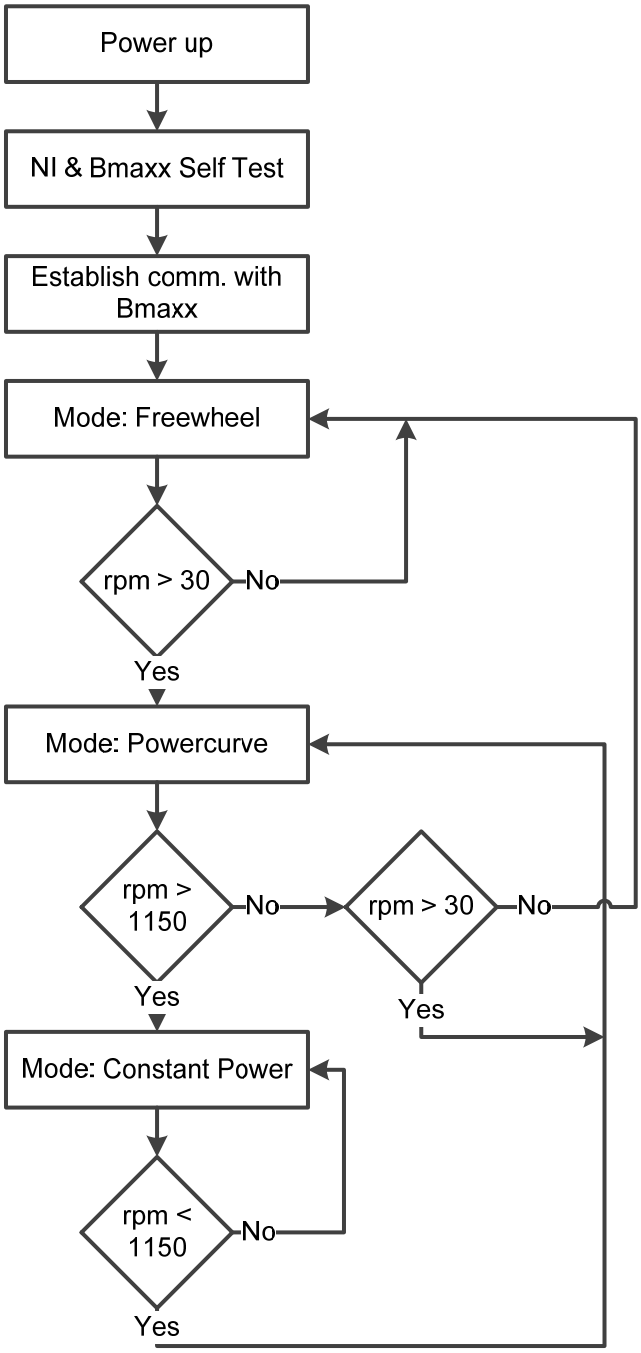

Figure 13: simplified block diagram of the MPPT software

5 Approach and Methods

To test the WindRail system, a new prototype was built based on the knowledge Anerdgy has gained from the earlier Prototypes A and B as well as R&D results since 2012. This prototype was installed on top of the Landi silo tower to evaluate its potential. To generate a scientific and independent statement, Anerdgy and ZHAW measured the energy output separately. The wind data was measured only by Anerdgy and provided to the ZHAW. The Anerdgy approach to check the produced energy is to calculate the produced power out of the torque, current and rpm provided by the drives. With these measured results Anerdgy continuously improved their MPPT routine design and modified the wind channel design.
The prototype unit was installed on the building rooftop. Placement on an existing building allowed the testing off all the functions, e.g. channel airflow over speed, rotor dynamics and processes related not only to wind energy production, but also system integration with existing infrastructure and the installation and maintenance concept. It will be disassembled from the site once further testing has finished.

5.1 Measurement concepts

5.1.1 Meteorological measurements in front and at the building

At the prototype, the temperature and barometric pressure were measured as well as the wind speed and direction from the reference point (see 3.3.1). In addition, a wind vane and an anemometer were placed in a vertical position on the building edge, in front of the prototype, in order to measure updraft speeds as well as direction. This data is all read and logged by the NI cRio system to enable analysis of power against wind speed and direction.

5.1.2 Wind and pressure measurements within the WindRail turbine

The Pitot Tubes used were 2000 mm Kimo FT-Debimo and were mounted horizontally in two places, one at the middle of the entrance to the WindRail channel and one directly in front of the rotor. These were connected to Halstrup Wacher Differential Pressure Transducers Model PS27. Figure 14 shows the technical scheme of the Pitot Tube.

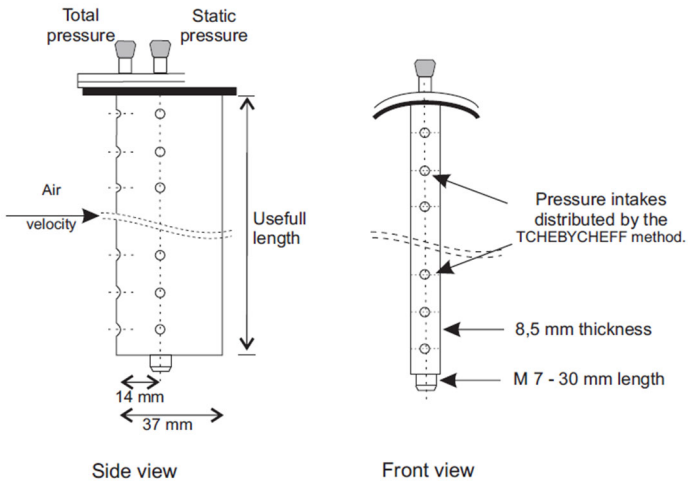

Figure 14: Pitot Tube technical drawing

The transducer voltage was measured through the NI Analog Input Card AI9205 and converted to wind speed, using the actual barometric pressure and temperature (Figure 15).

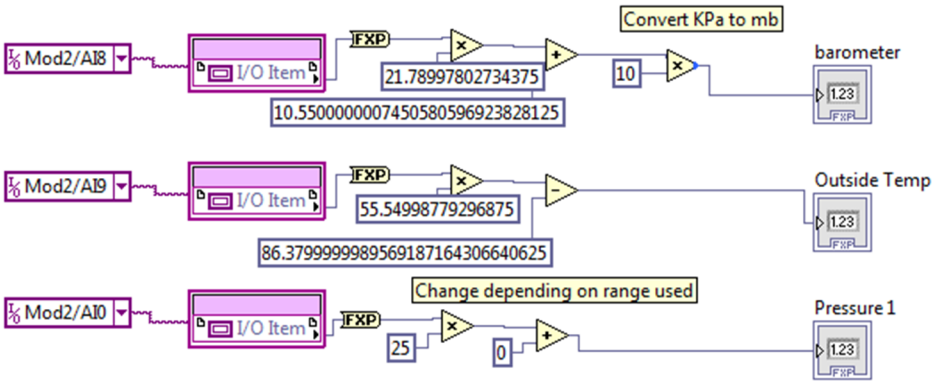

Figure 15: LabVIEW wind speed, barometric pressure and temperature calculation

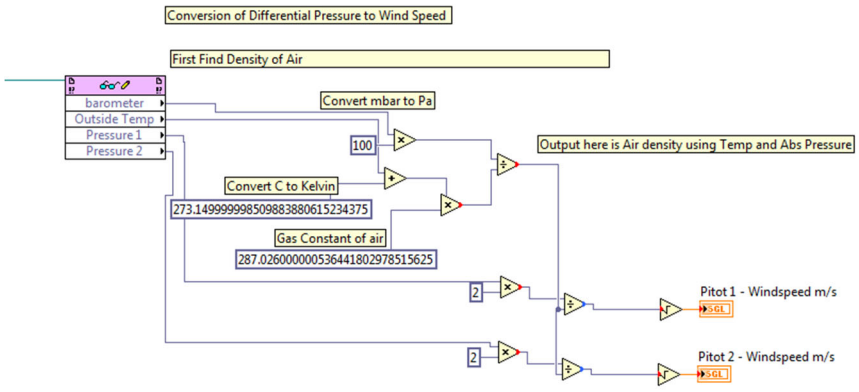

Figure 16: LabVIEW Pitot Tube wind speed calculation

The actual velocity is calculated using

$$V = \sqrt{\frac{(2 \cdot \Delta P)}{density}} \tag{5.1}$$

where ΔP is the differential pressure indicating from the manometer in Pascals in kg/m^3.

$$density = \frac{P_{abs}}{R \cdot (Temp + 273.15)} \tag{5.2}$$

Temp is the temperature of the flow in Celsius.
R is the gas constant $R = 287.026 \frac{joule}{kg \cdot Kelvin}$ for air, and
P_{abs} is the static pressure measured with the absolute pressure manometer in Pascals.
The according LabVIEW code is shown in Figure 16.
The position of the Pitot Tubes appears in Figure 17. A third pressure transducer was used to test the pressure difference between the front and back of the WindRail sys-

tem. The positive inlet was placed to measure the static pressure in front of the WindRail system and the negative inlet was placed to measure the static pressure behind it (not in the exhaust airflow of the channel).

Figure 17: pitot pipe positioning

5.1.3 Power output measurement for wind turbine and solar panels

The electrical energy in the AV-7 turbine was measured by the grid connection, whereas, in the WindRail, the energy was measured on the DC Bus. The measurement setup and the hardware used by the ZHAW are described in detail in Appendix A. The solar energy production is not measured because the solar potential is already well-reviewed, and accurate models are readily available. See Appendix B for further details and production figures.

5.1.4 Ease of installation

The measured values are the installation time and required equipment. The installation includes the following steps:

- Base frame connection to the roof top
- Module lifting and positioning
- Electrical connection
- Commissioning

Figure 18 shows the prototype hanging from the crane during installation.

Figure 18*: *The WindRail prototype on the crane

5.2 Environmental, Health and Safety standards (EHS)

The EHS standards were held through the following procedures and approaches:

- Environmental protection
    - Fire resistance
    - No air and water pollution
    - No bird and bat issues
- Health
    - Very low noise level
    - No shadowing
- Safety
    - Storm procedure and safety position
    - Remote access, control and shut down possibility
    - Secure connection to the roof top
    - Lightning protection

6 Results

The primary goal of this project was to investigate the principal concept. The set objectives were achieved as follows.

6.1 Building based wind and solar electrical energy generation

6.1.1 Wind turbine efficiency and control by output-power comparison

The first evaluation shows that the approach to build a ducted wind turbine, which is comparable to a HAWT low wind turbine, is successful. The WindRail produces more than 1.49 the energy per square meter (Appendix A). This leads to the conclusion that the pressure differences and the shape of the wind channel have a positive influence on the energy production. Furthermore the modifications on both the wind channel and MPPT routine increase the energy production. In addition, the generator produces the 2 kW power peak. For the ZHAW it is impossible to match the wind data with the energy data. This is because acquisition of wind and energy data does not occur simultaneously. Therefore, it is impossible to generate a wind-electrical power chart. Because the evaluated system is restricted by the angle the wind is blowing, it is not possible to evaluate the final energy power potential with the three wind cases in Appendix A.
The power curve of the system was calculated by Mr. Michael Webner from Ventego AG as shown in Figure 19. The reference document is [4].

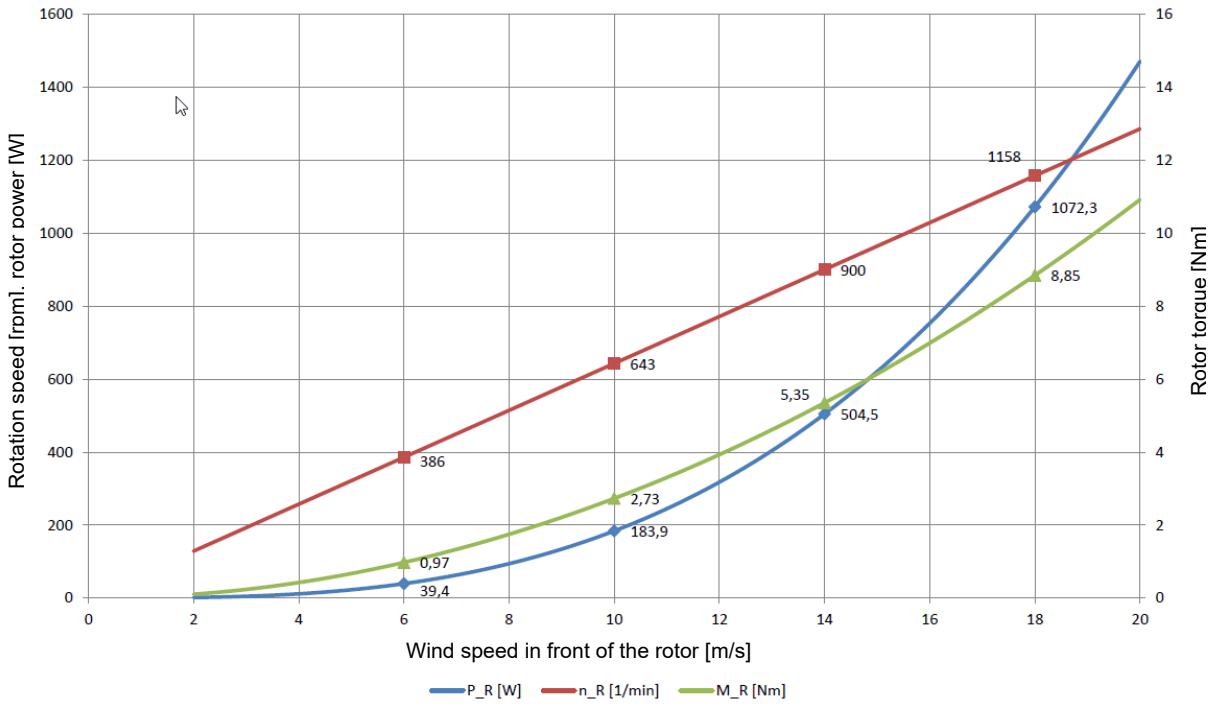

Figure 19: C30 rotor calculation at the optimal working point

The system was then run using this power curve and the mechanical power produced was in direct correlation to the expected power. The mechanical power is also shown in the ZHAW data in Appendix A.

6.1.2 PV combination functionality

The use of the PV panels ensures increased energy production per square meter of footprint including days when the wind is low. The system is independent from the underlying channel, only using the frame for mounting. In the final production system however, the PV panels will be combined into a single power control system and onto a single combined DC bus. This improves the system's overall efficiency by utilizing higher efficiency inverters as well as simplifying wiring on the roof area. This combination also simplifies the reducing of power output if required by the grid operator.

6.1.3 Summary energy production

The energy output from the system from 10.03.2015 to 30.08.2015 was 385 kWh in PV. This data is obtained directly from the Tigo optimizer website (Appendix B).

The WindRail single module utilizes a ±30° wind direction as demonstrated in green in Figure 20. The light yellow area from ±50° is the extended range of input with reduced efficiency due to the side walls at the WindRail (see also appendix C). Within the optimal input angle from 225° to 275°, 52 % of the wind power during May - July was detected. It represents E_{pot} of 32.7 kWh (see figure 21) in wind kinetic energy per square meter. Formula 6.1 shows how the kinetic wind energy was calculated.

$$E_{kin} = \sum_{n=0}^{n} \frac{Rho}{2} {v_n}^3 \tag{6.1}$$

The WindRail single module has converted 11.7 kWh (calculation based on the full 1 s data set recording with the formula 6.3) of electrical energy out of this with its 1.4 square meter inlet area A_{inlet}. The WindRail efficiency is calculated as

$$\eta_{WR} = \frac{E_{kin}}{E_{pot} \cdot A_{inlet}} = \frac{11.7\text{kWh}}{32.7 \frac{\text{kWh}}{\text{m}^2} * \ 1.4\text{m}^2} = \ 25.5\ \% \tag{6.2}$$

This leads to an overall efficiency of 25.5 % relative to the reference point. The given target of the project of 36 % has therefore not been reached over the full time period.

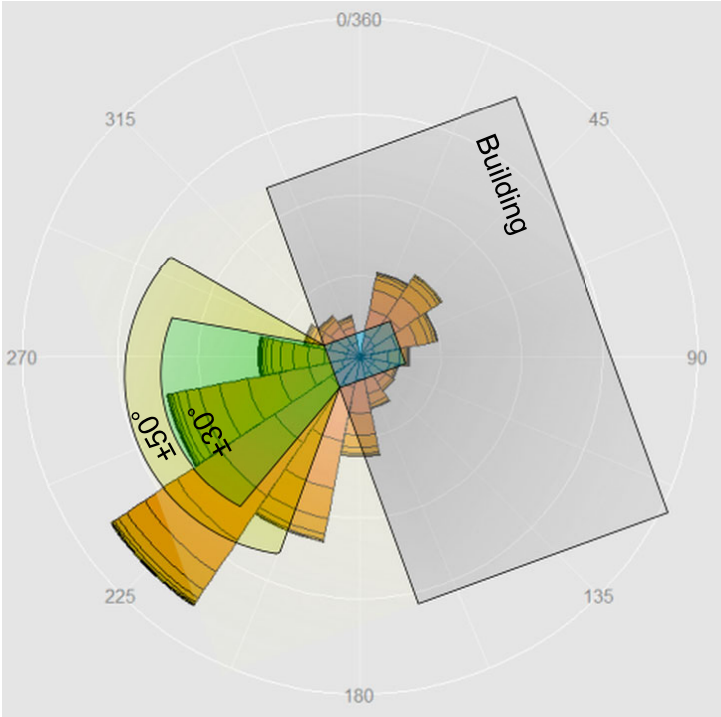

Figure 20: Wind input angle

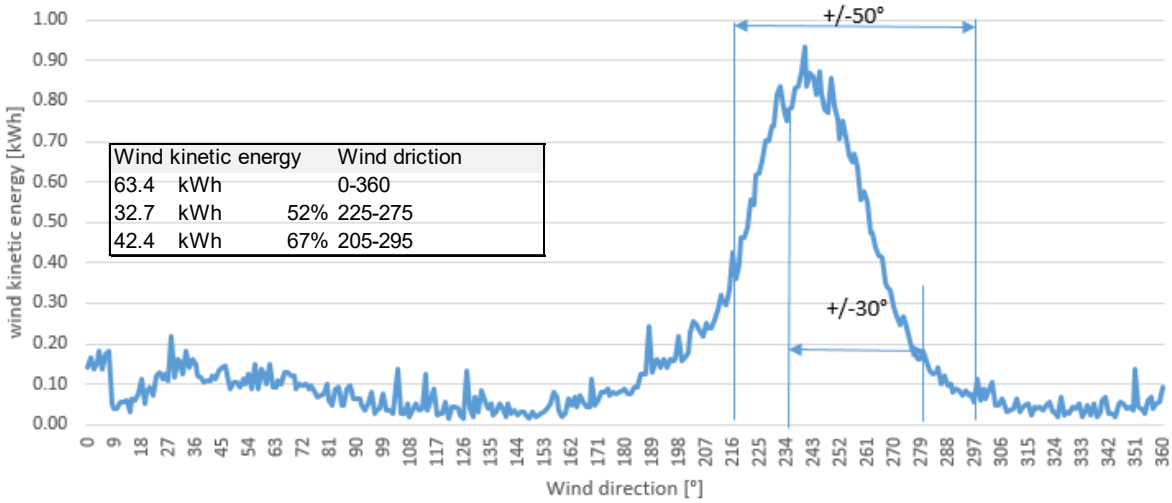

Figure 21: Wind kinetic energy versus wind direction – 01.05.2015 – 31.07.2015

The wind kinetic energy (Figure 21) was calculated with formula 6.1. For the period from 01.05.2015 – 31.07.2015 63.4 kWh per square meter wind kinetic was detected. The WindRail electrical output was calculated as

$$E_{el} = \sum_{n=0}^{n} A_n I_n \qquad (6.3)$$

Due to the control system update, beginning in July 2015 and the channel improvement by the end of July 2015 resulted in an efficiency η_{WR} of 38.9 % after 27.07.2015. This is calculated from the wind energy potential per square meter, in the ±30° range, of 11.6kWh. See formula 6.4 .. Therefore the WindRail TRS7 prototype has achieved the 36 %-target.

$$\eta_{WR} = \frac{E_{kin}}{E_{pot} \cdot A_{inlet}} = \frac{6.3\text{kWh}}{11.6\,\frac{\text{kWh}}{\text{m}^2} * \ 1.4\text{m}^2} = \ 38.9\ \% \qquad (6.4)$$

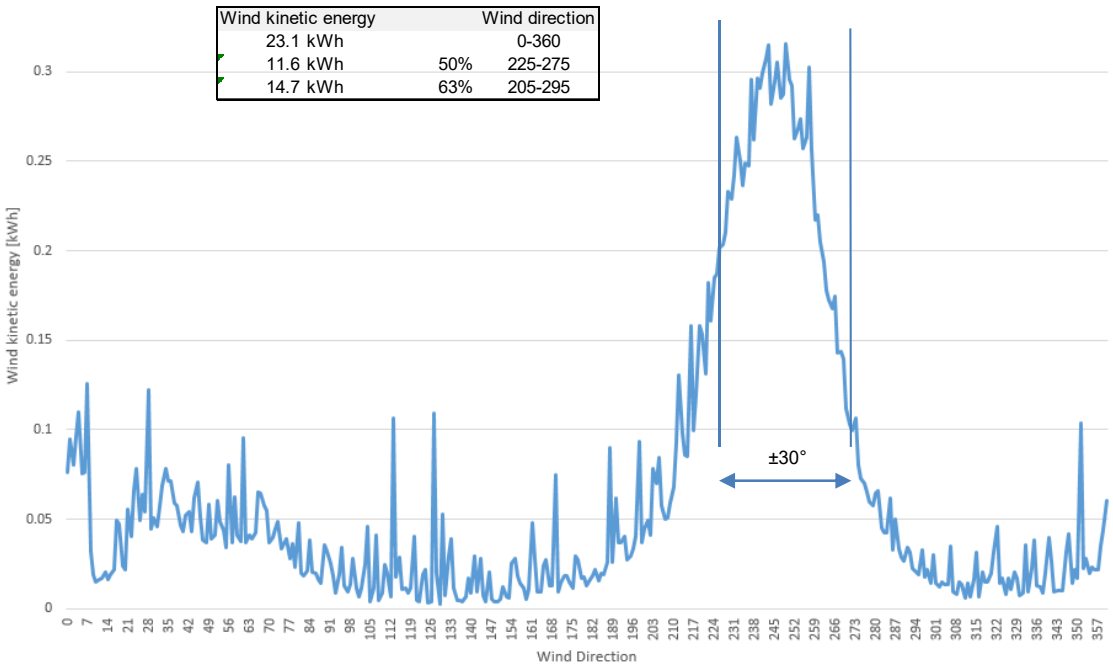

Figure 22: Wind kinetic energy 27thJul-24Aug

To extrapolate the wind speed data from May-July to a full year, the results were compared with the SMA wind data from Zürich Kloten [5]. For the measured summer season period, the average wind speed [m/s] at the reference point in Marthalen is 0.2 m/s lower than at Zürich Kloten.

Wind Data ZH/Kloten vs. Marthalen reference point

	Jan	Feb	Mrz	Apr	Mai	Jun	Jul	Aug	Sep	Okt	Nov	Dez	Average
langjähriges Mittel 1987—2006	2.5	2.5	2.6	2.4	2.3	2.1	2.1	1.8	2	2	2.1	2.5	2.2
1999	2.6	3	2.5	2.4	2	2	2.3	1.7	1.8	1.9	1.9	3.2	2.3
2000	2.5	2.8	2.7	2.2	2.1	2	2.2	1.5	1.8	1.7	2	1.9	2.1
2001	1.9	2.6	2.7	2.4	2.5	2.1	2.1	1.7	2	1.5	2.5	3.4	2.3
2002	2.1	3.8	2.7	2.7	1.9	2	2.2	1.8	2	2.3	2	2.4	2.3
2003	2.9	2.2	2.3	2.7	2.1	2	1.9	1.7	1.9	2.4	1.6	2.2	2.2
2004	2.9	2.6	2.3	2.7	2.3	2	2	1.9	2.1	1.8	2.1	2.2	2.2
2005	2.6	2.6	2.1	2.2	2.1	2	2	2	1.8	1.3	1.9	2.2	2.1
2006	2	2.4	3.4	2.1	2.3	2	2.1	2.1	1.7	1.8	1.9	2.2	2.2
2007	3.5	2.6	2.3	2	2.7	2.2	2.3	1.8	1.8	2.1	2.5	2.7	2.4
2008	2.2	2.2	3.5	2.4	2.5	1.9	2	1.8	2.2	1.9	1.9	2.3	2.2
2009	1.9	2	2.9	2.2	2.1	2.3	2.1	1.7	2.1	2	2.2	2.6	2.2
2010	2.2	2.6	3.1	2.7	2.6	2.4	1.9	2	1.8	2.2	2.4	2.2	2.3
2011	2.5	1.9	2.7	2.1	2.2	2.3	2.2	1.9	1.8	2	1.6	3.4	2.2
2012	3.3	2.8	2.1	2.9	2.4	2.1	2.2	1.9	2	2	1.9	2.9	2.4
2013	2.2	2.8	2.4	2.6	2.6	2.3	2.4	2	2.2	2	2.8	2	2.4
2014	2	2.3	2.1	2.2	2.8	2.6	2.2	2	1.9	2	1.9	2.6	2.2
2015	2.9	2.6	3.1	2.9	2.2	2.4	2.6	-	-	-	-	-	2

Average per season 1987-2006	2.5	2.2	1.9	2.4	
Average per season 2015		2.4			
Marthalen Landi		2.1	1.8	2.7	
Average Landi May-Jul		2.2			

Figure 23: Average wind speed in m/s

The seasonal wind speed estimation in Figure 23: Average wind speed [m/s] is used as a basis for the prototype yearly output calculation.
A single module, compared to a multiple module solution, has several restrictions due to:

- a smaller input angle point
- no significant pressure difference increase between roof top and façade
- only one direction

This results in a lower energy transformation level from a global wind potential view. Figure 24 shows the wind turbine electricity output estimation and prototype result. It indicates that the Anerdgy calculation against the estimated yearly output power based on the three months measurement period are within the same range. The channel and software improvements indicate a good improvement potential for the single module.

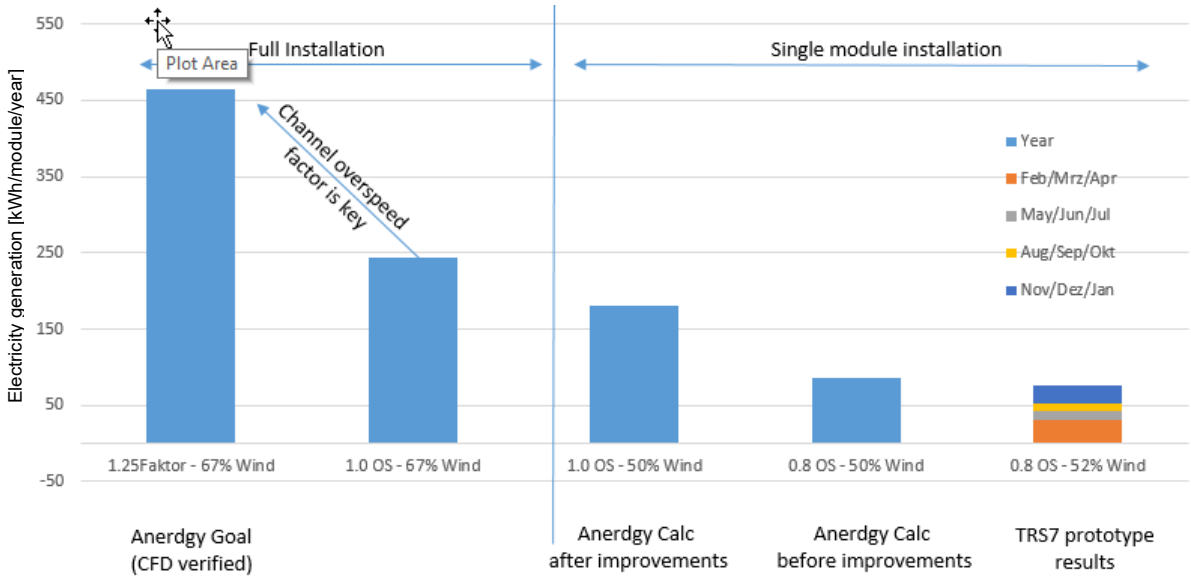

Figure 24: WindRail wind turbine electricity output estimation and prototype result

To improve the WindRail electricity output further the following steps are required: Step one: In order to increase the WindRail output, first a multi module installation must be employed on one side of the building. This increases the wind direction which can be used from ±30° to ±50°. This results in a 67 % wind power usage at Marthalen, rather than 52 % as of today (Figure 24).
Step two is to increase the over speed factor from the WindRail channel, as it is a major driver for a higher output. Anerdgy designed and verified, through CFD analysis, a new channel design based on the results and updates of the current prototype. Figure 25 shows the CFD analysis through one module. The new channel design in combination with a multi-module installation can realize a wind over speed factor of 1.25 compared to 1.0. The Wind-Rail channel over speed design is part of the Anerdgy IP and therefore not part of this publication.

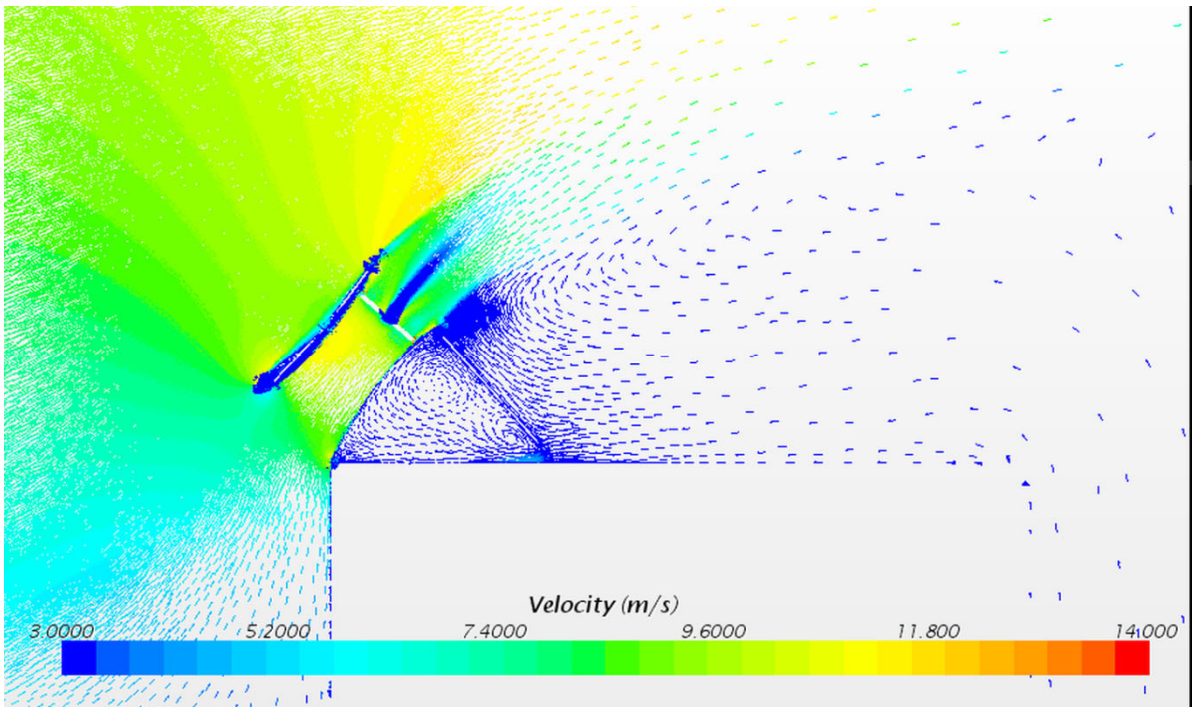

Figure 25: Wind flow through WindRail on one side in a multi module installation with turning rotors

6.2 Installation & Maintenance concept

The installation concept works well with a three hour installation time. Anerdgy performed some wind channel improvements during the testing period. As a result, all the maintenance main concept elements, e.g. removal and replacing of the rotor from the wind channel, PV pull back, module rear position (Figure 26) was tested.

Figure 26: Rotor maintenance functionality and WindRail maintenance position

Despite the positive results Anerdgy decided to further improve the installation concept towards a more simplified installation in order to minimize the usage of the crane as this is a major cost factor.

6.3 Function of the roof mounting and sliding system

The roof mounting and sliding system was installed in February 2015 and functioned without failure until the end of the test period in August 2015 (Figure 27). The WindRail module has the ability to roll backwards, through high wind force to an inner roof position. This reduces the wind forces to the module, the base frame, and to the building. Nevertheless the “Typenstatik”-a certificate in Germany which permits the use of a standardized method without static recalculation–indicates that an alterna-

tive safety system design is needed. This is currently under review and will be used in the next WindRail installations.

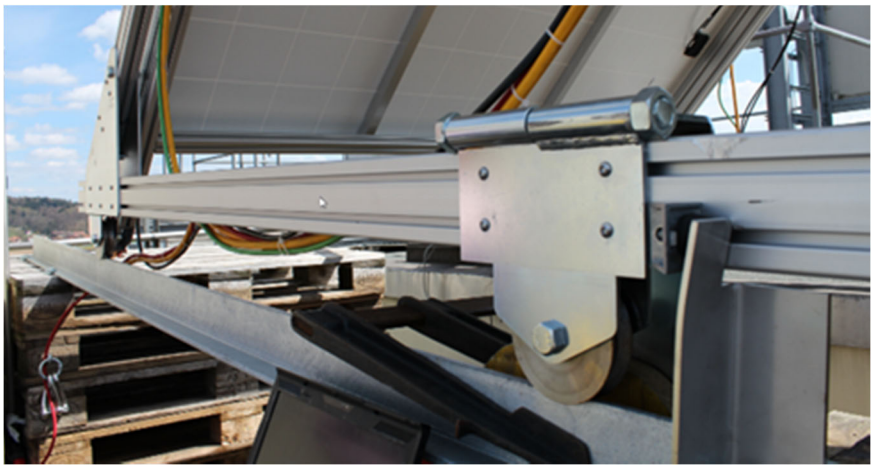

Figure 27: Rotor maintenance functionality and WindRail maintenance position

6.3.1 Electrical building grid connection

The grid connection was not realized for the wind turbine part in order to remove any restrictions from the inverter side, and allow a complete unfiltered power output from the generator and control unit. The WindRail inverters are sourced from third-party inverter manufacturers with all the necessary permanent grid tie/ anti-islanding norms required depending on the country of use. Anerdgy therefore ensures that an appropriate supplier is chosen depending on the country of installation. For PV the grid inverter was installed.

6.3.2 Validation of low noise level & vibrations

The validation of the low noise level is not yet fully completed. Based on the manual measurements and observations the level is very low over the full wind speed range. VibroAkustik Consulting & Technology GmbH is contracted to evaluate a noise certificate which is currently under preparation. Mr. Stan Pietrzko from ETHZ will perform the measurements planned for September 2015. The observed vibration level based on the wind rotor rpm change is compensated within the structure and results in very low levels transferring from the base frame to the building structure. Data measurements are not yet established.

7 Conclusion

More wind energy was produced by the tested WindRail prototype per square meter on 27.07.2015-28.07.2015, than by the AV-7 wind turbine. Hardware and software modifications, during the measurement period, increased the comparison coefficient from 0.73 to 1.49. Because of the varying measurement conditions and the limited measurement time it is not possible to calculate the yearly energy production effectively, particularly since within the period – 01.03.2015 - 31.07.2015 – the wind speed is lower than the average. The present estimation (chapter 6.1.3) indicates that the prototype performance is within the desired range and that a full WindRail installation should be tested and validated to qualify its full potential.

8 Discussion and Findings

The present measurements provide a valuable input on the energy potential of the new wind turbine. It allows estimation of the energy production in the measurement periods and shows that the basic principle works. The measurement results could directly be used to enhance the system and enabled a systematic optimization. Because of the variable measurement conditions and modifications of the system different results were achieved. These differences are technically explainable and reproducible.

9 Outlook

To provide a holistic evaluation of the WindRail system, a larger wind plant should be installed in the next project, ideally over an entire rooftop. This would lead to conclusions that are more accurate on how the modules work together. Furthermore, the wind-angle dependency should be reduced, and the real efficiency of the system including the standby losses, should be determined. Finally, to estimate the cost-effectiveness of the system, it is necessary to measure the exact amount of energy, which is produced and then fed back into the grid.

10 References

[1] Bundesamt für Energie BFE: BFE-Leuchtturmprogramm: Programmbeitrag zur Energiestrategie 2050 Konzept, 15.03.2013

[2] IEC 61400-12-1 2007;

[3] 150405_Auslegung_C30-Generator; Smartdrives GmbH; 05.04.2015

[4] 20140822_Aerodynamische Auslegungsrechnung Mantelturbine_c; Ventego AG; 22.08.2014

[5] Monatswerte der Windgeschwindigkeiten Station Zürich Kloten: http://wind-data.ch/messdaten/monate.php?wmo=66700: 25.08.2015

[6] Leistungskurve der Leichtwindanlage AV-7: http://www.aventa.ch/leistungskurve-av7.html: 30.09.2013

[7] LMG670 Precision Power Analyzer: Power Analysis2 Two Bandwidths Simultaneously: en 05/2014

[8] CFD report CFS; 30.04.2015

[9] Photovoltaic Geographical Information System: http://re.jrc.ec.europa.eu/pvgis/apps4/pvest.php: 25.08.2015

[10] The Weibull Distribution: A Handbook: 1st Edition: ISBN-10: 1420087436: 20.08.2015

[11] Windkraftanlagen; Grundlagen, Technik, Einsatz, Wirtschaftlichkeit: 5., neu bearbeitete Auflage: ISBN 978-3-642-28876-0: 2014

[12] Grant, A., Johnstone, C. & Kelly, N. Urban wind energy conversion: The potential of ducted turbines. Renewable Energy 33, 1157–1163 (2008).

A Appendix: Electrical Energy-Production Measurement (ZHAW)

A 1 Introduction

This chapter describes the measurement goal, WindRail and the AV-7 turbine. It also shows the original measurement concept.

A 1.1 The measurement goal

The goal of the measurement is to evaluate the WindRail and its wind-power production efficiency. Therefore the energy produced by both wind turbines, the WindRail turbine and the AV-7 turbine is continuously measured. The efficiency per module is determined using the measured data. The focus is on the wind production and, thus, the produced solar power is not measured. In addition the solar potential is already well reviewed, and its accurate models are readily available.

A 1.2 The wind turbines

This chapter describes the WindRail by Anerdgy and the AV7 turbine by Aventa. The Figure A 1-1 shows the two turbines on the silo.

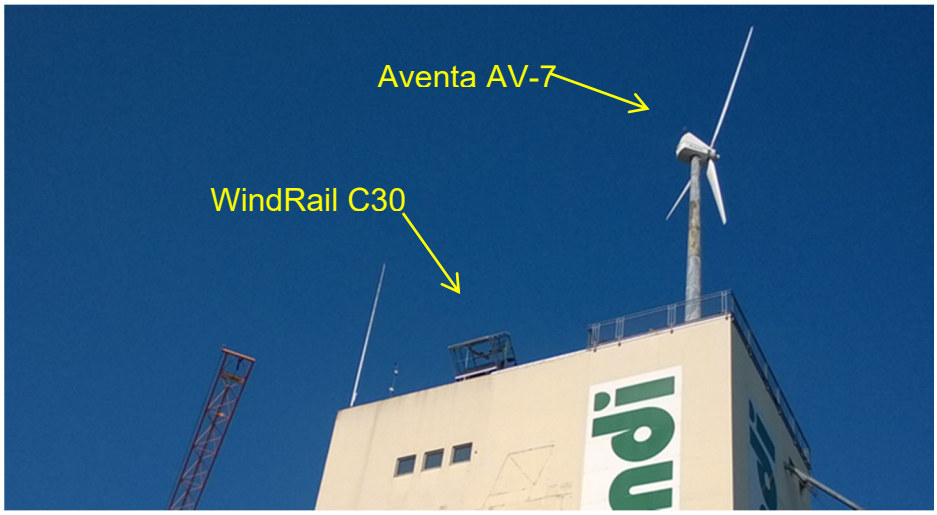

Figure A 1-1: The WindRail and the AV-7 turbine on the tower

A 1.3 The WindRail

The WindRail by Anerdgy is a 3-in-1 building-based renewable electricity generation system. It is a scalable modular system, which is installed on the edge of flat roof. It takes advantage of the building layout to harness wind, pressure difference, and solar energy sources readily available in the natural building environment, day and night, throughout the seasons. Figure A 1-2 shows one WindRail system (they are normally placed in a row) with the wind flow and solar radiation. The system is suitable for both new and existing buildings of various types industrial, residential, and commercial.

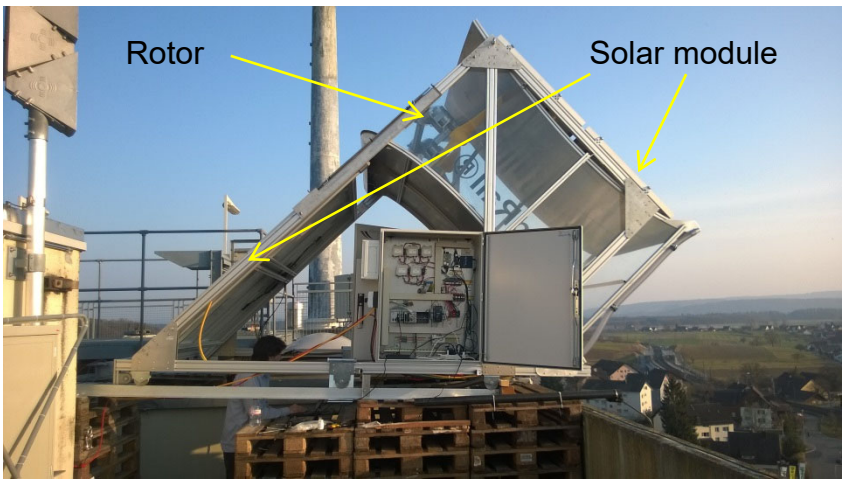

Figure A 1-2: WindRail by Anerdgy

The WindRail, Type C30 has a surface-flow area of 1.4 m^2 and its inlet measures 3 m^2. Inside the WindRail, there are two servo generators, which generate a maximum power of 2 kW. The WindRail also has four photovoltaic panels PW290 manufactured by Swisswatt, two on top and two at the rear. Every panel has its own MPPT to ensure peak power production.

A 1.4 The Aventa AV-7 Turbine

The AV-7 turbine by Aventa Ltd. is a classical horizontal-axis wind turbine (HAWT), especially designed for low wind speeds. Ideal sites for wind energy exploitation are those with average annual wind speeds 3.0-4.5 m/s. The rotor is mounted on top of an 18 m high hub. It has three blades with a rotor area of 129 m^2. The permanently excited synchronous generator produces maximum 6.5 kW. Figure A 1-3 shows the power curve of the AV-7.

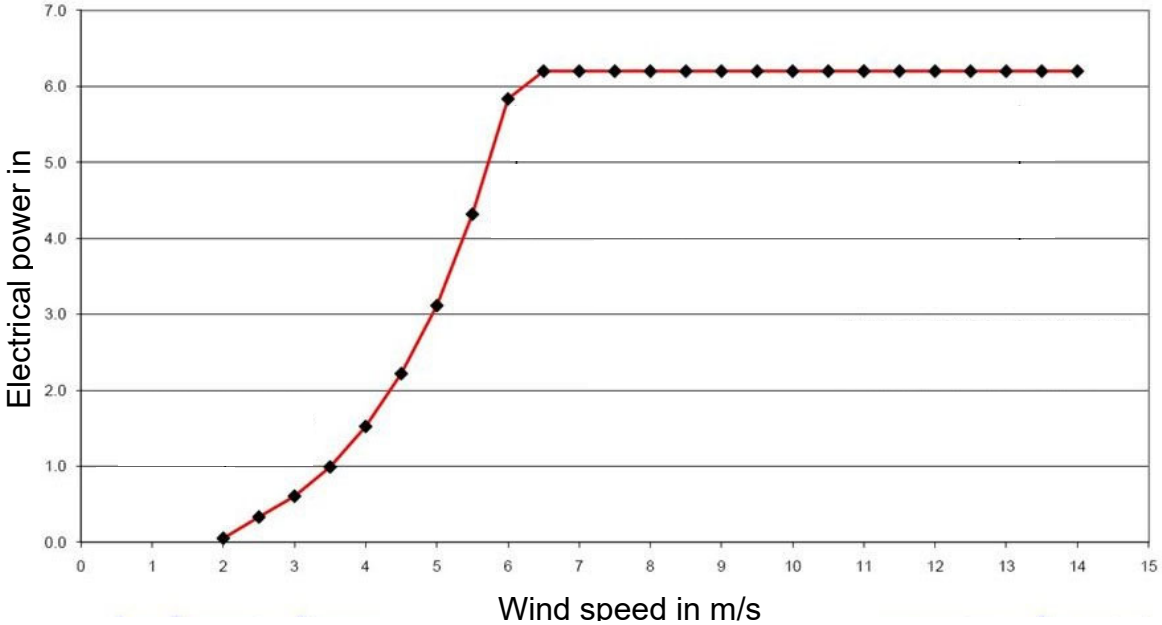

Figure A 1-3: Power curve of the AV-7 turbine [6]

A 1.5 Differences between the turbines

Table A 1-1 compares the turbine's features.

Table A 1-1: Differences between the turbines

	WindRail C30	**AV-7**
Turbine Type	**HAWT**	**HAWT**
Position	**Attached to roof top**	**18 m mast**
Direction following	**Fixed ±35°**	**360 °**
Pressure usage	**Yes – via Venturi channel**	**No**
Rotor blade per unit	**C30: 2 Rotors with 2 blades**	**3 Blades**
Blade pitching	**No**	**Yes**
Security position	**Module lower position**	**Blade pitch**
Surface flow area	**C30: 1.4 m^2**	**129 m^2**
Nominal generator power	**C30: 2 kW**	**7 kW**
Generator type	**Permanent Magnet Synchronous**	**Synchronous**

A 1.6 Original measurement concept

The measurement concept was established in a meeting between Anerdgy, the BFE coach and ZHAW, and it appears in Figure A 1-4. To measure the energy production of the WindRail system and the AV-7 turbine, the ABB A43 energy meter should be used. Because the WindRail produces DC power, which goes to a braking resistor without being transformed into AC power, the ABB A43 meter cannot be used. Furthermore as the current and voltage forms created by the breaking resistor are pulsed DC including high ripple content, it's only measureable with a sample rate above 2 MS/s and with an accuracy of 16 Bit as a power analyzer would offer [7]. This means also that only the Aventa AV-7 turbine is measured with the ABB A43 meter.

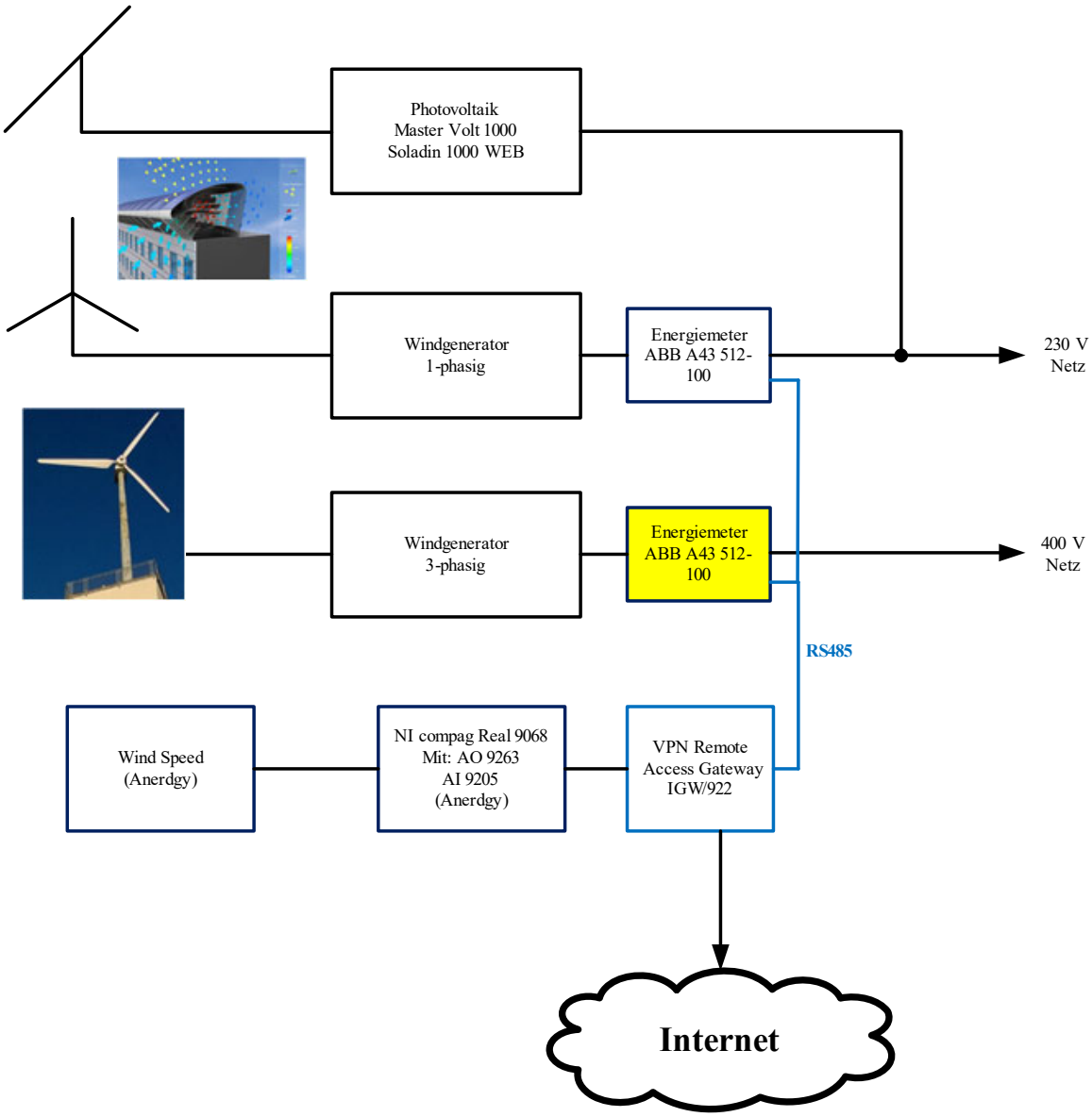

Figure A 1-4: The original measurement concept

A 2 Measurement setup

This chapter describes the location, at which the measurement is setup, the equipment used for the measurement, and the method, by which the measurement systems are connected. Furthermore it provides a detailed overview of the used ZHAW measurement software.

A 2.1 Location

The location to test the device is significant for all further discussions and evaluation. Therefore it was important to find a suitable location within an agreeable distance. The Landi silo tower (referred to as the tower hereinafter), is a good location to test the WindRail systems. The tower is high enough to deliver the desired building facade boost which increases the wind power production, and the tower is easily accessible at all times (Figure A 2-1).

In addition, there is already an Aventa AV-7 turbine install on top of the tower, which can be used to validate the measurements, enabling some benchmarking to a common HAWT turbine.

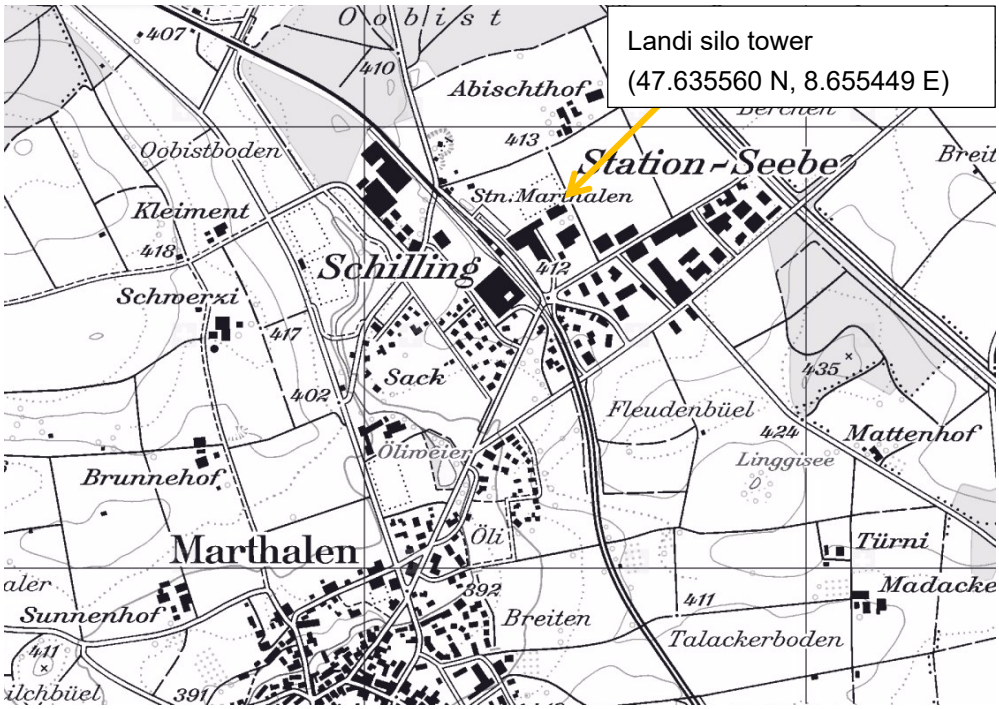

Figure A 2-1: Marthalen and the Landi silo tower

A 2.2 Setup

Figure A 2-2 provides an overview over the tower rooftop and shows the associated equipment. The WindRail system is directed to 237°, therefore the relevant wind direction is 237° - 2° = 235°. Figure A 2-3 shows all the equipment and their connections. In comparison to the AV-7 turbine, the WindRail is shown with its internal structure, because the measurement takes place internally. In addition, the solar part of the WindRail is shown but the solar power production is not measured, because it is already well-reviewed, and available.

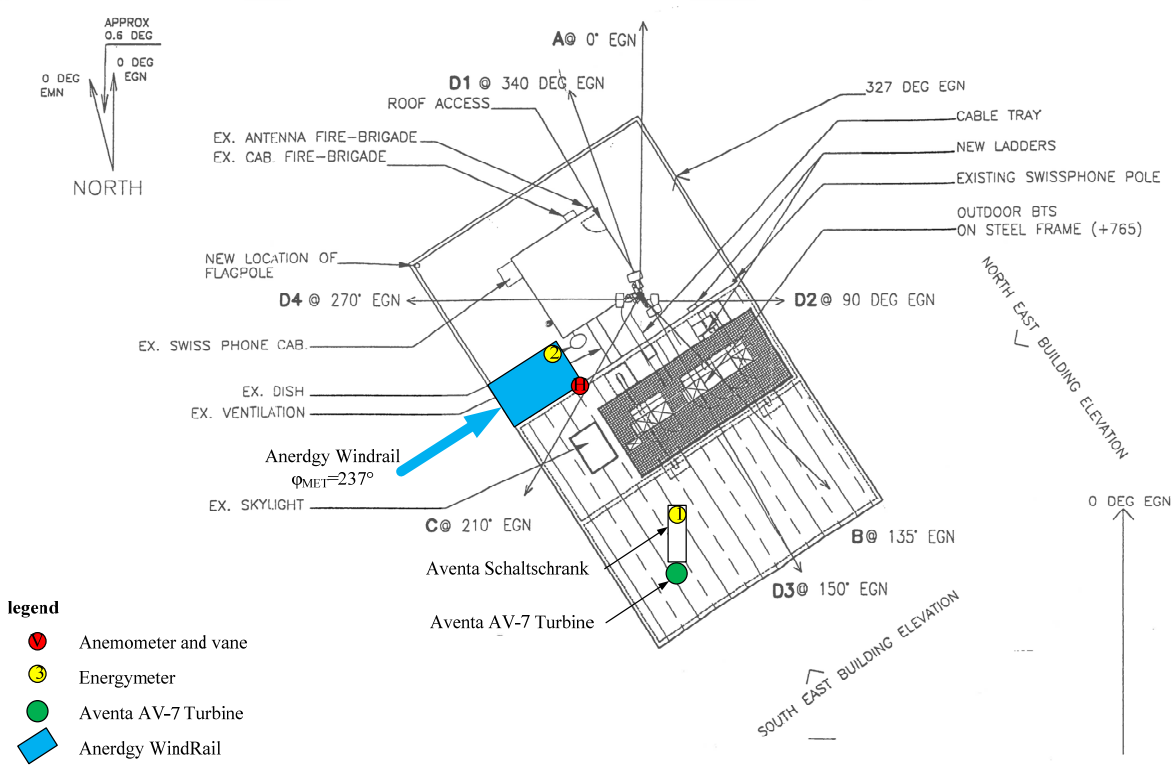

Figure A 2-2: Overview over the tower roof

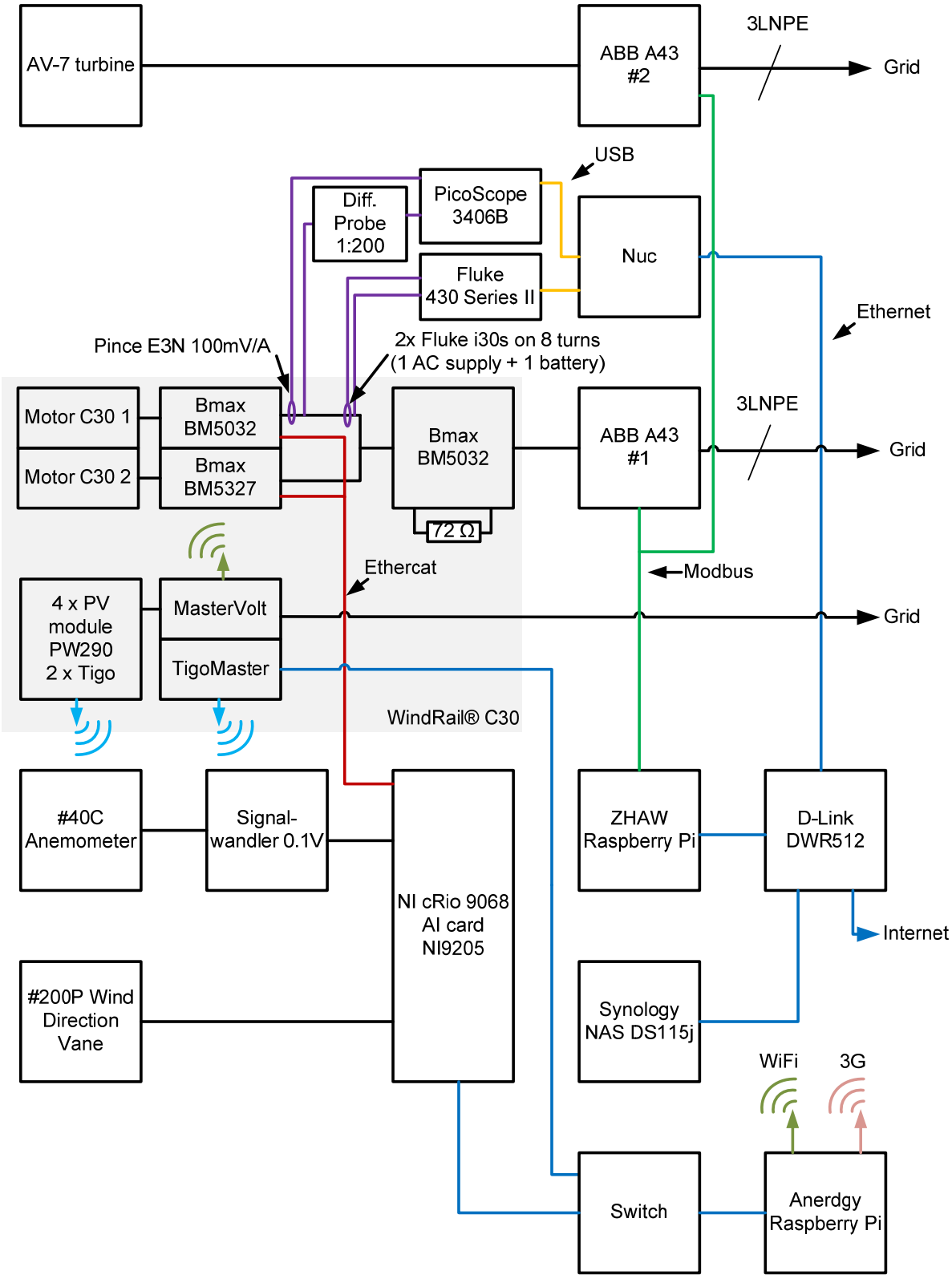

Figure A 2-3: Overall schematic of the setup

The Table A 2-1 lists the equipment used with their manufacturers and serial numbers.

Table A 2-1: Equipment

	Manufacturer	**Type**	**Serial number**
AV-7 Turbine	Aventa	AV-7	S01-01.003
ABB A43 #2	ABB	A43 512 100	

	Manufacturer	Type	Serial number
PicoScope 3406B	Picotech	3406B	CY056/112
Diff. Probe 1:200	Sapphire	SI-9000	
Pince E3N 100mV/A	Chauvin Arnoux	P01120043A	186627 LLV
Fluke 430 Series II	Fluke	Fluke 430-II	25653101
Fluke i30s	Fluke	i30s	
Motor C30 1	SmartDrives GmbH	Motor C30	
Motor C30 2	SmartDrives GmbH	Motor C30	
Bmax BM5032	Baumüller	Bmax BM5032	310047615 00425338
Bmax BM5327	Baumüller	Bmax BM5327	312006842 06500138
Bmax BM5323	Baumüller	Bmax BM5323	3120035467 06500257
ABB A43 #1	ABB	A43 512 100	
Solar modul	Swisswatt	PW290	
Tigo	Tigo	MM-2ES50	8-1011664FW 881-11664FN 8-1010688DG 881-10688DT
TigoMaster	Tigo	MU-ESW ES-GTWY	TG013124566 00158D000014DB 8E
MasterVolt	Mastervolt	Soladin 1000 WEB	D000A0115
#40C Anemometer	NRG Systems	#40C	179500222517
#200P Wind Direction Vane	NRG Systems	#200P	
Signalwandler 0.1V	ZMM Electronics		
NI cRio 9068	National Instru-ments	cRio 9068	18DD4BD
AI card NI 9205	National Instru-ments	NI AI 9205	12E9CA5
ZHAW Raspberry Pi	Raspberry Pi Found.		000000003f15b79f
D-Link DWR512	D-Link	DWR512	
Anerdgy Raspberry Pi	Raspberry Pi Found.		
Synology NAS DS115j	Synology	DS115j	
Switch	D-Link		

A 2.3 Measuring equipment

A 2.3.1 Power Quality and Energy Analyzer

The Fluke 430 Series II (FW V04.02) is a power quality and energy analyzer which also enables logging data over a long period. Thus, it is used to measure and log in the power production by the WindRail system. The power is calculated from the voltage and the current of the DC bus between the drives and the BM5032. Whereas, the used i30s current probe from Fluke has a low sensitivity range it is desirable to the sensitivity of the probe. To measure a small current, the sensitivity of a current probe increases by wrapping multiple turns through the primary (Figures A 2-6 and A 2-7).
The Fluke 430 Series II is calibrated to log in the data every second in the internal SD-card. The data files can be transferred over an USB connection to the connected Nuc with the Power Log – software V 4.3.1. Figure A 2-5 shows the selected values and the log setup. The Table A 2-2 shows the logged data and the assigned case number.

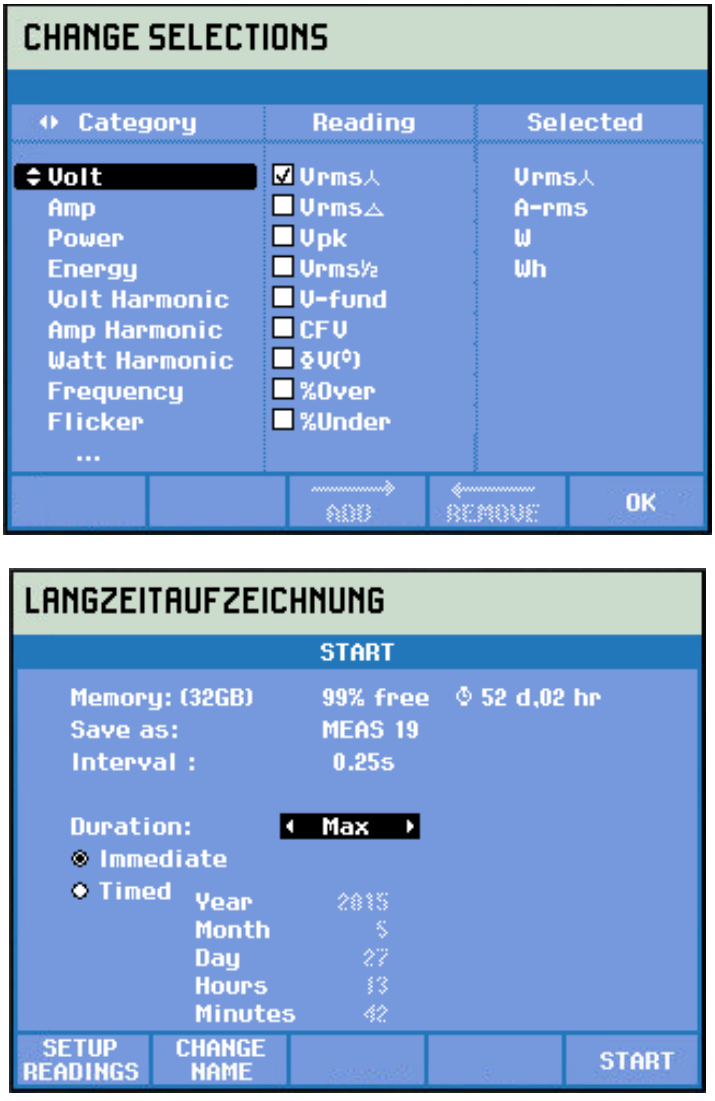

Figure A 2-5: Selected values and log setup

Figure A 2-6: The Fluke energy meter in action

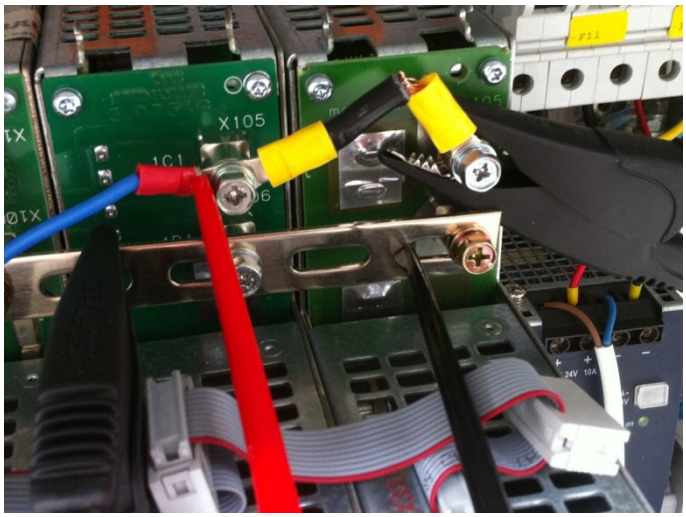

Figure A 2-7: connection to the DC-Bus

Table A 2-2: Logged data overview

Measurement Raw-Data-File	Case	Start	End
MEAS 9 -- SD-Karte.fpq	Case-01	08.05.2015 16:30	08.05.2015 20:15
	Case-02	12.05.2015 13:00	13.05.2015 00:00
MEAS 10 -- SD-Karte.fpq			

MEAS 11 -- FLUKE 430-II (COM3).fpq	Case-03	13.05.2015 15:20	13.05.2015 16:30
MEAS 13 -- FLUKE 430-II (COM3).fpq	Case-04	14.05.2015 04:30	15.05.2015 06:00
	Case-05	16.05.2015 18:28	16.05.2015 19:51
MEAS 15 -- FLUKE 430-II (COM3).fpq			
MEAS 16 -- FLUKE 430-II (COM3).fpq			
MEAS 17 -- FLUKE 430-II (COM3).fpq	Case-06	19.05.2015 09:00	19.05.2015 11:00
MEAS 18 -- FLUKE 430-II (COM3).fpq	-		
MEAS 19 -- FLUKE 430-II (COM3).fpq			
MEAS 20 -- SD-Karte.fqp	Case-12	28.05.2015 07:12	29.05.2015 00:00
MEAS 21 -- SD-Karte-A.fpq	Case-14	29.05.2015 17:45	01.06.2015 23:35
MEAS 21 -- SD-Karte-B.fpq	Case-15	02.06.2015 19:45	02.06.2015 22:15
MEAS 24 -- SD-Karte.fpq			
MEAS 26 -- SD-Karte.fpq			
MEAS 0 -- FLUKE 430-II (COM3)			
MEAS 1 -- FLUKE 430-II (COM3)			
MEAS 2 -- FLUKE 430-II (COM3)	Case-18	12.06.2015 17:23	12.06.2015 19:36
		13.06.2015 04:46	13.06.2015 19:55
		14.06.2015 00:56	14.06.2015 01:40
MEAS 3 -- FLUKE 430-II (COM3)	Case-26	07.07.2015 12:00	09.07.2015 16:30
MEAS 5 -- SD-Karte	Case-30	11.07.2015 09:08	11.07.2015 19:29
	Case-31	12.07.2015 11:20	12.07.2015 18:49
	Case-32	13.07.2015 07:36	13.07.2015 18:44
	Case-33	14.07.2015 06:56	14.07.2015 18:19
	Case-34	19.07.2015 09:43	19.07.2015 19:09
	Case-35	25.07.2015 03:16	25.07.2015 20:29
	Case-36	27.07.2015 06:00	28.07.2015 20:26

used for evaluation

A 2.3.2 Oscilloscope

A picoscope is used to determine the voltage and the current form on the DC-Bus. The results are used to define a conversion coefficient. To measure the voltage, a differential probe from Sapphire Instruments Co. Ltd. with a conversion factor of 1/200 is used (Figure A 2-8). The current is measured with a current clamp from Chanvin Arnoux with a conversion factor of 100 mV/A.

Figure A 2-8: Differential probe configuration and picoscope

A 2.3.3 Energy meter

The A43/A44 is a directly connected meter to measure currents smaller than 80 A. The meter comes with a Modbus interface, which allows reading of the measured data. The meter is therefore connected to an embedded Linux computer with the ZHAW measurement software running. The program records the following data:

- Voltage: L1 to N, L2 to N, L3 to N, L1 to L2, L2 to L3, L3 to L1
- Current: L1, L2, L3, N
- Frequency
- Time
- Apparent Power: L1, L2, L3, N, Total
- Reactive Power: L1, L2, L3, N, Total
- Apparent Energy: Import, Export, Total
- Reactive Energy: Import, Export, Total

A 2.3.4 ZHAW measurement software

The ZHAW measurement software collects the data from the ABB A43 meter and saves it on the internal storage. The software runs on the Raspberry Pi and uses a FTDI USB to a RS485 cable to interface the meters. Every hour a new CSV-file is generated and the old one is pushed to the NAS. Figure A2-9, A2-10, and A2-11 describe the software further.

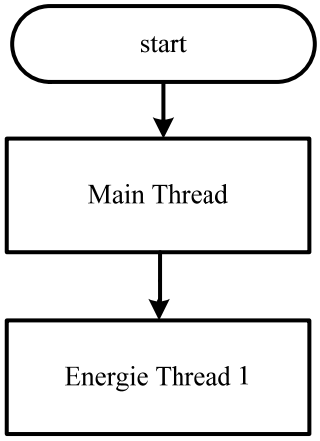

Figure A 2-9: Call graph

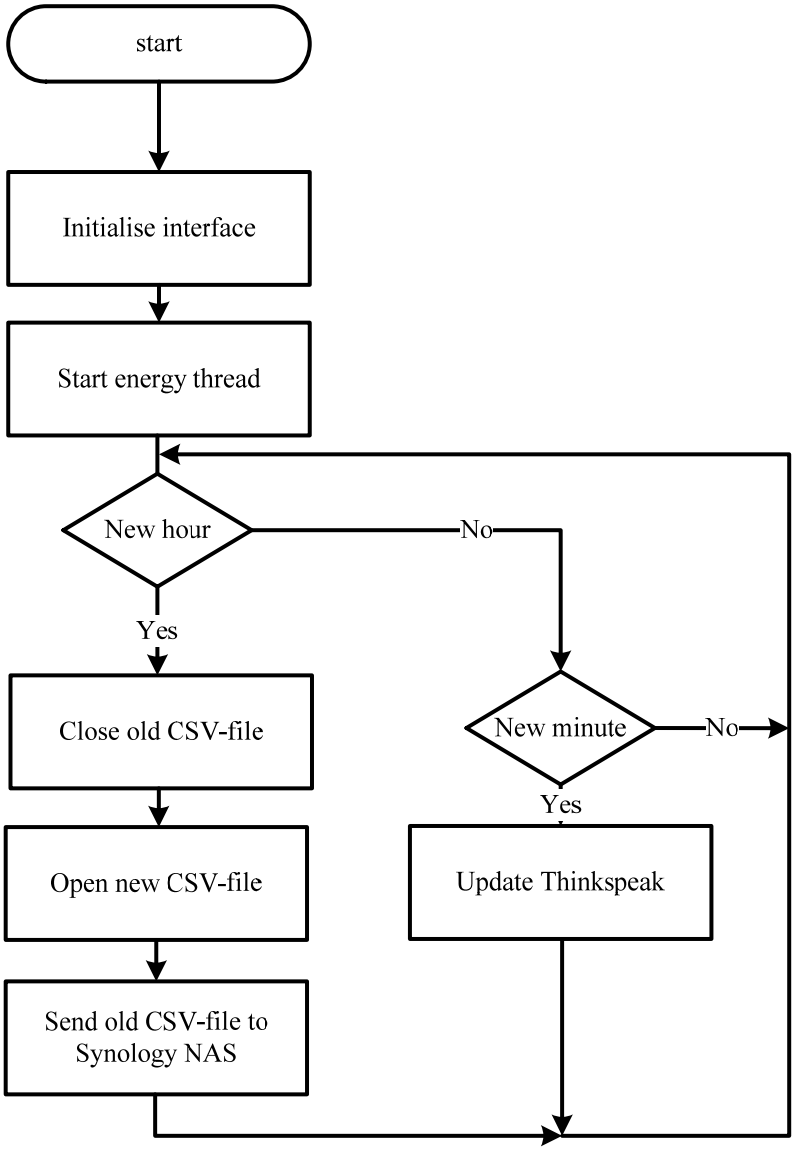

Figure A 2-10: Flow graph of the main thread

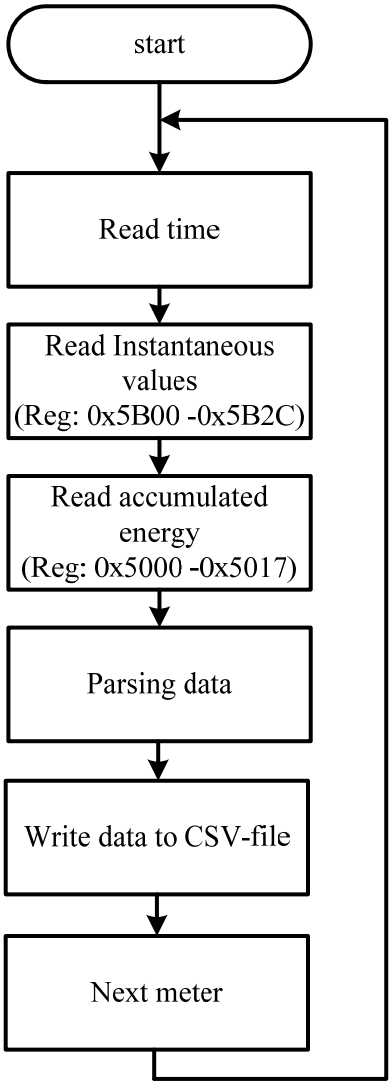

Figure A 2-11: Flow graph of the energy thread

A 2.3.5 Wind sensor

Wind is measured every second and logged in as a CSV-file. The sensors are measured on the NI cRio at the AI card 9205. The conversion of the wind direction is shown in equation 2.1 and the implementation in Figure A 2-12. The anemometer delivers an output signal which is frequency-coded. Therefore, the time between the rising edges is measured and converted into the speed using equation 2.2. The corresponding LabVIEW code is shown in Figure A 2-13.

$$\varphi_{MET} = \frac{U_{vane}}{U_{supply}} \cdot 360° \tag{2.1}$$

$$v_{wind} = \frac{1}{\Delta t_{in}} \cdot 0.744140625 \, \frac{\frac{m}{s}}{Hz} + 0.369140625 \, \frac{m}{s} \tag{2.2}$$

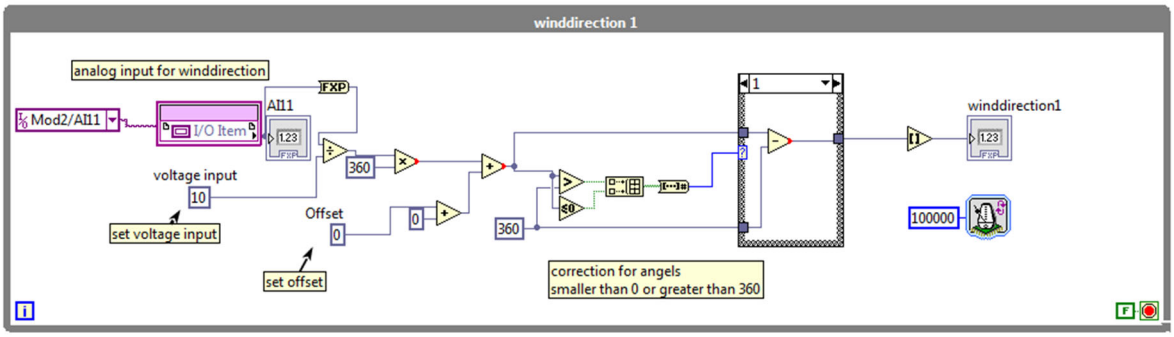

Figure A 2-12: LabVIEW code for wind direction

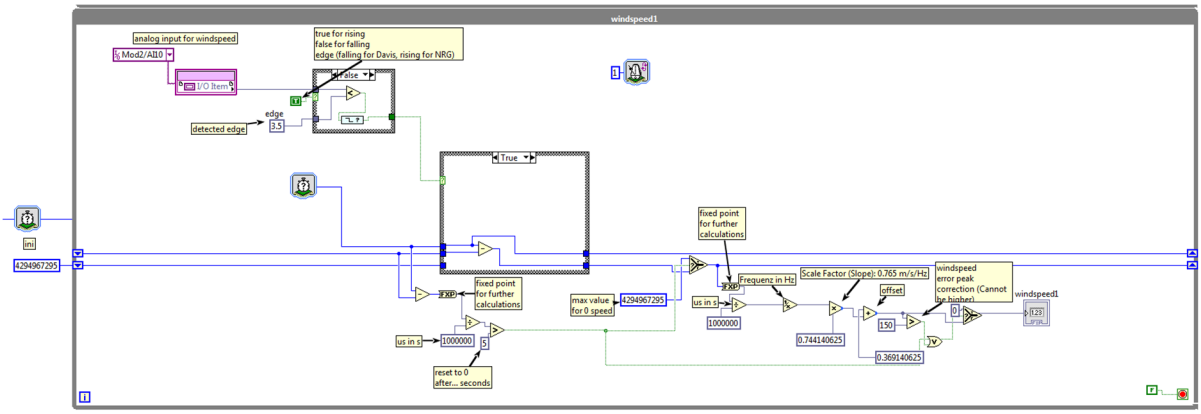

Figure A 2-13: LabVIEW code for wind speed

A 2.3.6 Data storage

To provide enough data storage, a Synology NAS is installed, on which all the collected data is stored. The D-Link DWR512 router maintains the access to the Internet and allows remote servicing.

A 2.3.7 Mechanical energy production

The generator provides the applied torque *M* in Nm and angular speed n in 1/min to the NI cRio over EtherCAT. As a result the produced energy E_{mech} can be calculated with Formula 2.3.

$$E_{mech} = \int \frac{n}{60\,\frac{s}{min}} \cdot 2\pi \cdot M \; dt \qquad (2.3)$$

A 3 Measurement Results

The energy measurements for the Aventa AV-7 turbine and the Anerdgy WindRail are compared and matched to the wind data. The first comparison, on 28.05.2015 was performed with inappropriate controller settings and no mechanical energy data is available. The settings were then adapted for the second test of the 07. - 09.07.15. In the third case, from 27.07.2015 - 28.07.2015, the wind channel was modified and the controller's torque constant was updated.

A 3.1 Test 1 (28.05.2015)

A 3.1.1 Wind data

Figure A 3-1 contains the raw speed and direction data of the wind sensor. Figure A 3-2 shows the wind distribution in a 2-axis plot.

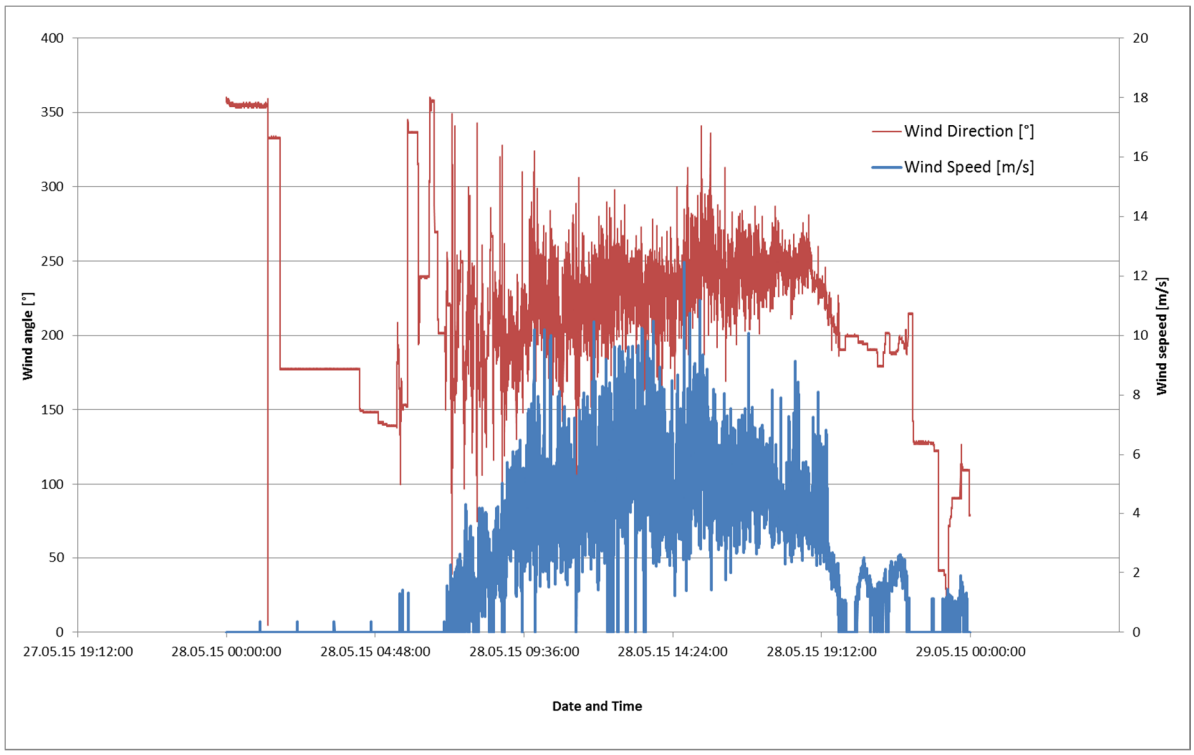

Figure A 3-1:: Wind direction and speed, 28.05.2015

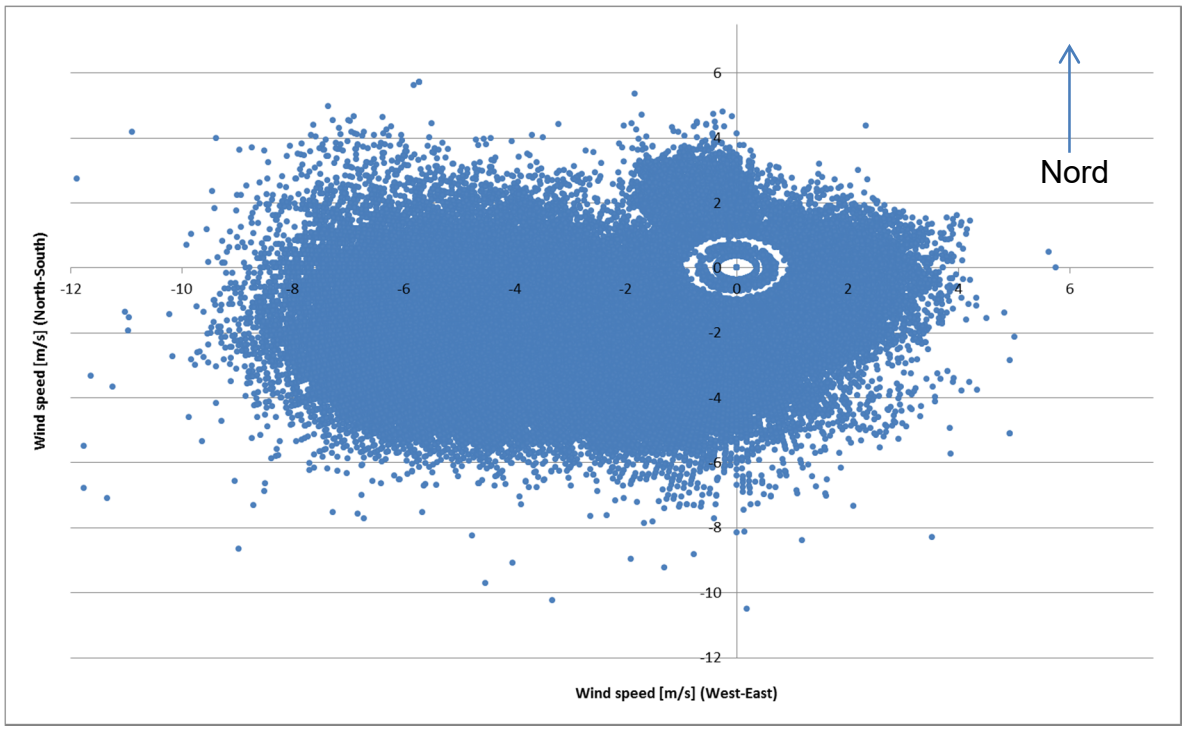

Figure A 3-2: Wind rose, 28.05.2015

A 3.1.2 Energy production

The energy production is calculated from the electrical data provided by the measuring equipment. For the AV-7 turbine, the momentary power is recorded and shown in Figure A 3-3. For the WindRail, the power has to be calculated from the voltage and the current measurements.

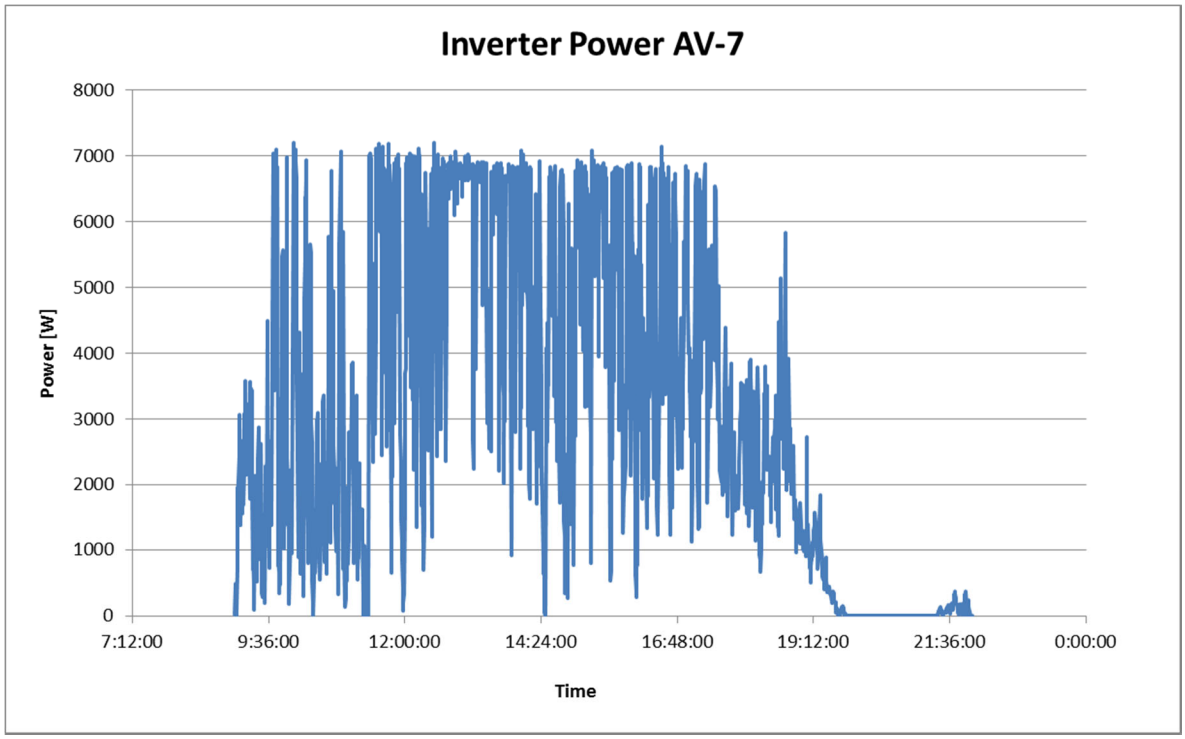

Figure A 3-3: Power of the AV-7 turbine, 28.05.2015

For the WindRail the power has to be calculated from the voltage and current measurement shown in Figure A 3-5 (Original data in Figure A 3-4). For measuring the current, there was 1 turn used. In Figure A 3-6 the power output of the Anerdgy WindRail is shown. Figure A 3-7 shows the energy production over the evaluation period of both devices.

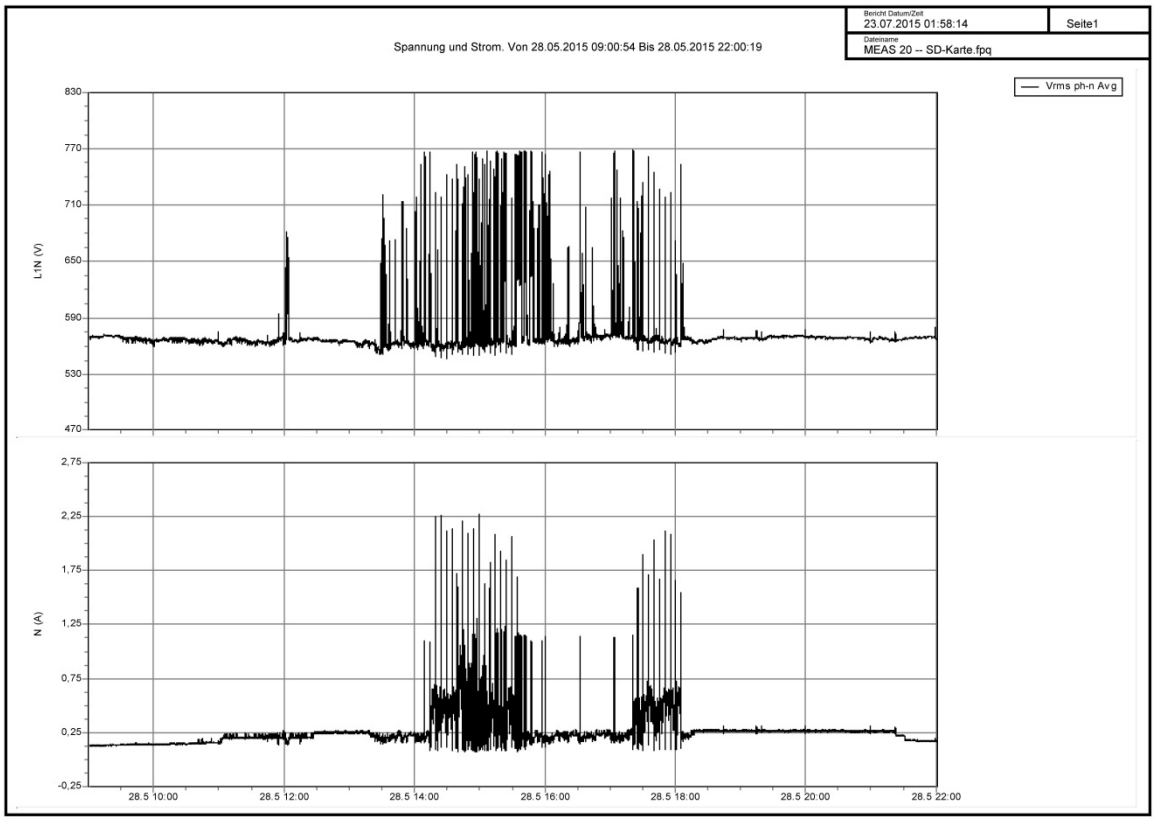

Figure A 3-4: Original Fluke measurement data, U and I of the Anerdgy WindRail, 28.05.2015

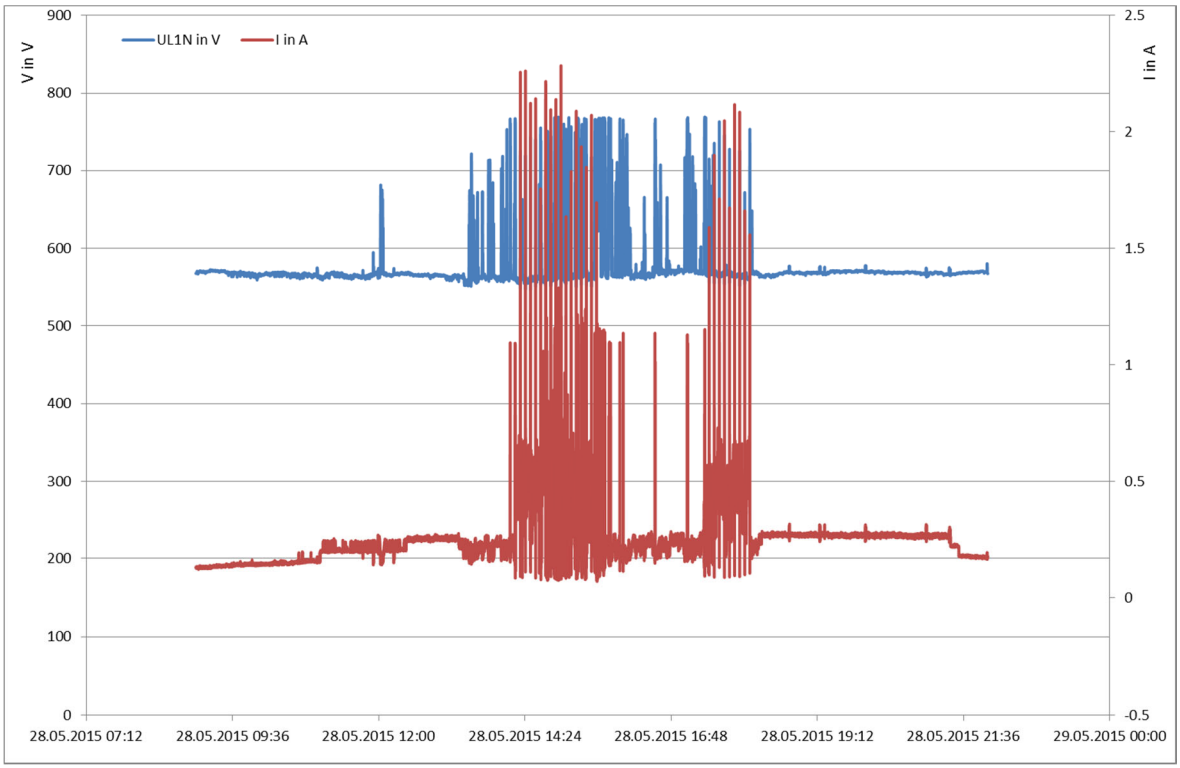

Figure A 3-5: Voltage and current of the Anerdgy WindRail, 28.05.2015

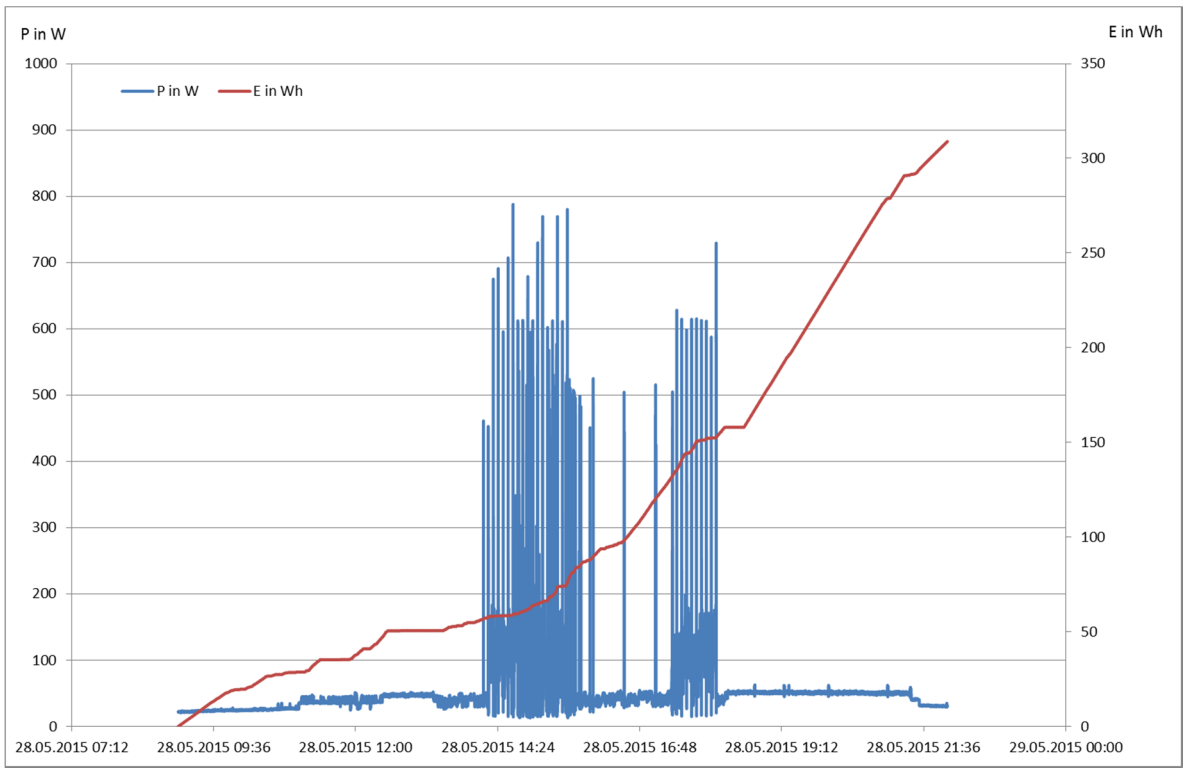

Figure A 3-6: Power of the Anerdgy WindRail, 28. 05.2015

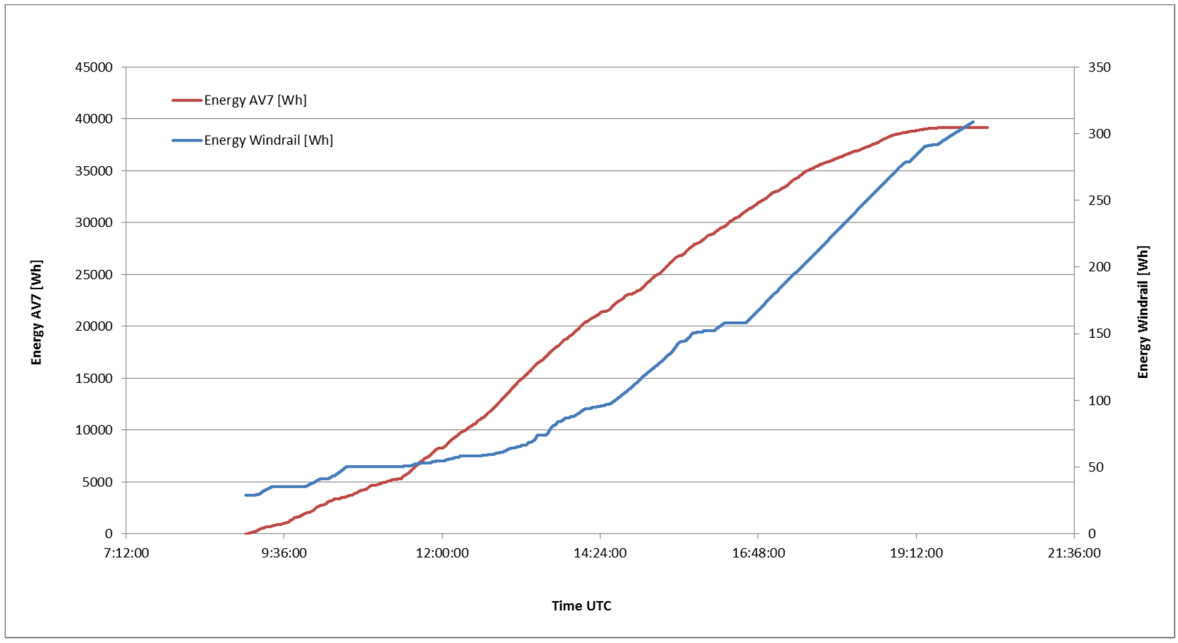

Figure A 3-7: Energy production, 28.05.2015

A 3.2 Test 2 (07.07.2015 - 09.07.2015)

A 3.2.1 Wind data

Figure A 3-8 shows the raw speed and the direction of the wind sensor. Figure A 3-9 presents the wind distribution in a 2-axis plot.

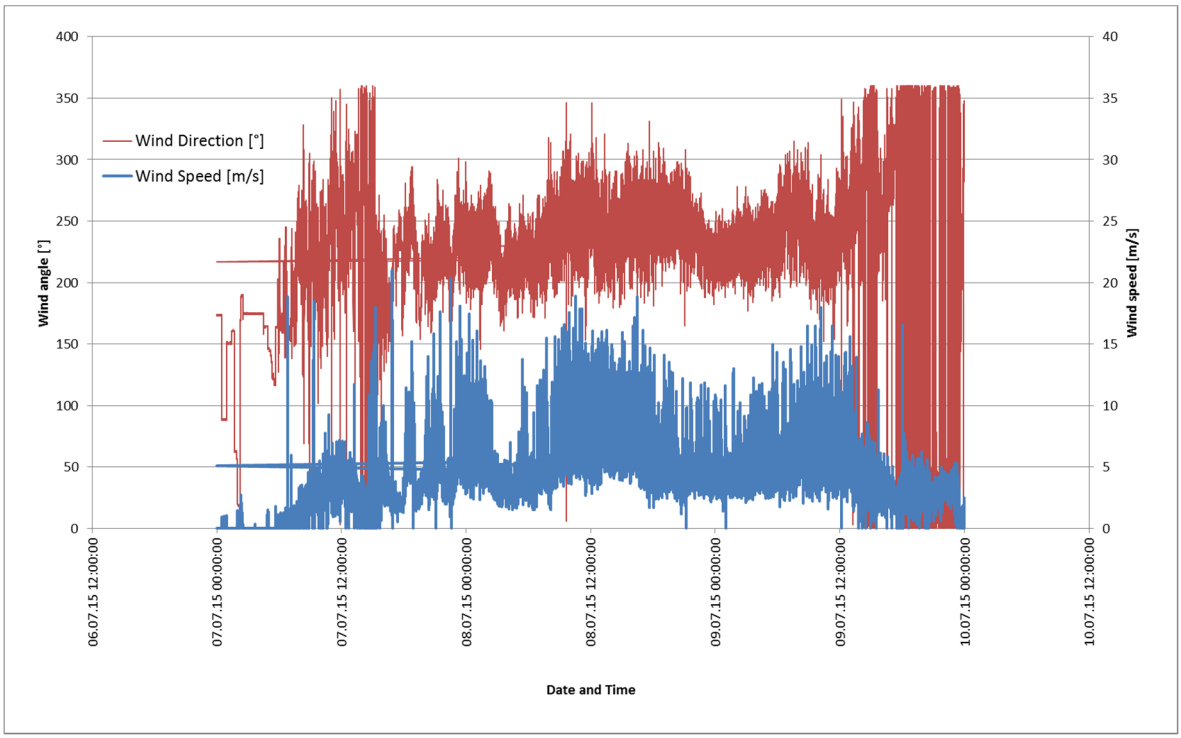

Figure A 3-8: Wind direction and speed, 07.-09.07.2015

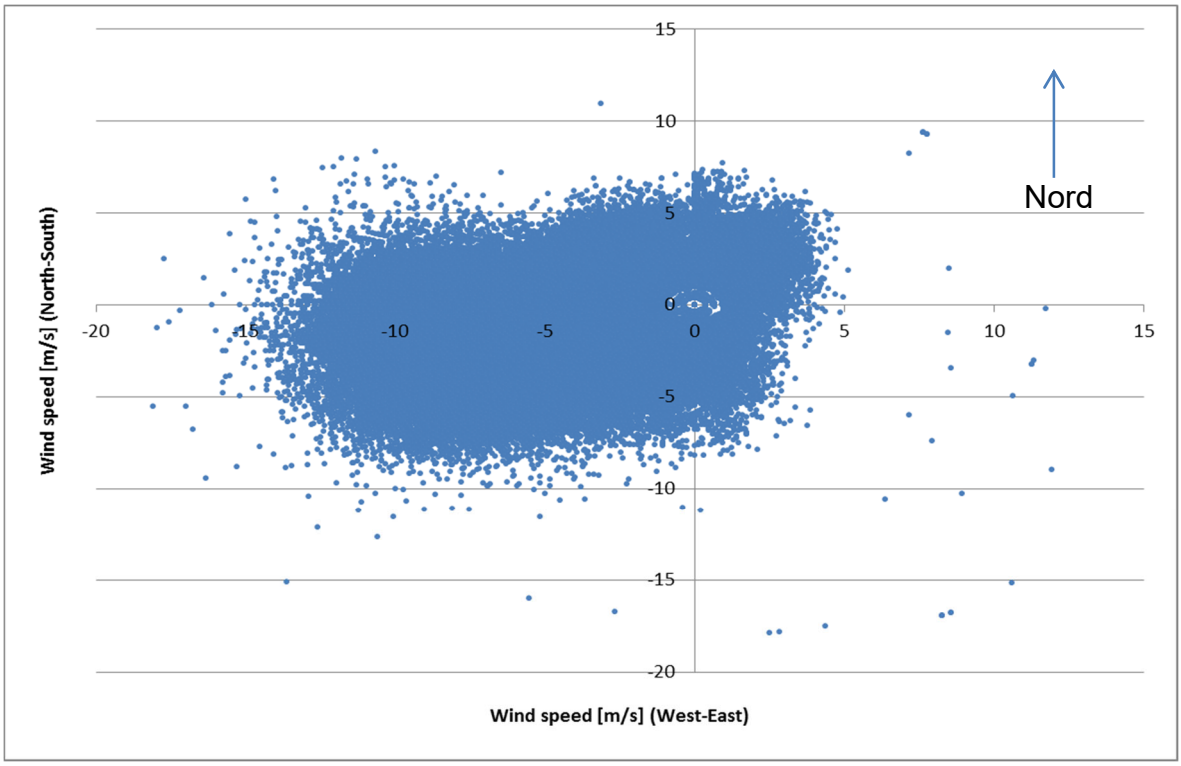

Figure A 3-9: Wind rose, 07.07.2015 - 09.07.2015

A 3.2.2 Energy production

The energy production is calculated from the electrical data provided by the measuring equipment. For the AV-7 turbine the momentary power is recorded and shown in Figure A 3-10.

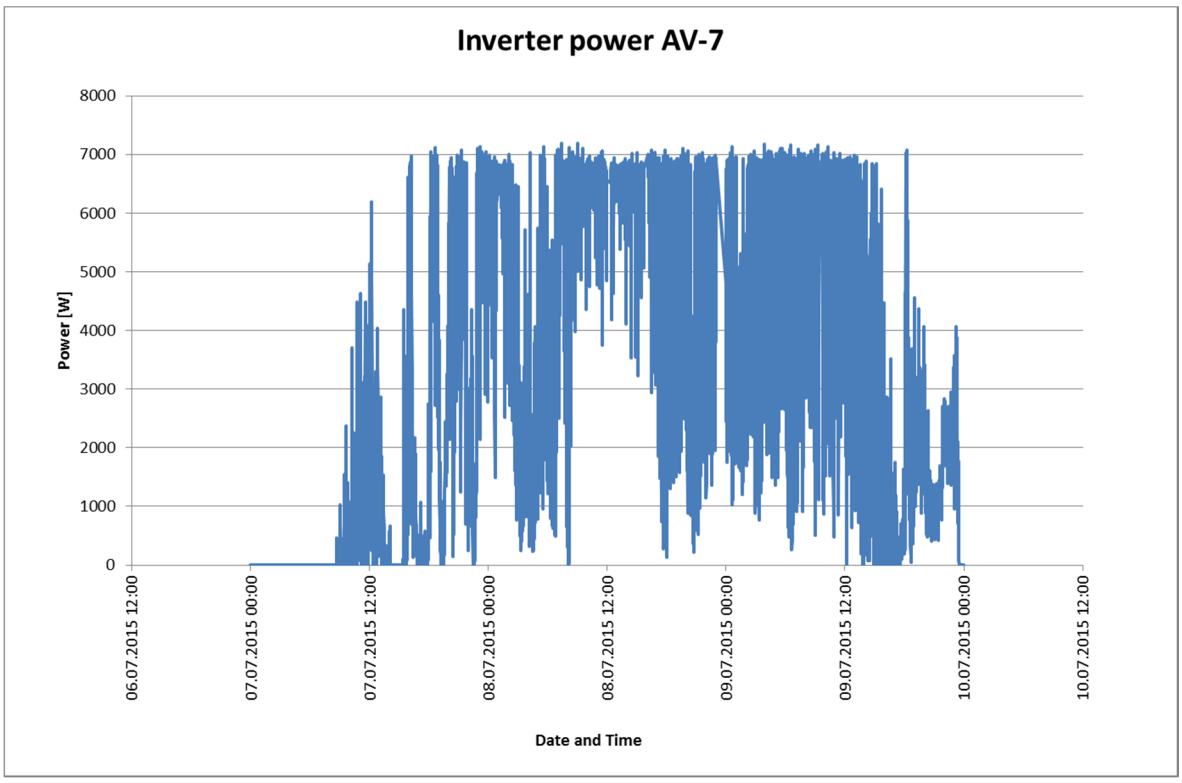

Figure A 3-10: Power of the AV-7 turbine, 07.07.2015 - 09.07.2015

For the WindRail the power has to be calculated from the voltage and current measurement shown in Figure A 3-12 (original data in Figure A 3-11). For measuring the a small current, the sensitivity of the current probe was increased by wrapping eight turns through the primary. In Figure A 3-13 the power output of the Anerdgy WindRail is shown.

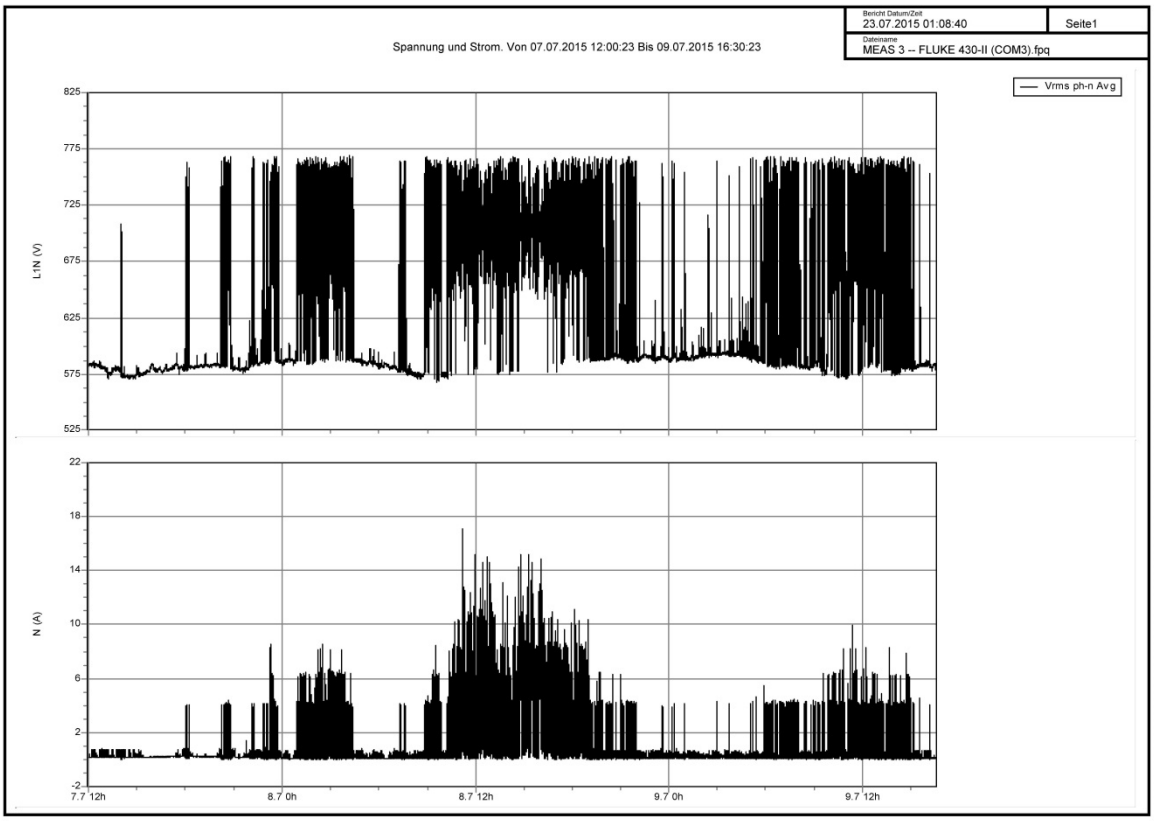

Figure A 3-11: Original Fluke measurement data, U and I of the Anerdgy WindRail, 07.07.2015 - 09.07.2015

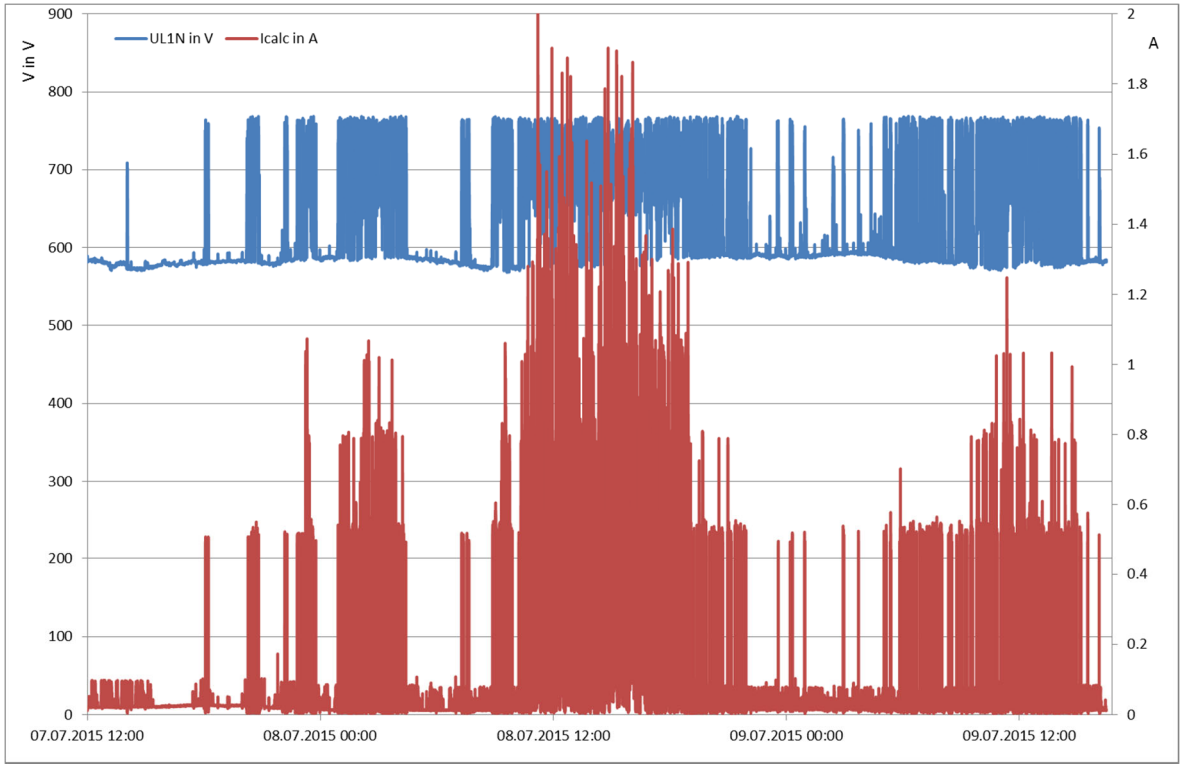

Figure A 3-12: Voltage and current of the Anerdgy WindRail, 07.07.2015 - 09.07.2015

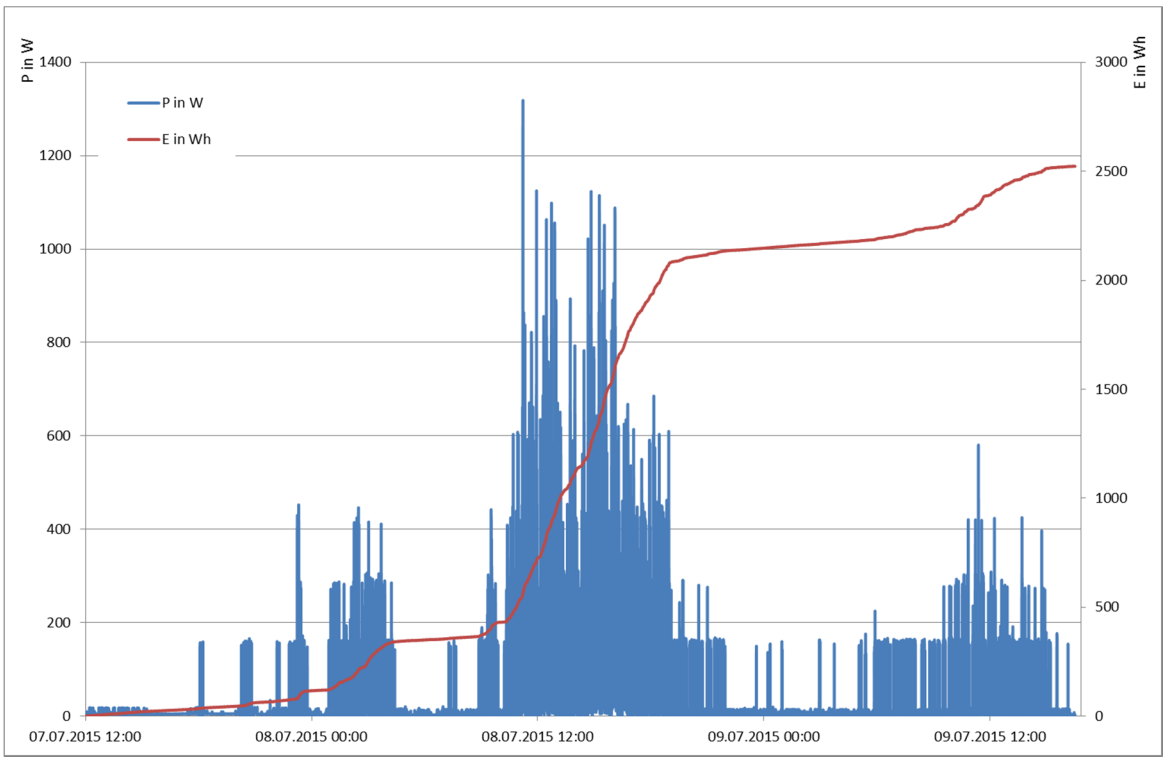

Figure A 3-13: Power of the Anerdgy WindRail, 07.07.2015 - 09.07.2015

Figure A 3-14 shows the energy production over the evaluation period for both systems. Additionally, the mechanical power calculated from the generator controller is shown for validation.

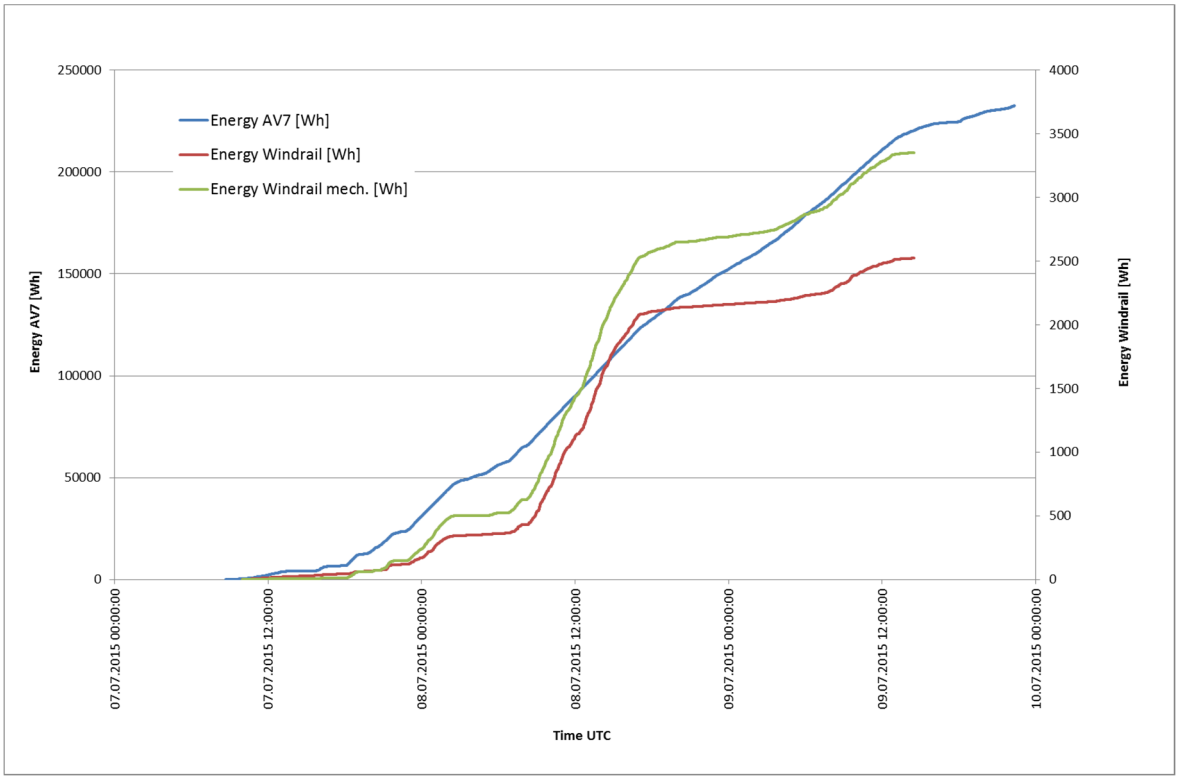

Figure A 3-14: Energy production, 07.07.2015 - 09.07.2015

A 3.3 Test 3 (27.07.2015 – 28.07.2015)

A 3.3.1 Wind data

Figure A 3-15 shows the raw speed and the direction of the wind sensor. Figure A 3-16 shows the wind distribution in a 2-axis plot.

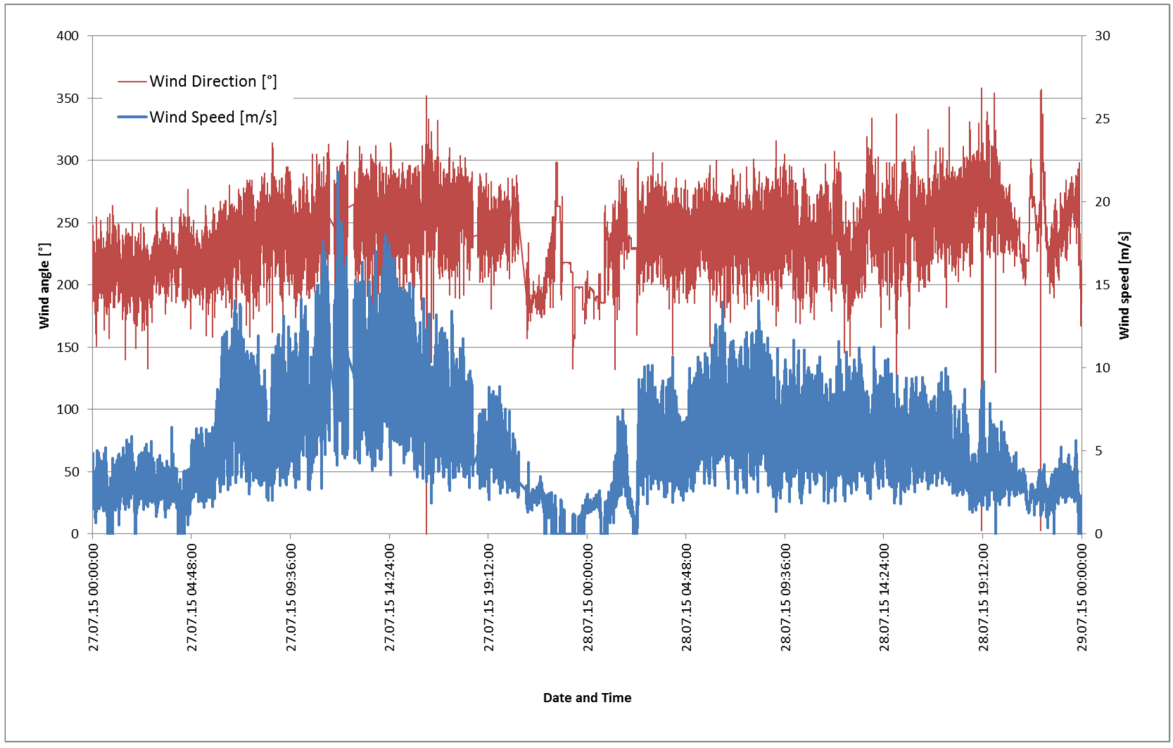

Figure A 3-15: Wind direction and speed, 27.07.2015 – 28.07.2015

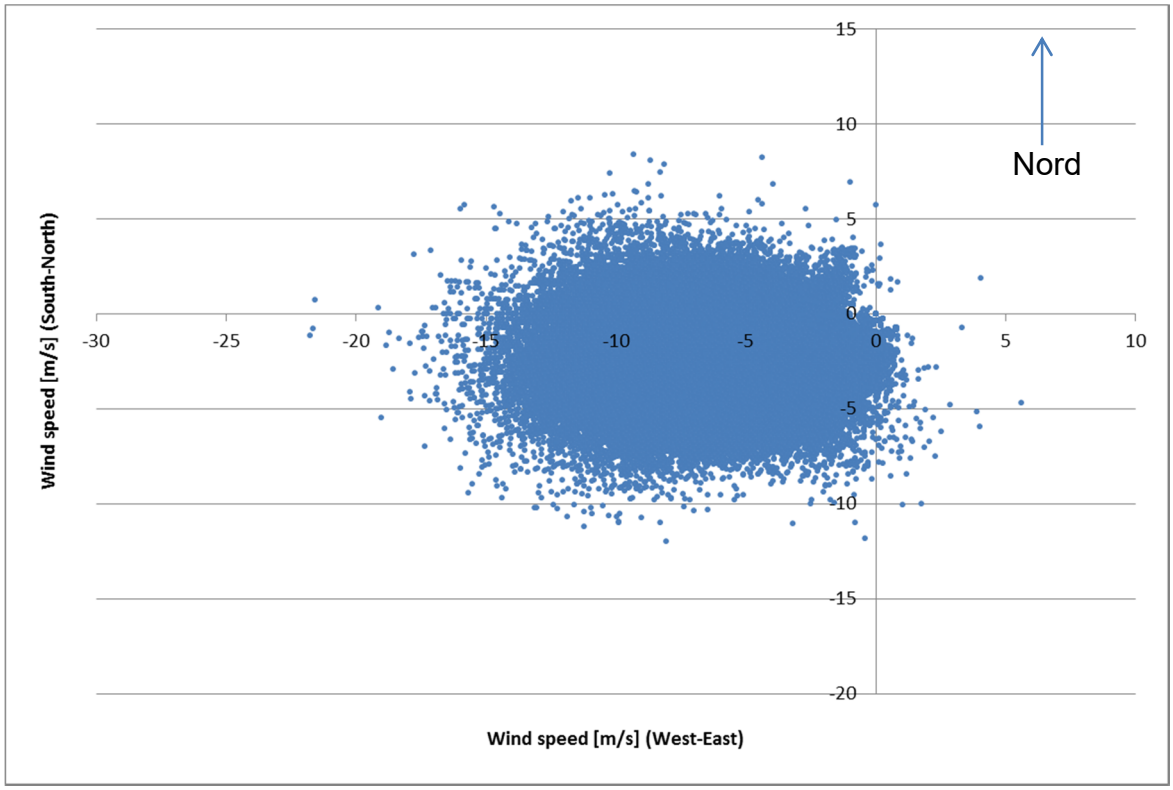

Figure A 3-16: Wind rose, 27.07.2015 – 28.07.2015

A 3.3.2 Energy production

The energy production is calculated from the electrical data provided by the measuring equipment. For the AV-7 turbine, the momentary power is recorded and shown in Figure A 3-17. The data log starts at 12:39 UTC.

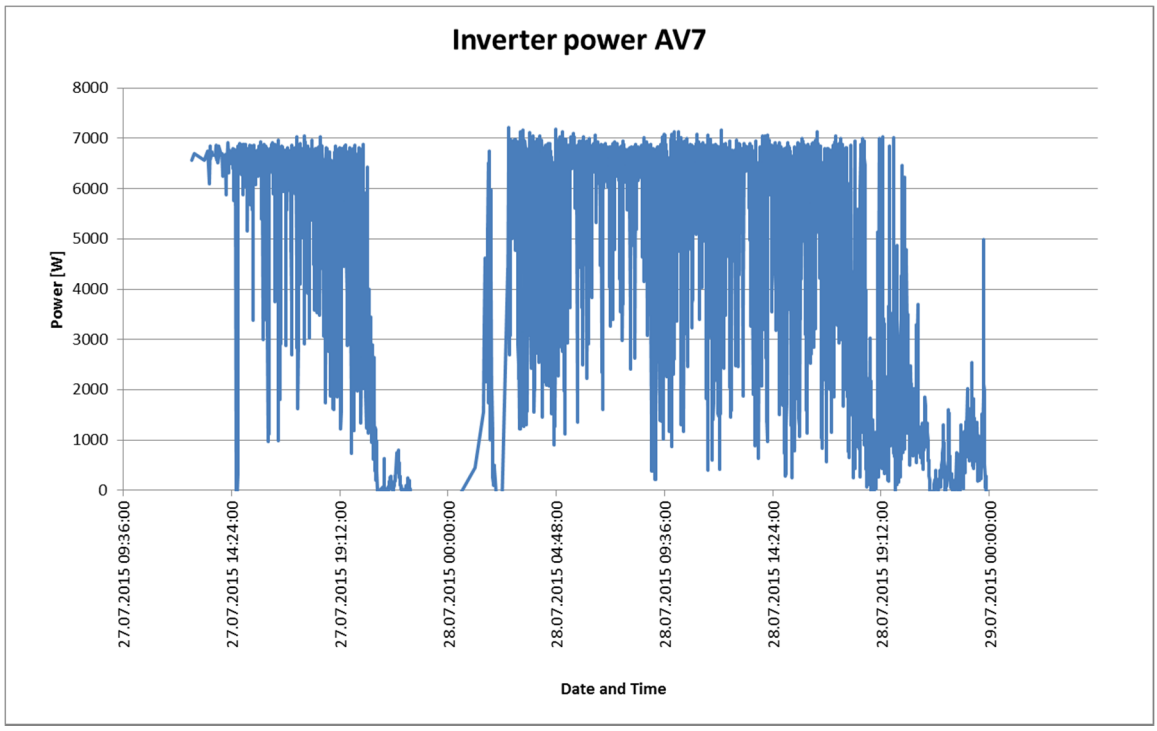

Figure A 3-17: Power of the AV-7 turbine, 27.07.2015 – 28.07.2015

For the WindRail the power has to be calculated from the voltage and current measurement shown in Figure A 3-19 (Original data in Figure A 3-18). For measuring a small current, the sensitivity of the current probe was increased by wrapping eight turns through the primary. In Figure A 3-20 the power output of the Anerdgy WindRail is shown.

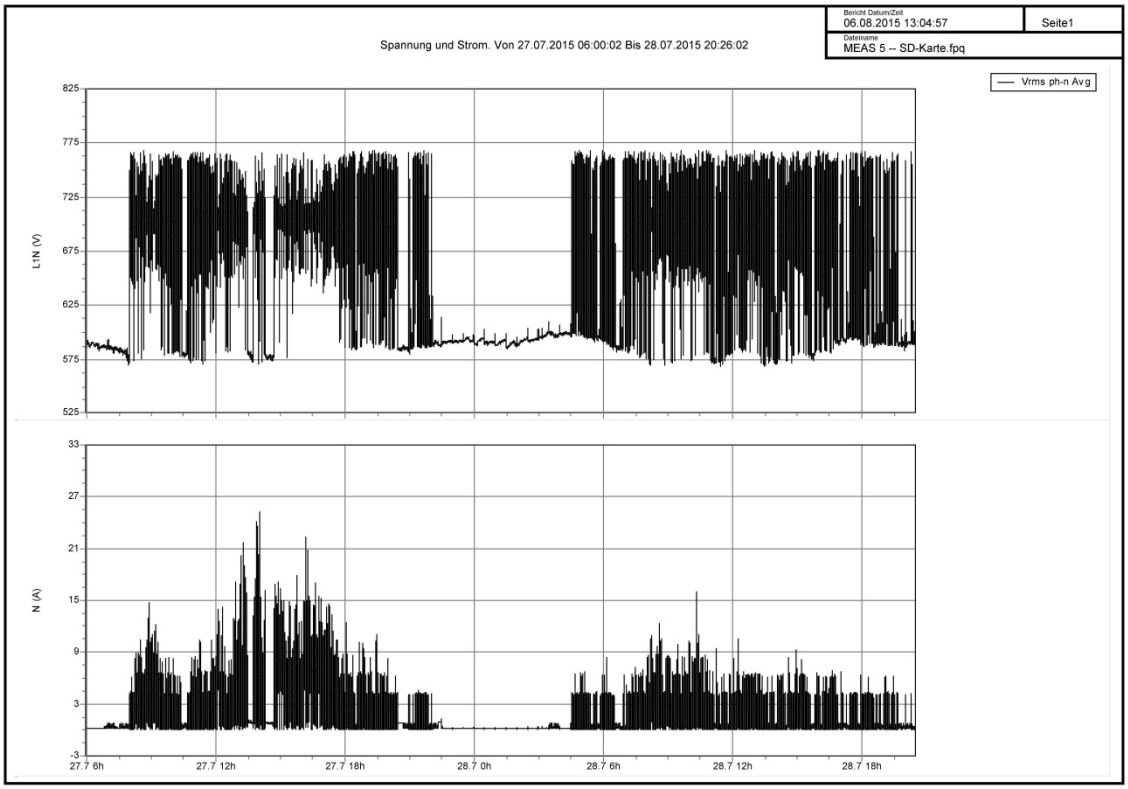

Figure A 3-18: Original Fluke measurement data, U and I of the Anerdgy WindRail, 27.07.2015 – 28.07.2015

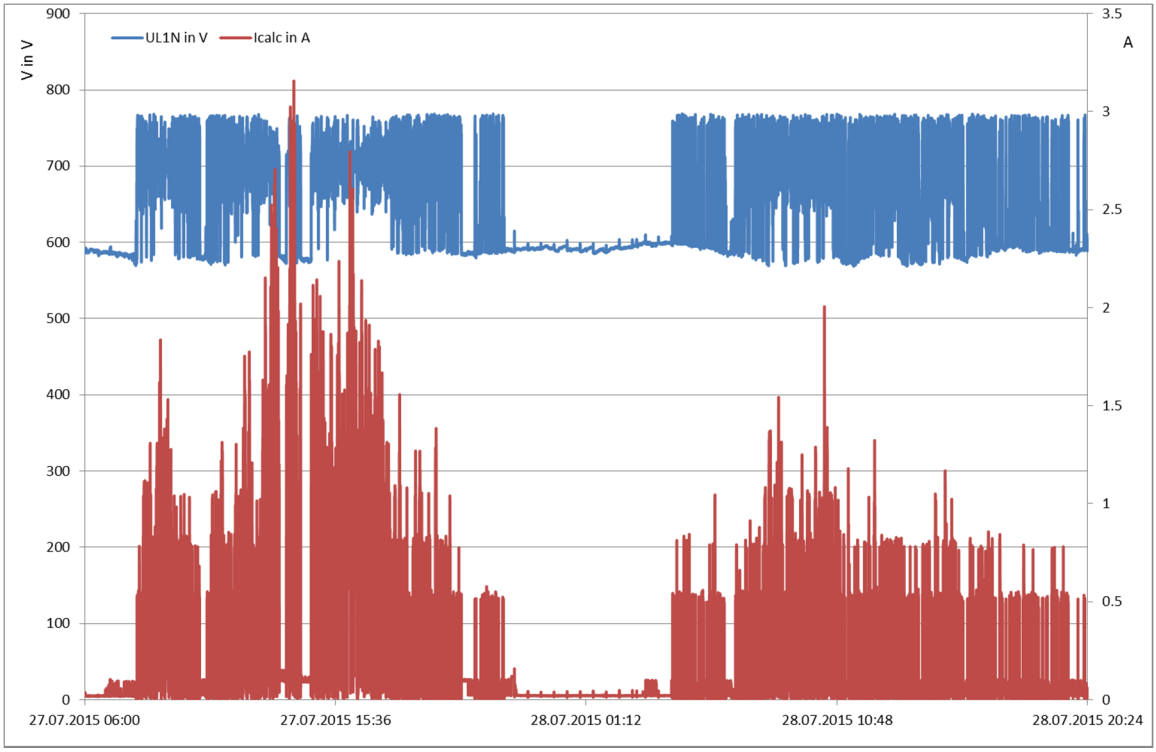

Figure A 3-19: Voltage and current of the Anerdgy WindRail, 27.07.2015 – 28.07.2015

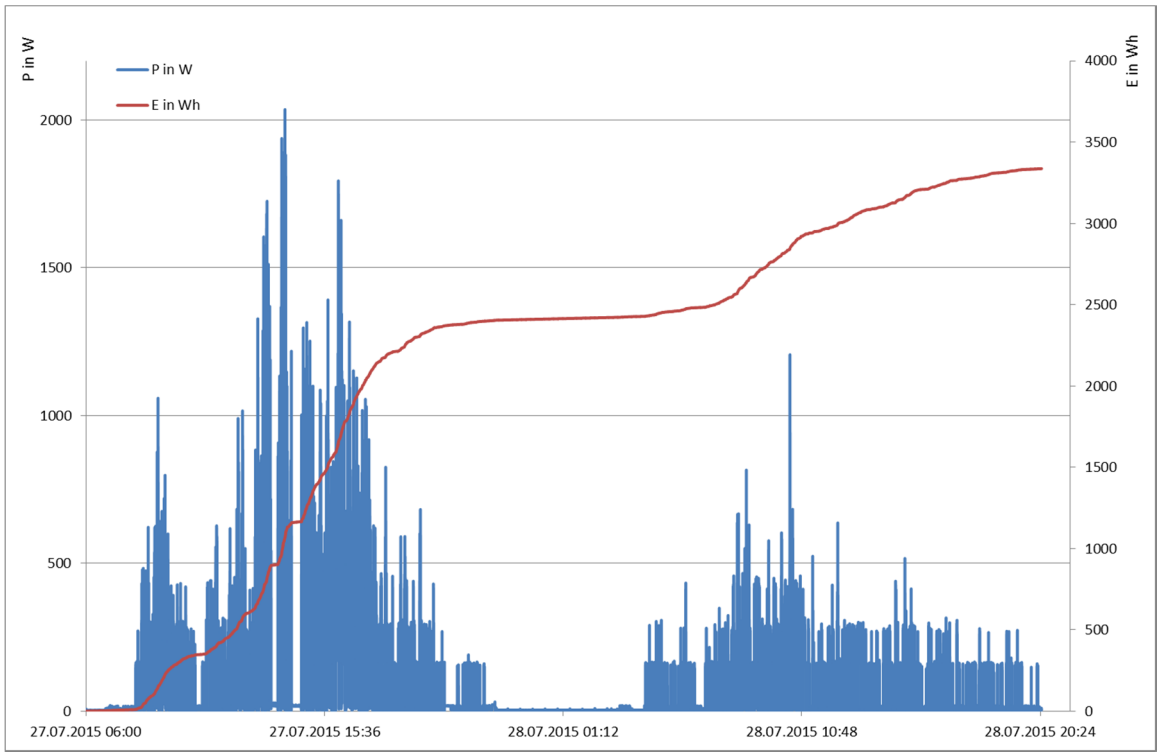

Figure A 3-20: Power of the Anerdgy WindRail, 27.07.2015 – 28.07.2015

Figure A 3-21 shows the energy production over the evaluation period for both systems. Additionally, the mechanical power calculated from the generator controller values is shown for verification.

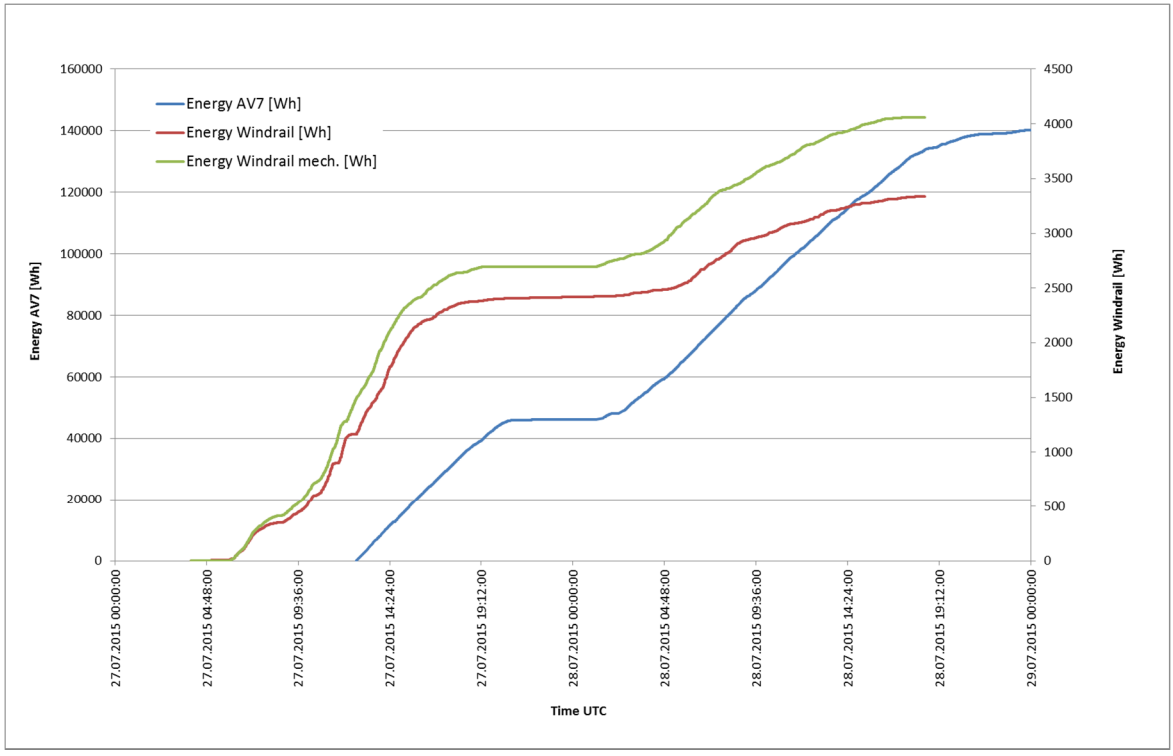

Figure A 3-21: Energy production, 27.07.2015 – 28.07.2015

A 4 Evaluation

The electrical power data was acquired at different sample rates for the different measuring equipment according to Eq. 5.1. I_{avg} is calculated from IRMS (measurement data) using the conversion coefficient α given in Eq. 8.1.

$$P(t) = I_{avg}(t) \cdot U(t) = \frac{1}{\alpha[I_{RMS}(t)]} \cdot I_{RMS}(t) \cdot U(t) \tag{5.1}$$

The energy production is calculated as the sum of the produced power with respect to the time between two samples according to Eq. 5.2. In addition, the energy production calculated from the generator controller data is given as a comparison. The results are given in Table A 4-1 and Table A 4-2.

$$E_{tot} = \sum_{k=0}^{N} [T(k+1) - T(k)] \cdot P(k) \tag{5.2}$$

The energy production of both systems is then weighted with the active area (rotor area) of each device according to Eq. 5.3. The results are given in Table A 4-1 and Table A 4-2.

$$E_{sqm} = \frac{E_{tot}}{A_{Rotor}} \tag{5.3}$$

A_{Rotor} Aventa AV-7: 129 m^2
A_{Rotor} Anerdgy WindRail: 1.4 m^2

Table A 4-1: Results Aventa AV-7

Evaluation period	**Energy production E_{tot}**	**Energy production per m^2 E_{sqm}**
28.05.2015 07:00-20:00 UTC	39’150 Wh	303.5 Wh/m^2
07.07.2015 - 09.07.2015 10:00-14:30 UTC	220’360 Wh	1708 Wh/m^2
27.07.2015 - 28.07.2015 12:40-18:30 UTC	134’010 Wh	1039 Wh/m^2

Several hardware and software changes on the Anerdgy WindRail apply for the different evaluation periods. The first measurement on 28.05.2015 was performed with inappropriate controller settings and, thus, yielded a low energy production. No mechanical energy data is available for this evaluation period. The settings were then adapted for the second measurement on 07.07.2015 - 09.07.2015. For the third measurement period (27.07.2015 - 28.07.2015), the wind channel was modified and the controller’s torque constant was updated. The difference in the two energy values is explained in A 6.4. To estimate the efficiency of both facilities, the energy production per square meter is compared in Table A 4-3.

Table A 4-2: Results Anerdgy WindRail

Evaluation period		Energy production E_{tot}	Energy production per m² E_{sqm}
28.05.2015 07:00-20:00 UTC	Fluke	309 Wh	220.7 Wh/m²
	Generator	-	-
07.07.2015 - 09.07.2015 10:00-14:30 UTC	Fluke	2523 Wh	1802 Wh/m²
	Generator	3350 Wh	2393 Wh/m²
27. 07.2015 - 28.07.2015 12:40-18:30 UTC	Fluke	2172 Wh	1551 Wh/m²
	Generator	2572 Wh	1837 Wh/ m²

Table A 4-3: Comparison between the two systems

Evaluation period	E_{sqm} WindRail Fluke / E_{sqm} AV-7	E_{sqm} WindRail Generator / E_{sqm} AV-7	Remarks
28.05.2015	0.73	no data	with improper controller settings
07.07.2015 - 09.07.2015	1.06	1.40	with proper controller settings
27. 07.2015 - 28.07.2015	1.49	1.77	with updated controller settings and wind channel modifications

A 5 Conclusion

The presented measurements are only indicative, yet they indicate that the WindRail system produces more power per square meter active area as compared to the AV-7 turbine. The modifications during the measurement increased the efficiency from 0.73 to 1.44. However, no estimation for a yearly wind energy production is possible as only isolated cases were investigated and conditions and settings differed between the measurements.

For further evaluations several improvements should be made, such as

1. increasing the efficiency further
2. reducing the power path losses
3. reducing the production cost
4. closing the power path to the grid for further measurements
5. verification of the wind measurement setup

The WindRail right now is a well-developed A-prototype, which should be further optimized in order to become a series product.

A 6 Verification

A 6.1 Power Quality and Energy Analyzer data

The following figures show the current measurement on channel L1 und N with the battery change.

New Battery in Current Clamp 07.05.2015 13:11
Empty Battery in Current Clamp_L1 08.05.2015 20:30

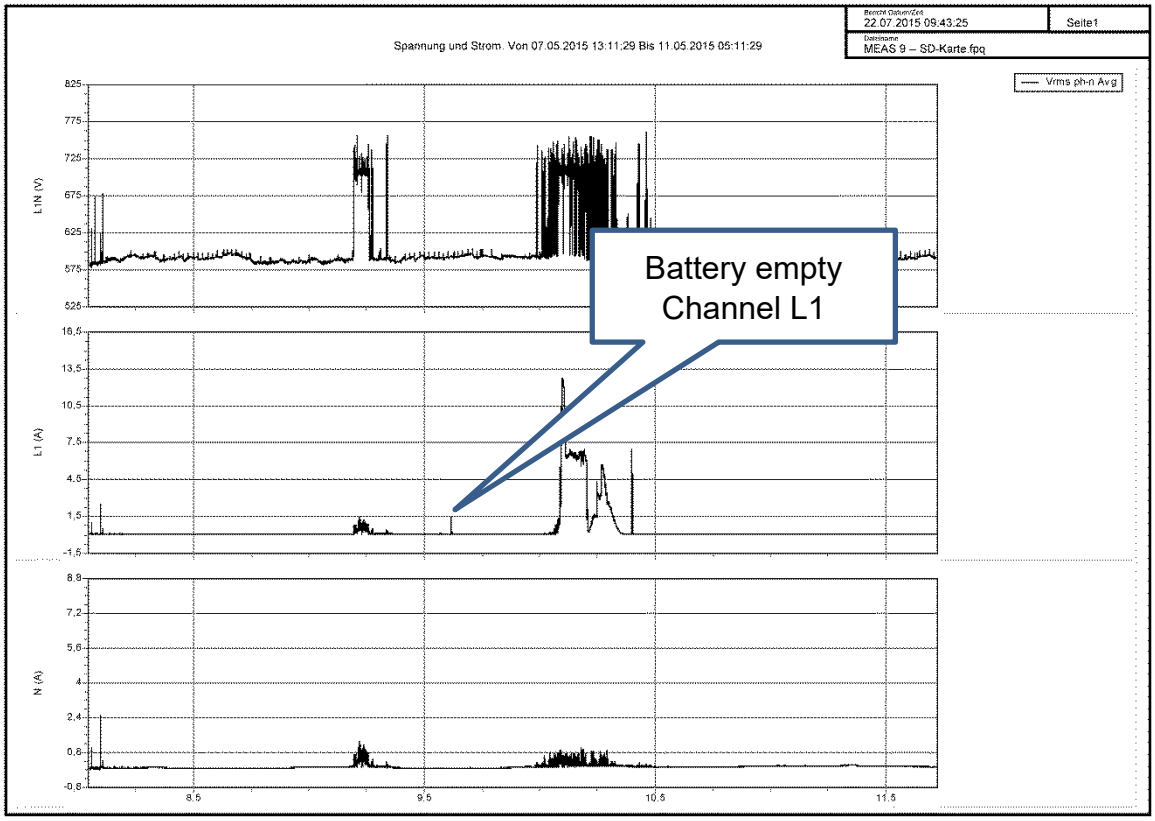

Figure A 6-1: Voltage L1N, Current IL1 und Current IN 07.05.2015 to 11.05.2015

New Battery in Current Clamp	04.06.2015 16:54
Empty Battery in Current Clamp_L1	06.06.2015 05:16

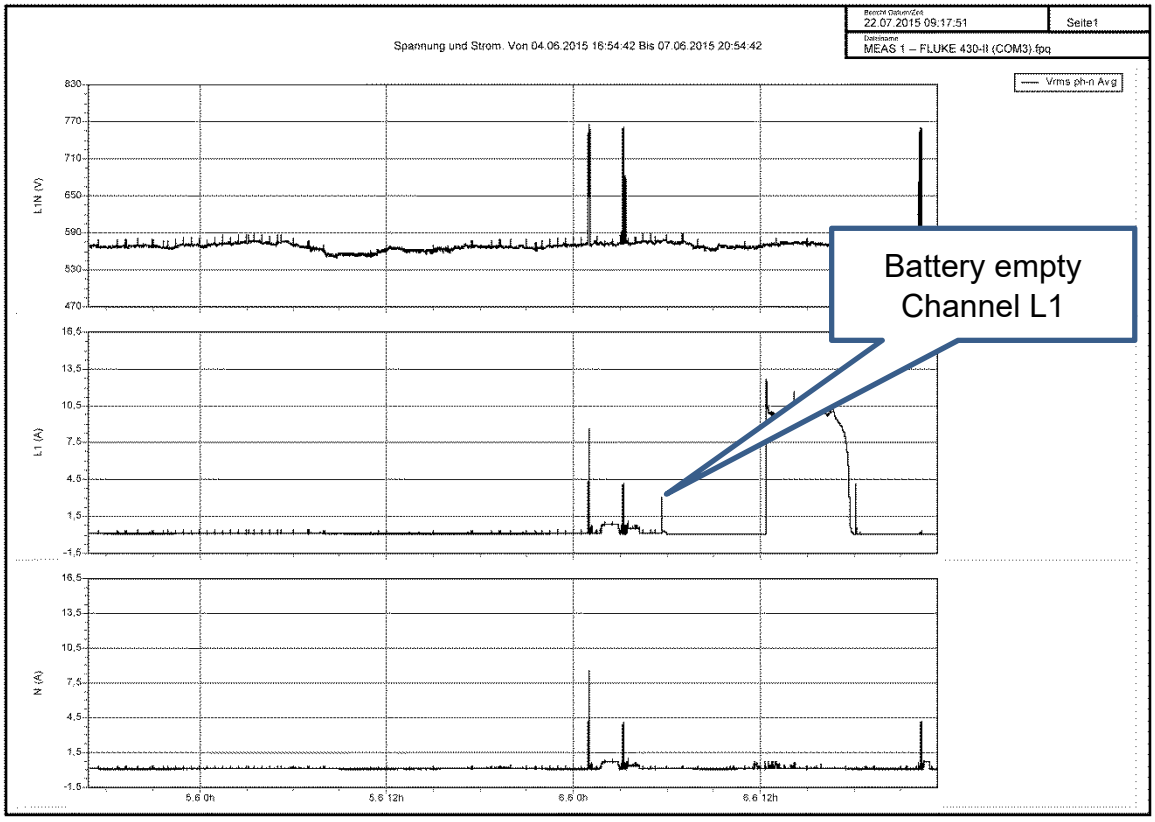

Figure A 6-2: Voltage L1N, Current IL1 und Current IN 04.06.2015 to 06.06.2015

A 6.2 Conversion coefficient for I_{RMS}

Due to the converter setup, the measured output power of the WindRail has a pulsed waveform (Figure A 6-4). Therefore, the I_{avg} values instead of the I_{RMS} values have to be used to calculate the DC power of the WindRail correctly. The waveforms are shown in Figure A 6-4 where red is the current and blue the voltage. The I_{RMS} values can be converted to I_{avg} values using the conversion coefficient α. A qubic function for α was derived through polynomial fitting (see Eq. 8.1, Fig. A 6-3).

$$\alpha(x) = -0.086x^3 + 0.7733x^2 - 2.3155x + 3.3854 \qquad (8.1)$$

To verify the waveforms of the picoscope, it is possible to compute the value of the breaking resistor R_{br}. To do so, the Formula 8.2 is used.

$$R_{Br} = \frac{t_{on} \cdot I_{on,avg} + t_{off} \cdot I_{off,avg}}{t\_on} \cdot U_{on,avg} = 74.29\ \Omega \qquad (8.2)$$

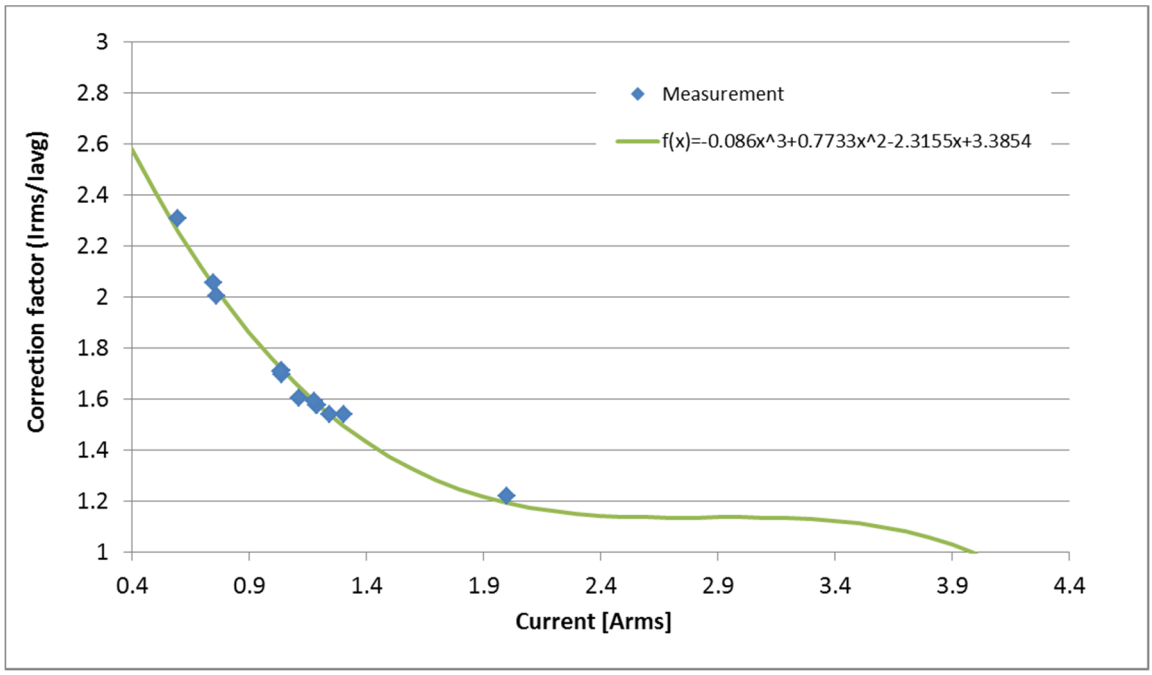

Figure A 6-3: Conversion coefficient I_{RMS} / I_{avg}

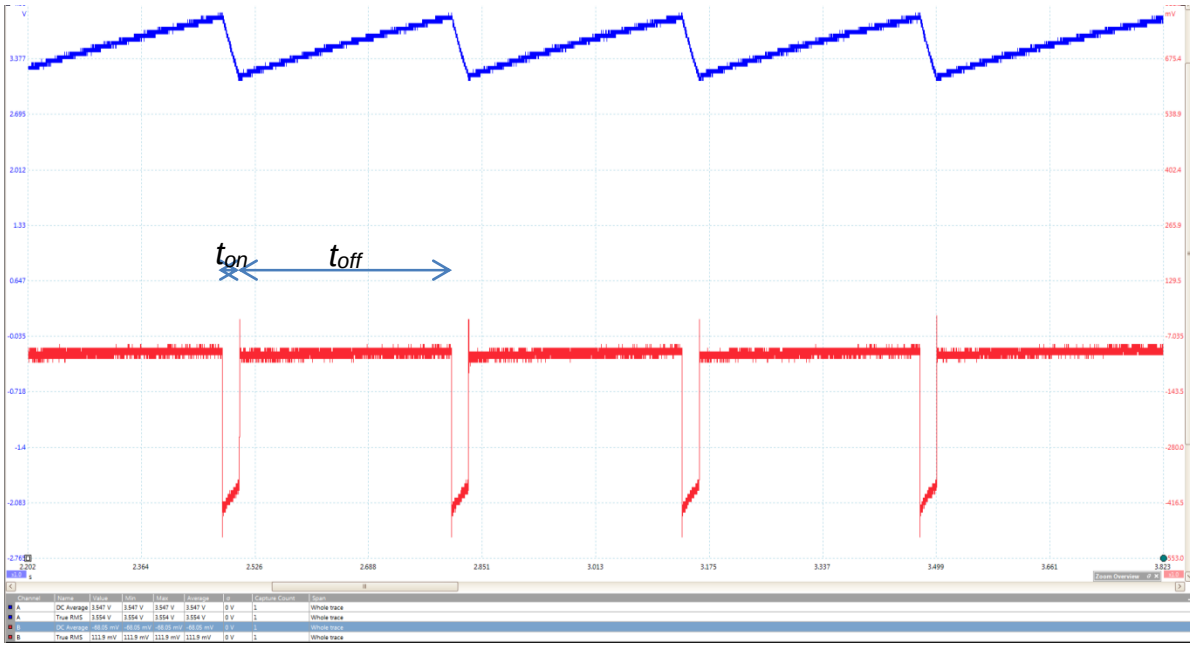

Figure A 6-4: Picoscope DC-bus measurement

A 6.3 Validating AV-7 data

To validate the measured data from the ABB A43 meter installed in the AV-7 turbine, a histogram of the sampling time is derived. A software problem influenced by a critical environment, with massive EMC radiation on the roof, produced by the GSM antenna, the drives and the frequency converters, led to a data loss. This shows the histogram in Figure A 6-5, which includes the data from 06.06.2015 00:00 to 10.07.2015 08:14. Further analysis shows that the received data are not corrupted, the energy is monotonously increasing, and the sampling time still fits the requirements.

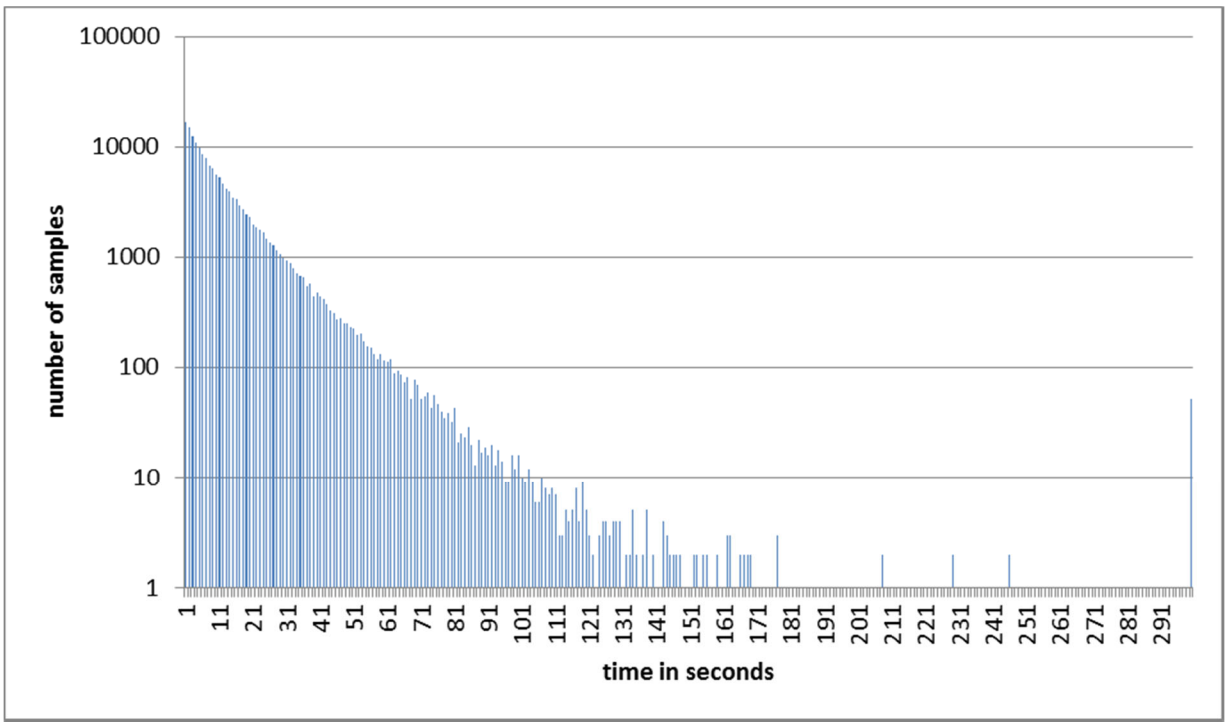

Figure A 6-5: Sampling time histogram

A 6.4 Generator losses

Figure A 3-14 and A 3-21 show a considerable difference in energy production when comparing the Fluke measurement data and the controller's values. This is most probably due to internal losses in the converters Bmax BM5323 and BM5327.
The average power difference over the investigated periods is 17 W.

B Appendix: Solar data

B 1 Setup

The WindRail prototype is equipped with four industrial crystalline PV panels from Swisswatt POLYWATT 290W-72c. Each panel has a TIGO power optimizer MM-2ES50 and runs on a Mastervolt Soladin 1000 Web 1kW inverter.

Figure B 1-1: WindRail Layout

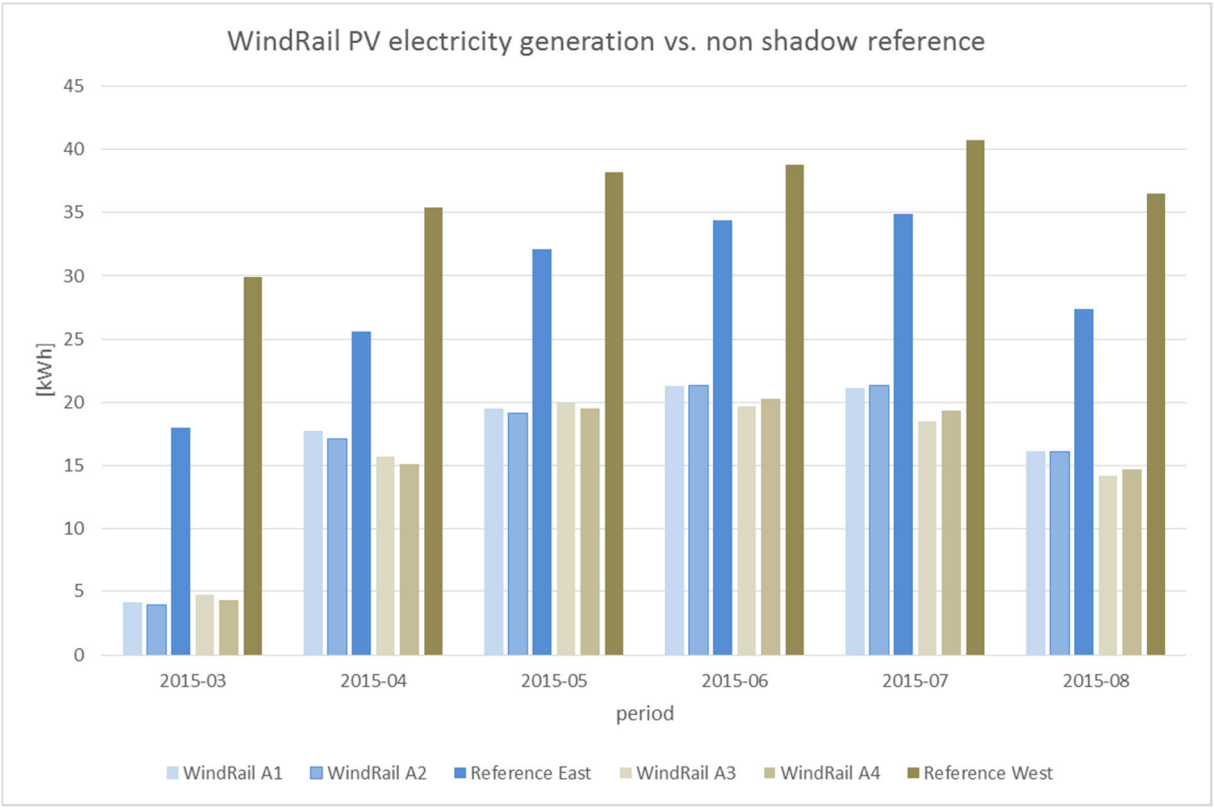

Figure B 1-2: generated PV electricity vs. reference w/o shadow effect

The Theoretical power data was obtained from the Joint Research Centre Institute for Energy and Transport (IET) of the European Commission using their Photovoltaic Geographical Information System (PVGIS) [9].

B 2 Data

The solar PV data was recorded by TIGO software. The given data period is from 10.03.2015 to 30.08.2015. 385 kWh were produced in this period.
The main purpose of this prototype was to test the various fitting and installation methods when PV modules are attached to the WindRail system. Two panels are mounted on top of the wind channel and two at the rear.
The Aventa HAWT is southeast of the Anerdgy WindRail (Figure A 2-2) and, therefore, casts a shadow most of the day on the PV panels, which explains the reduced output power of the panels against the possible theoretical power (Figure B 1-2).
The position of the WindRail is not ideal for PV due to large shadowing effects from the Aventa HAWT turbine as well as other antenna structures such as GSM and also the anemometer used for the reference data. (Figure B 2-1)

Figure B 2-1: Shadowing effects on the WindRail PV panels

In order to reduce the negative effects of such shadowing, WindRail uses MPPT power optimizers at individual panel level as opposed to long strings. Figure B 1-2 shows that different energy production was achieved using a separate MPPT per panel, which re-enforces the approach Anerdgy took to consider each PV panel individually to minimise overall system degradation due to shading objects which Anerdgy has no influence over.
As proof of concept for this method a Tigo system was used, set up as below but with only 4 panels.The inverter used was a Mastervolt Soladin 1000 Web unit to convert the PV DC bus to single phase AC (Table B 2-1).

Table B 2-1: used PV components

	Manufacturer	**Type**	**Serial number**
Solar modul	Swisswatt	PW290	
Tigo	Tigo	MM-2ES50	8-1011664FW 881-11664FN 8-1010688DG 881-10688DT
TigoMaster	Tigo	MU-ESW ES-GTWY	TG013124566 00158D000014DB8E
MasterVolt	Mastervolt	Soladin 1000 WEB	D000A0115

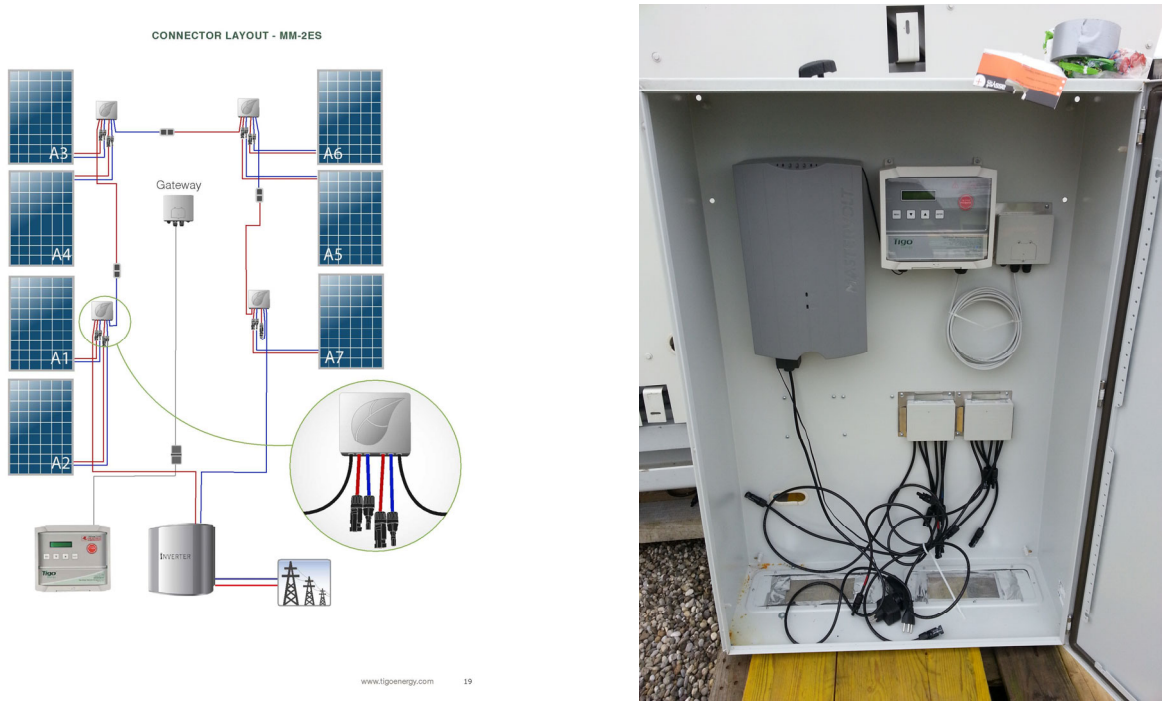

Figure B 2-2: PV string principle and actual WindRail installation

The power production data is sent directly and automatically to the Tigo website through the internet with logging taking place every two seconds. The Tigo website creates the charts from this data. The precise calculations used are not known by us, but they are the same as are provided for all their installations worldwide. The raw data can be downloaded from their website and an extract follows:

DATETIME	TimeStamp	GMT	MM_A1_Vin	MM_A1_Iin	MM_A1_Temp	MM_A1_Power	MM_A2_Vin	MM_A2_Iin	MM_A2_Temp
56:05.8	1402052166	7200	31.9	1.7675	32.019375	56.38325	60.2	1.7675	27.37875
56:07.7	1402052168	7200	32.05	1.7625	31.933437	56.488125	60.15	1.7625	27.37875
56:09.6	1402052170	7200	32.05	1.7575	31.933437	56.327875	60.15	1.755	27.37875
56:11.6	1402052172	7200	32.05	1.755	31.8475	56.24775	60.05	1.75	27.37875
56:13.6	1402052174	7200	34.8	1.725	31.933437	60.03	60.25	1.72	27.37875
56:15.5	1402052176	7200	35.3	1.725	31.933437	60.8925	60.25	1.7275	27.37875

Figure B 2-3: Tigo solar data part 1

MM_A2_Power	MM_A3_Vin	MM_A3_Iin	MM_A3_Temp	MM_A3_Power	MM_A4_Vin	MM_A4_Iin	MM_A4_Temp	MM_A4_Power
106.4035	52.25	1.7675	28.06625	92.351875	61.1	1.7675	29.699062	107.99425
106.014375	52.1	1.7625	28.06625	91.82625	61.1	1.76	29.699062	107.536
105.56325	52.1	1.7575	28.06625	91.56575	61.05	1.7525	29.699062	106.990125
105.0875	52.1	1.755	28.06625	91.4355	61.05	1.745	29.699062	106.53225
103.63	52.5	1.7325	28.06625	90.95625	61.15	1.7175	29.699062	105.025125
104.081875	52.55	1.73	28.06625	90.9115	61.15	1.7225	29.699062	105.330875

Figure B 2-4: Tigo solar data part 2

The use of PV enables energy to be produced on more occasions than with just Wind Alone. By utilizing both forward and rearward facing aspects of the WindRail Surfaces, energy production is maximised over a longer period of sunlight without requiring additional roof space. One or both of these aspects, could be easily converted for Solar Hot Water production as necessary.

C Appendix: WindRail – further findings

C 1 Airflow channel acceleration

The following findings were calculated out of the cRio data set from 27.07.2015. The WindRail airflow channel acceleration is the main factor for higher output power on the wind turbine. Over the relevant wind speed range the acceleration is constant with a 175 % mean between inlet area (Pitot 1) to in front of the rotor (Pitot 2). Figure C 1-1 shows the correlation between the inlet airflow speed and that in front of the rotor.

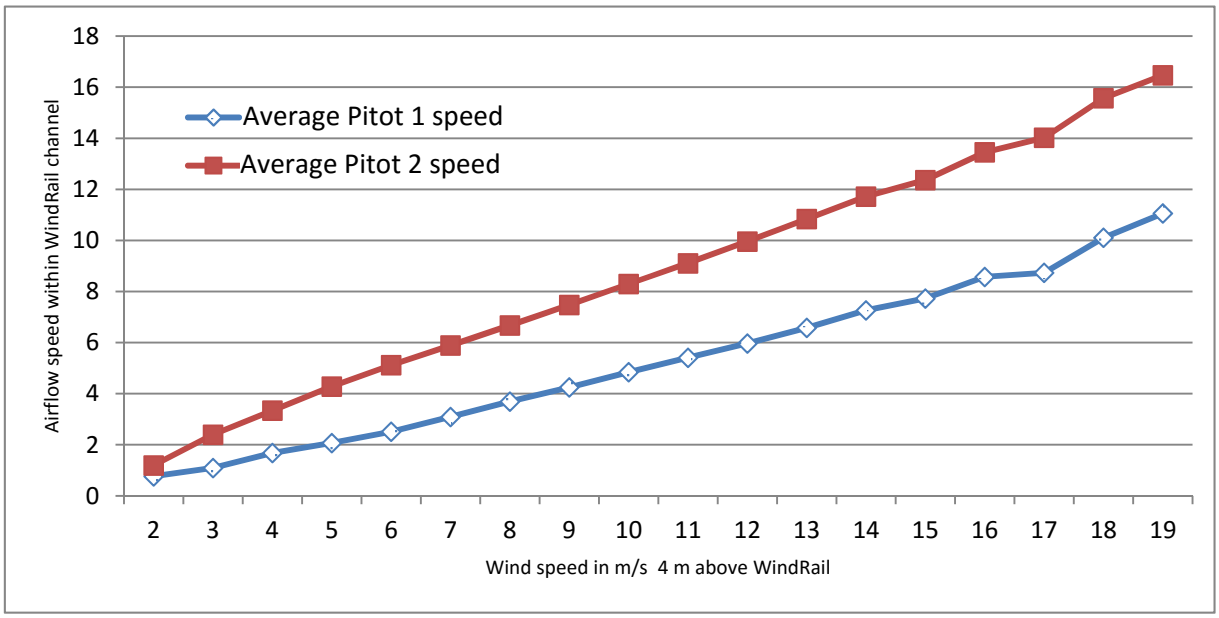

Figure C 1-1: Airflow channel acceleration with rotating rotor in geno mode

C 2 Influence of Wind direction

Based on the obtained data-set example for 27.07.2015, the influence of the wind direction was analyzed. A front flow with a relative wind direction angle of ±30 ° relative to WindRail installation direction shows a rather stable output power (Figure C 2-1). From a relative angle of >30° and <50° the power output drops significant. This is mainly due to a single module being tested as the side wall installation blocks the lateral wind significantly. CFD simulations show that a WindRail line with multiple modules shall be able to work with ±50° wind angle [8].

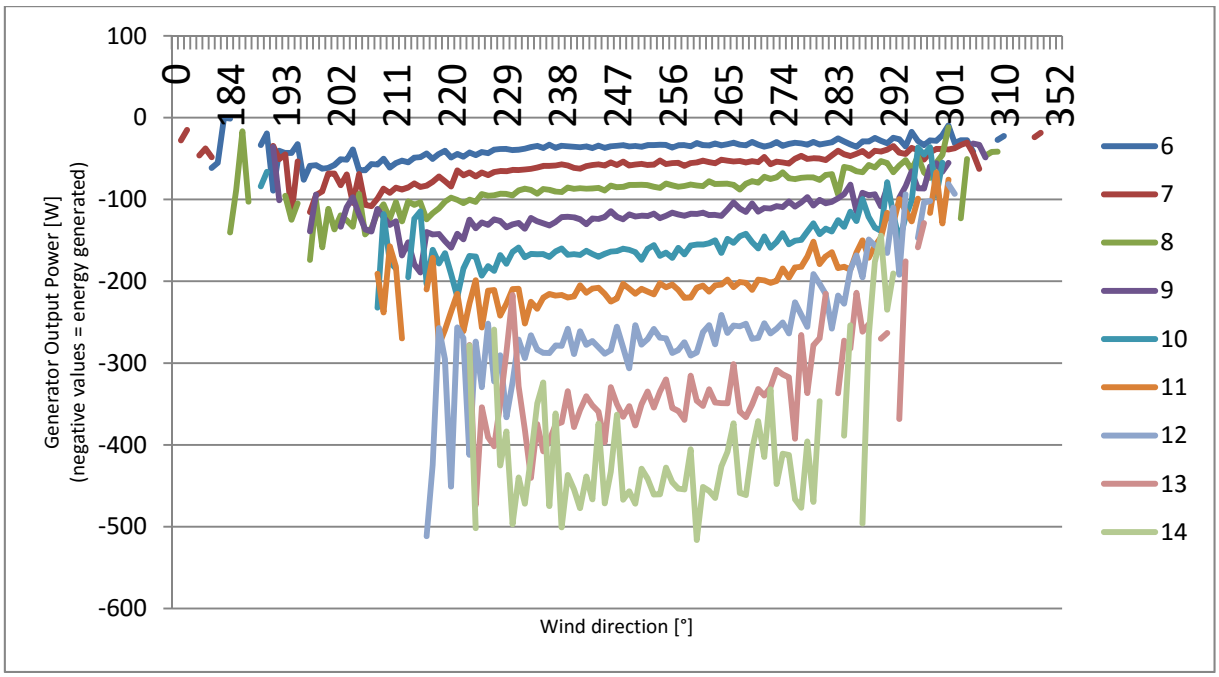

Figure C 2-1: Wind direction versus output power

C 3 Rotor differences

The rotor-generator output power curves demonstrate a similar behavior for both turbines (Figure C 3-1). The observed differences above 14 m/s wind speed are due to the wind direction side effects as demonstrated in Figure C 2-1.

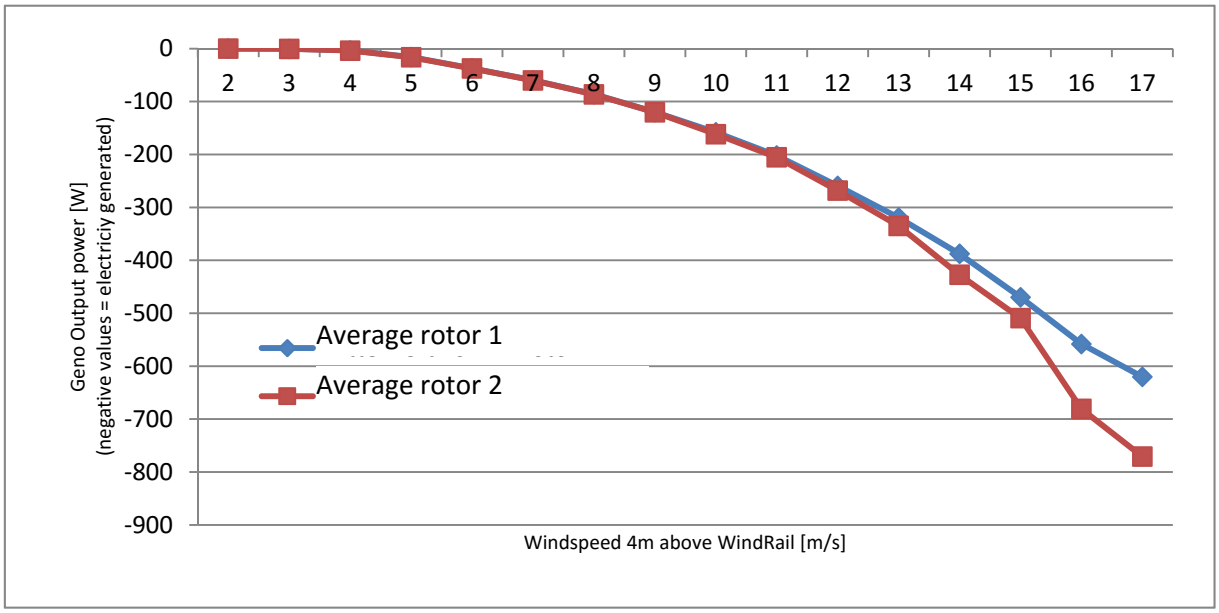

Figure C 3-1: Wind direction versus output power